STRUCTURE-BORNE SOUND TRANSMISSION ALONG PIPING ON SHIPS

Anıl Gülsar

20171735

FIRST REVIEWER	SECOND REVIEWER
Prof. Dr. Eng. Patrick Kaeding	Dr.-Ing. Dietrich Wittekind
Chair of Ship Structures	Managing Director
University of Rostock	DW-ShipConsult GmbH
Albert-Einstein-Str. 2	Lise-Meitner-Str. 9
18059 Rostock	24223 Schwentinental
Germany	Germany

July 17, 2019

Contents

List of Figures

List of Tables

List of Symbols

Sign	Unit	Description
A	mm^2	Section Area
C	–	Correction Factor
c	–	Damping Coefficient
D	m	Static Deflection
d	mm	Diameter
E	MPa	Young's Modulus
F	N	Normal Reaction Force
F_0	N	Reference Reaction Force
G	m/s^2	Gravitational Acceleration
I	mm^4	Moment of Inertia
K	N/m	Spring Stiffness
K_a	N/m	Beam Axial Stiffness
K_r	N/m	Beam Radial Stiffness
l	mm	Length
m	kg	Mass
μ	kg/m	Unit Mass
ω	$1/m$	Natural Frequency
R_i	mm	Inner Radius
R_o	mm	Outer Radius
S	Pa	Shear Modulus
t	mm	Wall Thickness

List of Abbreviations

3D	Three-dimensional
ABN	Air Borne Noise
ABS	American Bureau of Shipping
BC	Boundary Conditions
CAD	Computer Aided Design
CPU	Computational Time
DNV GL	Det Norske Veritas Germanischer Lloyd
DOF	Degrees of Freedom
FE	Finite Element
FEA	Finite Element Analysis
FEM	Finite Element Method
HPC	High Pressure Compensators
HRA	Harmonic Response Analysis
IMO	International Maritime Organization
LPC	Low Pressure Compensators
MSUP	Mode Superposition
RPM	Revolutions per Minute
SBN	Structure Borne Noise
SDOF	Single Degree of Freedom
SPL	Sound Pressure Level
STL	Sound Transmission Loss
VS	Visual Studio-Software by *Microsoft* to Solve Mathematical Problems
WBN	Water Borne Noise

Declaration of Authorship

I declare that this thesis and the work presented in it are my own and have been generated by me as the result of my own original research.

Where I have consulted the published work of others, this is always clearly attributed.

Where I have quoted from the work of others, the source is always given. With the exception of such quotations, this thesis is entirely my own work.

I have acknowledged all main sources of help.

Where the thesis is based on work done by myself jointly with others, I have made clear exactly what was done by others and what I have contributed myself.

This thesis contains no material that has been submitted previously, in whole or in part, for the award of any other academic degree or diploma.

I cede copyright of the thesis in favour of the University of Rostock.

Date: Signature

1. Abstract

In ships, the pipe structure represents very complex system of noise and vibration with under effect of by the engine, compensator and specific pipe components. Structure borne noise can cause discomfort to passengers and hearing damage to the crew and in this regard the need for a safe work environment is growing. Due to these effects, noise and vibration analysis must be studied and adequately monitored during the design stage. In this thesis, various possible pipe structures are discussed with the norms of noise and vibration for ships concerning the machinery. The objective of this thesis was to assemble knowledge and experience in the area of piping vibration measurements and study in some depth what are the best practices to perform the measurements. Analysis are made a carefully with consultancy of *DW-ShipConsult*, a German vibration and noise consulting company and few recommendations are made for the future structure borne noise studies.

Gemilerdeki boru bağlantıları; motor, kompansatör ve özel boru bileşenlerinin etkisiyle çok karmaşık bir gürültü ve titreşim sistemini temsil eder. Yapı kaynaklı gürültü yolculara rahatsızlık verebilir ve mürettebatın işitme duyusuna zarar verebilir. Bu konuda güvenli bir çalışma ortamına olan ihtiyaç artmaktadır. Bu etkileri nedeniyle, dizayn aşamasında gürültü ve titreşim analizleri çalışılmalı ve yeterince izlenmelidir. Bu tezde, makine dairesindeki olası boru bağlantıları gürültü ve titreşim normlarıyla tartışılmıştır. Bu tezin amacı, boru titreşim ölçümleri alanındaki bilgi ve deneyimleri bir araya getirmek ve bu ölçümleri gerçekleştirmek için en iyi uygulamaların neler olduğunu derinlemesine çalışmaktı. Bir Alman titreşim ve gürültü danışmanlık şirketi olan *DW-ShipConsult* danışmanlığı ile analizler titizlikle yapılmıştır ve gelecekteki yapı kaynaklı gürültü çalışmaları için birkaç öneride bulunulmuştur.

2. Introduction

While ship design industry develops, in order to meet the demands of customer, particularly with regard to structural optimization, noise and vibration problems tend to get more severe. This expresses itself in some cases in the difficulty of reaching a satisfactory solution within the ship's operational and design constraints, while in other cases development has brought new sources to the surface.

National and international organizations have set noise and vibration exposure boundaries over the years. These limits have improved over the years as the environment of crew and customers onboard have been improved through observations and research.

The *IMO* set standards for onboard ships in 1981 for noise and vibration. Since then, numerous studies and research have created results and conclusions which have improved conditions of commercial and military vessels. *DNV, IMO, ABS* and other organisations collect and update information. The limitations do not differ so much from standard to standard, but these norms need to be fulfil in design process for each ship.[14]

The design process includes model tests, calculations and deterministic assumptions from previous experience. In the ship building, the design of piping systems with regard to the internal pressure,material properties or temperature are studied variously before. However the deep understanding of the pipe vibrations are still remained poor.

By introducing electronic computers and *Finite Element Method (FEM)*, solving of the vibration problems on board has got new progress. This enables to perform vibration analysis of very complex ship structures caused by main engine excitation. Severe vibration on ships may cause difficulties to owners and shipyard staff during trials and subsequent service period.

The current introduction section covers a clear description of the field of work, studied problem and an outline of the report.

2.1. Field of Work

The scope of the piping systems are relatively large. In this large spectrum of variations, some piping systems are more critical and more difficult to design than others with regard to vibration. The poor designed pipe structures can add enormous and detrimental force and moment to the pipe supports and connections due to the vibration.

The objective of the thesis is to assemble knowledge and experience in the area of piping vibration measurements,analytical and numerical solutions on the ships. The vibrations of the pipes concern the pipe structure, pipe support and resilient mounts. The numerical solutions are done with Finite Element Analysis.

Finite Element Analysis (FEA) is a numerical method in mechanics, more precisely in computational mechanics. Hereby, the computational mechanics also cover different fields, such as nano and micromechanics and systems, nevertheless for the given purpose continuum mechanics are used for solids and structures. Nowadays *FEM* provides one of the most, if not the most powerful tool to analyse pipe structures in their behaviour on a computational way. It has itself proven to be very precise in prediction of, for example, stresses and deformation of a component or even a whole piping structure.[15]

The best practice to how pipe vibration should be measured and managed but also how the process parameters that influence the vibrations can be measured in order to better capture the big picture. By setting up a guideline for pipe analysis based on experience the problem can be resolve in the most efficient way and selection of appropriate precaution can also be verified according to best practice.

2.2. Problem Statement and Outline

It is observed in practical systems that *Structure Borne Noise (SBN)* attenuation along the compensator is very limited and levels on the pipe are very high. Nevertheless the negative effect on overly *SBN* transmission from the source is uncritical in most cases.

The thesis will investigate *SBN* transmission from the resiliently mounted source to the ship via the compensator, pipe and pipe supports and compare it to the typical *SBN* transmission of the resilient mounts.

The initial pipe structure to investigate *SBN* transmission is showed in Fig. 1 below:
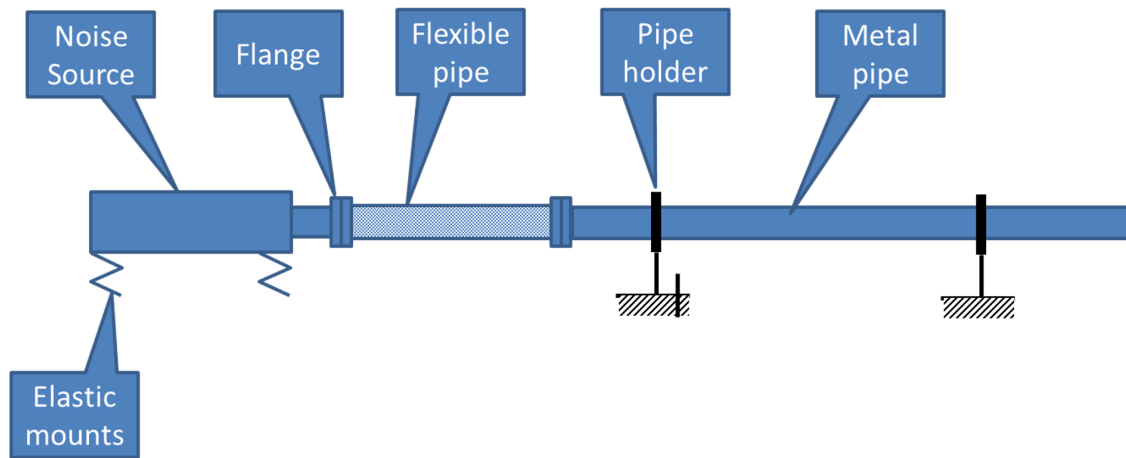
Figure 1: Problem statement.

If necessary, analytical approaches to solve the problem will be consider. Moreover, analysis will carried out with the *FEM* tool Ansys *Harmonic Response Analysis (HRA)*. Different set-ups for the *Finite Element Analysis (FEA)* will test to compare the results for each analysis.

The given Fig. 2 shows the test results for dynamic stiffness of the required compensator. The test hold by *DW-ShipConsult* before. The dimensions and boundary conditions are stated on the given graph.

The characteristics of the compensator will be search with respect to given graph with reverse engineering. The found will be use for the next analysis which contains compensator. After *SBN* transmission analysis for linear pipe structures which showed above, the new *SBN* transmission analysis will be evaluate to various type of pipe structure.
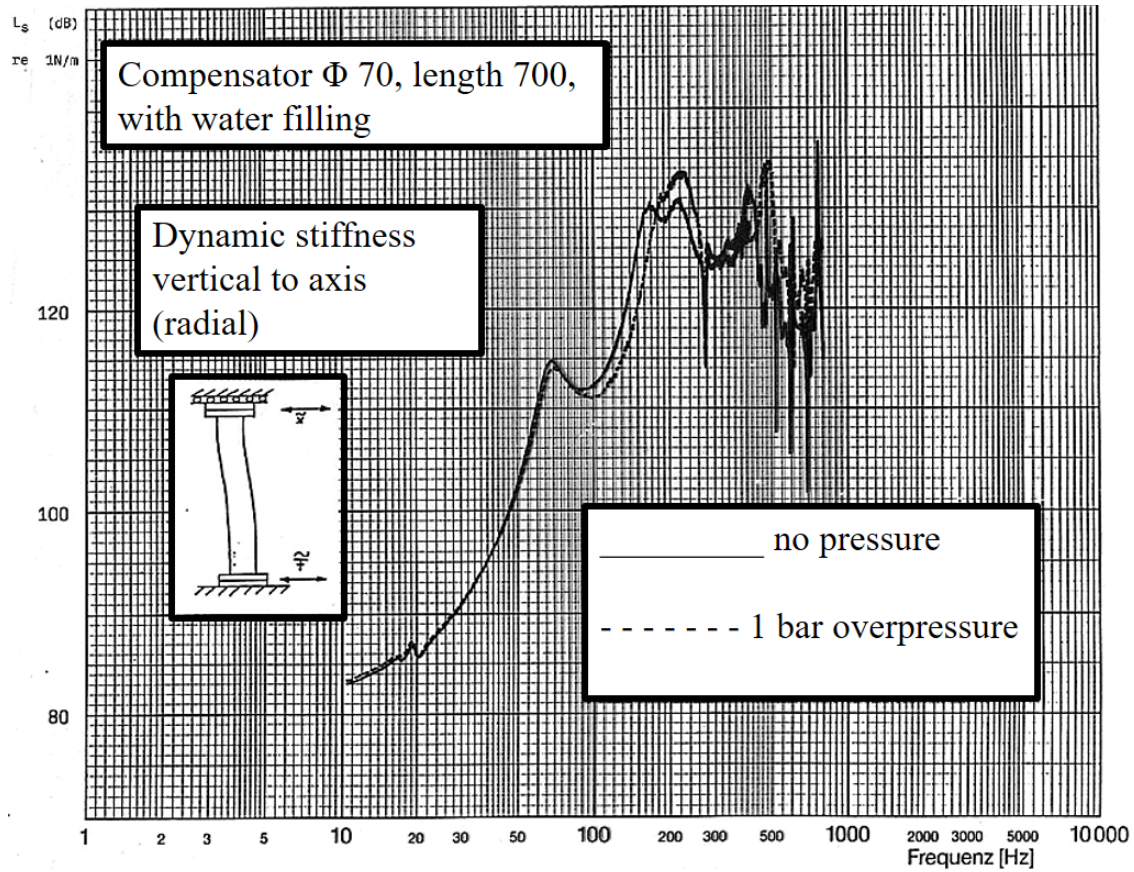
Figure 2: Dynamic stiffness analysis of given compensator.[26]

Afterwards, how the compensator length would effect on *SBN* transmission from the resiliently mounted source to the clamps will be studied. Moreover, various type of compensator and the location of the first clamp will be analysed with a regard of *SBN* transmission. Later, the effect of the rigid and resilient mounted clamps for *SBN* transmission will be determined. The criterion for the comparison is the reaction force acting on the ship structure.

Lastly, a case study will investigate *SBN* transmission from a double resiliently mounted source and intermediate mass to the hull via the two compensator, bended pipe and pipe supports. The results will examine both real measurement and numerical solutions. Additionally, optimization possibilities are proposed and tested to improve the pipe structure performance.

3. Background and Scope

3.1. What is Noise and Vibration?

Noise   Noise is an intense, troubling and uncomfortable sound. Over the top noise can lead to hearing impairment. Noise, known as impulses, containing sudden, strong sounds, is especially damaging. Noise is one of the most prevalent cause of illnesses for human-beings. People can discover disturbing even small noise levels when working in open-plan offices, for example, involves concentration. It's up to the individual what a person experiences as noise.

Vibration   The study of noise on ships can be well identify with clarify vibration concept. It is the movement on the decks,bed plates,frames or pipes which caused by an impact. Since the impact is transformed energy, the vibration is the energy which might lead to occurrence of noise if it is uncontrolled.

Harmful vibrations are vibrations of the body transmitted from a instrument to one's side or whole-body vibrations transmitted to the individual from a platform, such as the seat of a working machine. Generally noise is the sound that has negative or damaging effect on the living beings or the way of living.[13]

Frequency   It can be sum as noise is created when airborne vibration hits the eardrum. Since the noise can be subjective to each person, it is better to determine sound. Whether a sound is high or low is determined by frequency which are measured by cycles per second.

Generally the human ear can recognise vibrations between *20-15000 Hertz*. Hertz can be define as cycle per second and shown as *Hz*.

Natural Frequency   Natural Frequency occurs in all constructions, elements, components, engines, pipes etc. As already described in the above frequency is the individual item´s or geometry´s own cycle per second. It is dependent to the weight and geometric rigidity.[7]

Resonance   Resonance occurs when a body or element is exposed to impact with a frequency equal to its own natural frequency. If the impact is strong enough the element vibration will intensify and create resonance noise.[7]

Sound Pressure Level (SPL) The range of sound pressure between the hearing limit and the human ear's pain tolerance which is:

$$2.10^{-5}\,Pa = \; 10^{-12}\,W/m^2 \iff 20\,Pa \; = \; 1\,W/m^2 \tag{1}$$

Sound pressure covers a factor of 1 million. The representation in logarithmic form has been introduced to better display the hearing range. When comparing loudness, the ear treats noise in a logarithmic manner. The representation is standardized as 10 times the base 10 logarithm. It holds the *Decibel(dB)* unit and is called Level. The use of decibel scale is practical as it indicates the sound volume. The scale relates to the noise and provides a clear image of the risk of hearing is present or not.[24]
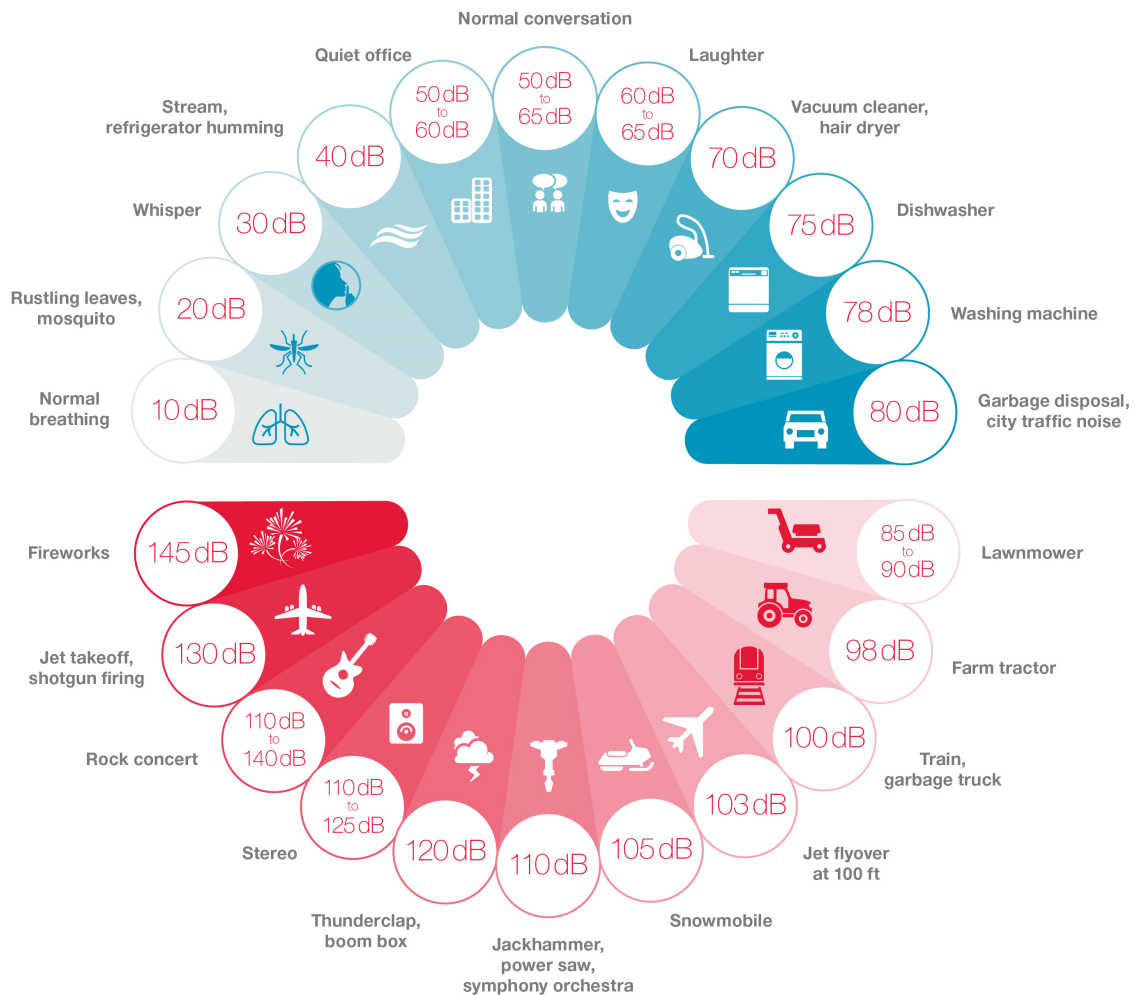
Figure 3: Reception of sound pressure levels.[17]

Safe operation, availability and lifetime assessment of piping systems are of utmost concern for plant operators. Optimized plants and safe operation under changing surrounding and boundary

conditions are of concern. Integrity assessment in these cases is to be performed and demonstrated in corresponding experiments.

Sound transmission loss (STL)   is a quantification of how much sound energy is prevented from traveling through an acoustic treatment. Transmission loss quantifies the effectiveness of acoustic treatments for an engineering application. [3]

Sound transmission loss can be defined as a ratio of the sound energy transmitted through a treatment versus the amount of sound energy on the incident side of the material.

Noise Transmission Paths   Machine sources typically generate three types of noise: *Airborne noise, Water-Borne noise and Structure-Borne noise*. When talking about an airborne noise source, it refers to sound generated by the machinery that radiates directly into the surrounding air. This airborne noise can then travel to any receiver within the room, such as a manned work station.

Additionally, airborne noise can travel through decks and bulkheads that make up a compartment containing a source. The sound created in the compartments that are directly adjacent to the source compartment is called *Airborne Noise*. The path this sound takes through decks and bulkheads is called the *Airborne Noise Path*.
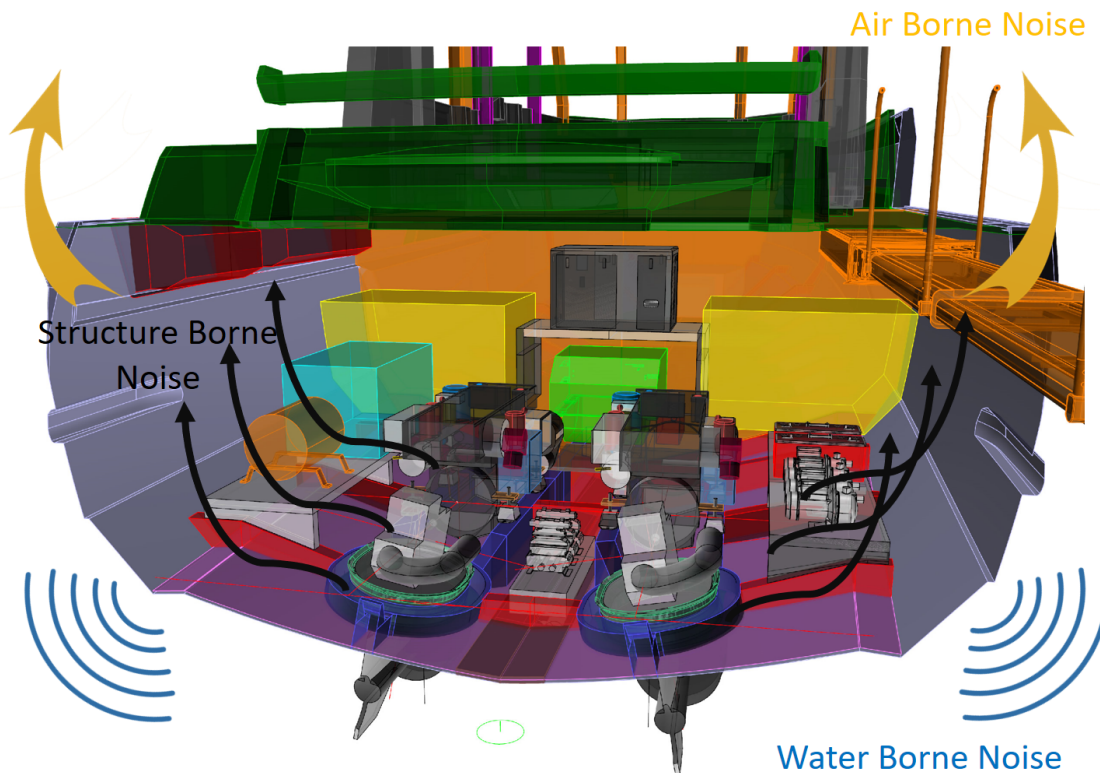
Figure 4: Acoustic paths.[18]

The second source of noise produced by machinery is vibration. Vibrations are transmitted through the equipment base from the mounting feet of the equipment to the vessel. The vibration then excites the adjacent deck and bulkheads, and travel across the ship. Essentially, any structure that makes up the ship will have some amount of vibration owing to a source of vibration, although the amount may be negligible for buildings far from the source. Vibrating decks and bulkheads forming any compartment on the vessel will radiate noise into the compartment's air. The noise produced by this route is called *Structure-Borne Noise*.[24]

In addition, another path deemed to be secondary structural noise. This route combines the noise paths of airborne and structure-borne. It is the consequence of airborne noise that excites the source compartment's surrounding structure and then crosses the entire vessel and radiates noise comparable to structure borne noise. This route can be very crucial, especially when the device is installed in isolation and there is a significant reduction in structure-borne noise.

Lastly, propeller, cavitation or the absence of propeller cavitation, machinery generated noise dominates a ship's underwater noise spectrum generate *Water-Borne Noise* . In the case where no isolation measures have been incorporated, structure-borne transmission dominates levels of *WBN*.

3.2. The impact of Noise

A highly advanced and delicate organ of the senses, the human ear perceives even minor sound changes. Usually do not pay much attention to the ear's function. Whether the sound is too high or annoying or calming, the action of hearing is become most important thing for humans.

The decibel scale is used when indicating the sound volume. A human with normal hearing can hear a sound level above *0 dB* with the decibel scale stated previous section. The pain threshold at the other end of the spectrum is reached at *120 dB* for most individuals. [11]

The decibel is a so-called logarithmic scale that doubles the sound energy reaching the ear if the sound pressure level increases at *3 dB*. If the level of noise is decreased by *3 dB*, noise may also be exposed twice as long without changing the risk of hearing impairment.

Thus for for a brief period of time a high *sound pressure / noise level* may have the same effect for a longer period of time as a low noise level. Tab. 3 demonstrates how long a noisy room can be stayed at different noise levels. For 8 hours the noise effect at *90 dB* is the same as for 10 minutes at *107 dB*. The sound energy level therefore determines how much time that people can stay in a space that is noisy.

Table 3: The sound level noise impact relationship.[13]

1 minute	117 dB
5 minute	110 dB
10 minute	107 dB
30 minute	102 dB
2 hours	96 dB
8 hours	90 dB
24 hours	85 dB

When it comes to person's perception of the change in the noise level, an increase of *10 dB* is considered as double the noise level. In other words, *90 dB* is twice as strong as *80 dB*. Even a small decrease of the noise can have an enormous effect.

In comparison the usual conversation is about *60 dB* in volume. If the surrounding noise exceeds *75 dB*, the voice must be raised. There will be no chance to be heard if the background noise exceeds *90 dB*.

3.3. Modal Analysis

Any object may be regarded a complex spring connection, and the system "*x*" can be provided for any input "*y*" applied by a factor of scaling as:

$$k \times x = y \tag{2}$$

This is comparable to the spring equation where "*k*" is the spring stiffness, "*x*" is the spring displacement, and "*y*" is the force applied. It can be rewrite for any generic system as,

$$[K][x] = [y] \tag{3}$$

where *x* may be displacement, temperatures, etc., while *y* is force, stream etc. The scaling factor of the matrix $[K]$ is more frequently called the stiffness matrix. For some response $x = a$, if $y = L \times a$ was the input used, *L* is known as the system's eigenvalues and the response of the system *a* are known as the *eigenvectors* corresponding to the *eigenvalue L*. The eigenfrequencies are those at which this eigenvalues is maximum.[9]

Each system can be defined as a stiffness matrix that links displacements (or system reaction) and forces (or system inputs). These frequencies are known as the system's natural frequencies and are supplied by the stiffness matrix's eigenvectors. These frequencies are also referred to as resonant frequencies.

The resonant frequencies associated with mechanical structures are known as mechanical resonance. As shown in Fig. 5. As the frequency of the load applied or input on the *x-axis* approaches the resonant frequency, the response amplitude nears the resonant frequency while the amplitude of response on the *y-axis* nears infinity.
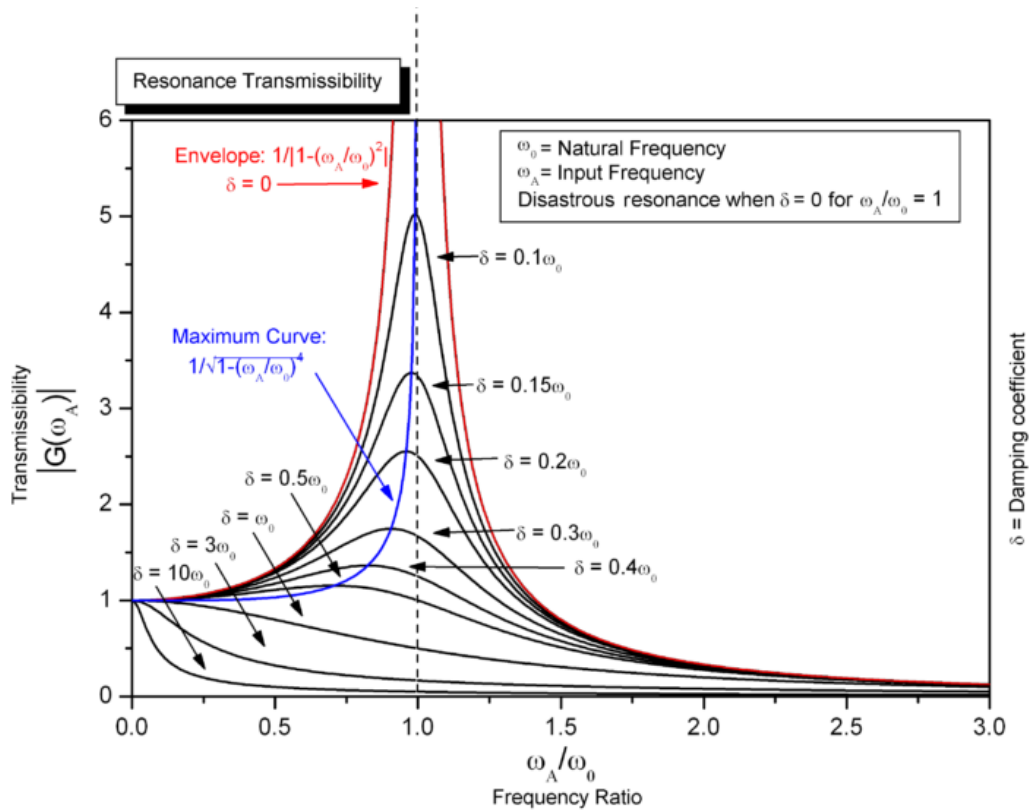
Figure 5: Amplitude of response as a function of the frequency ratio.[19]

Most structures like acoustic, thermal or electromagnetic can be made to resonate, i.e. to vibrate with excessive oscillatory movement. The vibration of the resonant is primarily due to the interaction of the materials inertial and elastic properties within a structure. Resonance is often the cause of many of the vibration and noise related issues that occur in structures and running machinery.

To better comprehend any structural vibration issue, a structure's resonant frequencies need to be recognized and quantified. Today, modal analysis has become a common means of identifying a machine or structure's modes of vibration.

Modal analysis is a method under vibrational excitation to study the dynamic characteristics of a structure. Modal analysis can be used to determine natural frequencies, mode forms and modal vectors of a structure. Modal analysis enables the design to prevent resonant vibrations or to vibrate at a certain frequency and provides engineers with a concept how the construction can meet distinct dynamic load kinds. The noise source and compensator such structures of that given pipe structure, the dynamic features of which can better be studied in modal analysis.

4. Source

4.1. What are the Noise Sources on Board?

Noise is a significant stressor on board ships. There are many distinct sources of noise and vibration in the engine room and it is often hard to define the precise issue, [11]. The individual sources of noise often strengthen each other. The main noise sources are:

Propeller   The propellers often cause a lot of noise and vibration problems on the ships. The problems are among others caused by the pressure momentum from the propeller blades each time they pass by the bottom of the hull. Varying forces and momentum from the propellers will also transmit through the steel structure.

Another problem is cavitation. Cavitation occurs when the pressure on the propeller blade front edge drops causing the water to boil. At low pressure water boils at a lower temperature. This creates bobbles again creating pressure load transmitting into vibration in the hull.

Machinery   The engine is installed on a bed-plate that is component of the vessel's entire steel structure, the vibration and noise produced here is transferred to the rest of the vessel. However on engine, the noise and vibration is either air borne or structure borne noise.

It differs how much noise and vibration the individual engine produces and how noise and vibration are transferred to the remainder of the ship. *Revolutions Per Minute (RPM)* and how the auxiliary equipment is mounted on the main machinery are important. When the machine is in service, turbo chargers, pumps, equipment etc. all contribute negatively to all noise levels.

Hydraulics   On board fishing vessels hydraulic systems are used as a source of energy for among others winches, pumps, cranes, steering gear, etc. Hydraulic systems are very dependable and therefore indispensable. Unfortunately they often create high noise caused by the impact motion created by the pumps of the hydraulic unit. In other words the higher pressure the more noise.

Ventilation   Noise produced by a ventilation system mainly comes from the ventilators and their drive motors and shafts, and is caused by their shape and circulation speed, and air intake and discharge vents.

4.2. Influence of Noise Sources

Noise from engines and auxiliary equipment tends to spread across the vessel. The noise level in engine rooms arises primarily from the various equipment. The overall noise level at one place is the total of the acoustic intensities that each equipment causes at this place and to which any sound reverberation impact on the walls is added. [11]

Most of the noise is transferred through pipes, floors and ceilings in common areas. Doors, furnishings and pipes that are deformed could affect the amount of noise in a specific location through the generation of parasite noise. The vibration energy that the propulsion system and propeller produce, primarily derives from noise that is transferred by pipes, floors and ceilings. Wall-mounted devices are also sources of unpleasant noise.

In proportion to the distance from the source of excitation and inversely proportional to the surface size and transmission coefficient, noise transmitted by the structures in question is decreased. Airborne noise can also be generated by exhausts of engines, ventilators and equipment such as hydraulic generators, steam valves etc. in addition to the noise from the structure.

The vast majority of ships are propelled by diesel engines. During the engine combustion process, aerodynamic noise happens. Gas generation generates sound waves in the cylinder that transmit as structure-borne noise through the inlet air and the combustion gas into the cylinder walls. The sound pressure level will initially depend on the process of combustion. The Also the noise transmission affects the cylinder lining and shape of the cylinder-head.

Mechanical vibrations from the column are transferred to the engine structure via the piston rod, shafts, tooth equipment, chains and journal rollers and are then transferred to the deck, cover, hatches, and other devices. Mechanical vibration also generates vibrations on both sides of the piston rod transferred from the sideways to the cylinders. The structure's noise is also enhanced by valves and other machinery.[25]

4.3. Engine

In this thesis the noise source will be think as a medium-speed diesel generator. Based on the *RPM* of the engine, a distinction can be made between "slow" engines with a relatively low noise level and "high-speed" or "medium-speed" engines, which are more powerful than other types of engine but which create more noise.
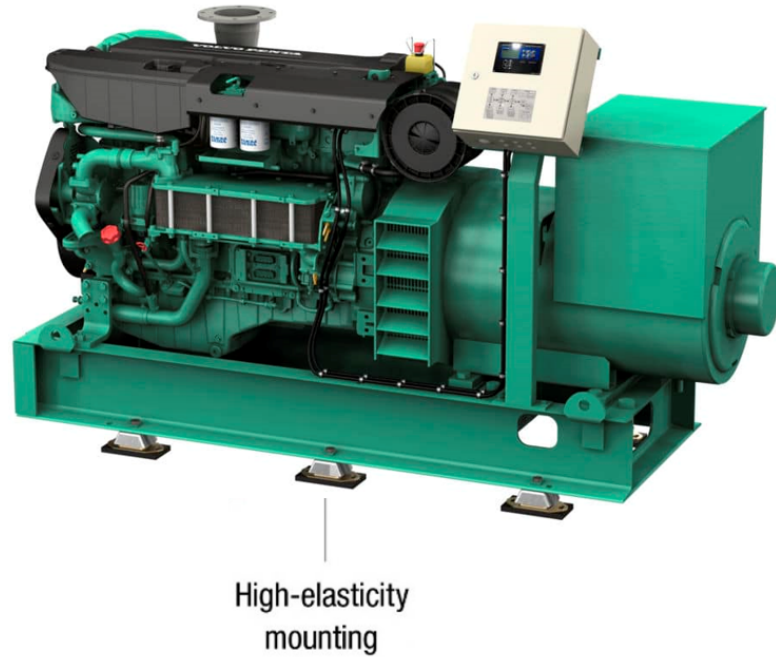
Figure 6: Typical diesel generator.[20]

Large ocean-going vessels typically have three generators powered either by dedicated 4-stroke-cycle medium-speed diesel engines or by diesel propulsion. Diesel generators are often installed resiliently, as they make a significant contribution to noise when they propagate throughout the structure and are radiated into rooms. [23]

Natural frequencies at multiple half rotational speeds characterize the noise of these diesels. Rotation velocity is connected to the 60 Hz frequency of the electric power supply. Therefore, a typical diesel generator turns *720 RPM* but there are also *600 or 900 RPM* index. A *720 RPM* Diesel has:

$$\frac{720 \ rev}{minute} \ \frac{1 \ minute}{60 \ seconds} \ \frac{1}{2} = 6 \ Hz \tag{4}$$

natural frequency and up to kilohertz range multiples. These scale is also important for the chose of engine weight with respect to its natural frequency.

The engine's noise and vibration are much harder to resolve by rebuilding the engine. The modifications in the surrounding machinery are often necessary to solve these issues. Resilient mounting of machinery is one way to reduce the noise due to the operation. Resilient mountings are effective vibration absorbers which are designed against increased dynamic and axial load. It is necessary to ensure that the bed-plate is rigid as the engine is not a part of the rigidity.

Figure 7: Type of resilient mountings.[21]

Resilient mounting of machinery also provides a reduction in the structure borne noise. When main machinery is fixed, the noise is transmitted through the bed-plate to the rest of the hull. To sum up, resilient mounted machinery isolates the engine from the bed-plate which means that the noise transmission can be reduced effectively.

4.4. Natural Frequency Analysis of Source

Although the primary assessment focus on the tube structure, noise can be generated from any source. The mass or material characteristics of source are not constrained by this study. However, natural frequency of the noise is important to know during full structure analysis. In this section the noise (vibration) source is defined both numerically and analytically. Later on results are crosschecked with each other.

4.4.1. Analytical Solution of Noise Source Vibration

The resilient mounted structures can express with the spring-mass single degree of freedom systems since the both have similar application. A *Single Degree of Freedom (SDOF)* system where the mass m can only move along the vertical $x - axis$ is described by the following equation;

$$m\ddot{x}(t) + c\dot{x}(t) + kx(t) = \omega(t) \tag{5}$$

This equation states that the sum of all forces acting on the mass should be equal to zero with an externally applied force, $m\ddot{x}(t)$ the inertial force, $c\dot{x}(t)$ the viscous damping force and $kx(t)$ the restoring force. The variable $x(t)$ stands for the position of the mass m with respect to its equilibrium point, i.e. the position of the mass when $\omega(t) \equiv 0$. [8]
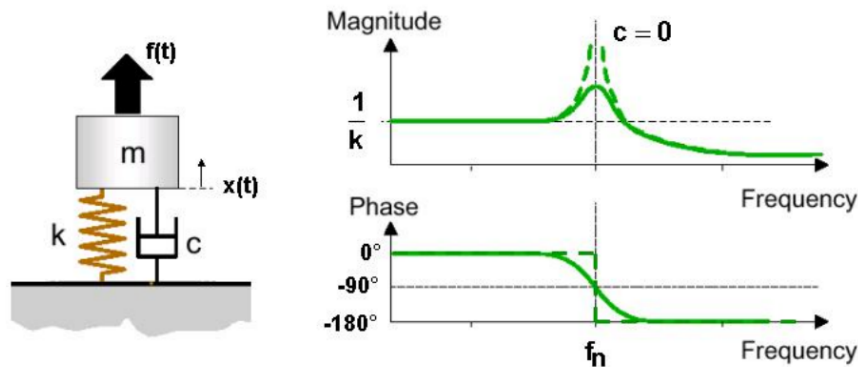
Figure 8: Single degree of freedom systems.[8]

The following analytical natural frequency estimation method can be used as a cross check for grounded finite element model modal analysis frequencies.

$$\omega = \frac{1}{2\pi}\sqrt{\frac{k}{m}} \tag{6}$$

Where;

- ω : Natural Frequency $[1/m]$
- m : Mass $[kg]$
- k : Stiffness $[N/m]$
- c : Damping Coefficient,
- G : Gravitational Acceleration $[m/s^2]$

The G is applying a downward body load on the mass and the static deflection D $[m]$ equation can be written as :

$$k = \frac{m.G}{D} \tag{7}$$

And finally the undamped natural frequency can thus be calculated from the static deflection for an *SDOF* systems.

$$\omega = \frac{1}{2\pi} \sqrt{\frac{G}{D}} \tag{8}$$

The general diesel generator engine rpm and natural frequencies are stated previous section. In order to get similar resilient mounted engine frequency range; the static deflection is set to 10 mm for the engine. The natural frequency and the inputs for chosen source modal is shown in Tab. 4 below.

Table 4: Single degree of freedom systems.

Static Deflection [D]	0,01	m
Mass [m]	3207,9	kg
Stiffness [k]	3,15E+06	N/m
ω	4,985	1/m

4.4.2. Numerical Solution of Spring Mass Vibration

In this thesis, different pipe structures are compared each other with their numerical solutions. Before comparison, the noise source properties are need to be set same for each structure. Noise weight has to evaluate for comparison between analytical numerical solution .
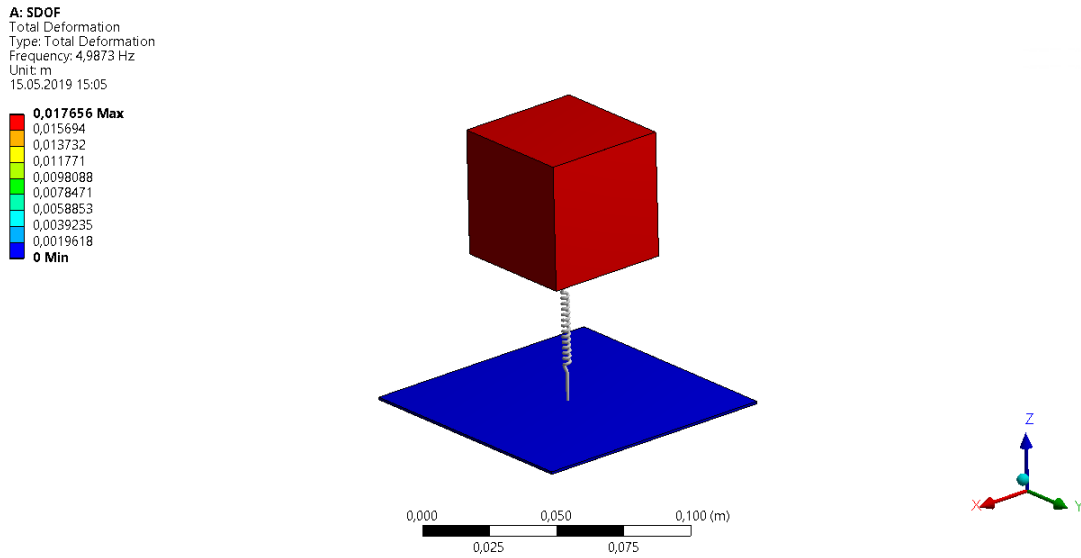
Figure 9: Ansys single degree of freedom systems.

In machinery, there are several type of forces are action on engines. Reciprocating compressors (and pumps) generate high dynamic forces. These forces are due to the inertia of the piston and other reciprocating and rotating components, gas,liquid forces and pulsation pressure induced forces in piping. However, the noise source only under axial force in this particular study. The finite element modeled through Ansys modal analysis and the total deformation of the model shown in Fig. 9 above. [1]

The importance of both analytical and numerical solution is the verification of the natural frequency within the range of commonly used engine *RPM* index. The possible engine *RPM* with the calculated frequency also can be find with the equation below :

$$RPM = 4,987 \times 60 \times 2 \quad where \approx 600 \, rpm \tag{9}$$

The numerical solution for similar mass and deflection inputs are matched with analytical solution. Final engine mass is evaluated regarded to the given analytical and numerical solutions.

4.5. Noise Weight Analysis

The challenge of the comparison of *SBN* transmission is the versatile force levels on pipe structure. There must be some reference values for all solutions which are not effect by different compensator type or clamp location. Since the engine properties and boundary conditions are similar for further analysis, it is important to have *SBN* force levels at engine foundations which are stable compare to the pipe structure.

To study effect of the source weight on the force levels of its foundation ; 7 different source weight is compared in same pipe structure with their own spring stiffness in Tab. 5.

Table 5: The weight and stiffness scale used for analysis.

	0,1 tonne	0,3 tonne	0,5 tonne	1 tonne	2 tonne	3 tonne	10 tonne
Spring Stiffness [N/m]	1,24E+05	2,99E+05	4,91E+05	9,76E+05	1,89E+06	3,15E+06	1,02E+07

Each system considered as *SDOF* with *10 mm* deflection. The increment of weight, result in greater spring stiffness. Tab. 6 indicate that the resonance frequency for each engine weight. Also the relative difference are stated below.

Table 6: Relative frequency difference respect to weight.

	Natural Frequency [Hz]	Difference
0,1 tonne	8,111	
0,3 tonne	6,579	18,89%
0,5 tonne	6,136	8,25%
1 tonne	5,337	7,04%
2 tonne	5,110	6,67%
3 tonne	4,989	4,77%
10 tonne	4,985	0,08%

The relative differences are show that the natural frequency of engine is start to converge above three-tonnes. The reason of the weight is chosen as *3207,9 kg* with respect to this convergence study.

In order to have better visualisation, the force levels with respect to frequency is showed in Fig. 10. The natural frequencies of the resilient engines are pointed. Pipe structures are identical for each solution and only the spring stiffness and the engine weight is varied through analysis. Selected engine weight solution is shown in black dashed pattern.
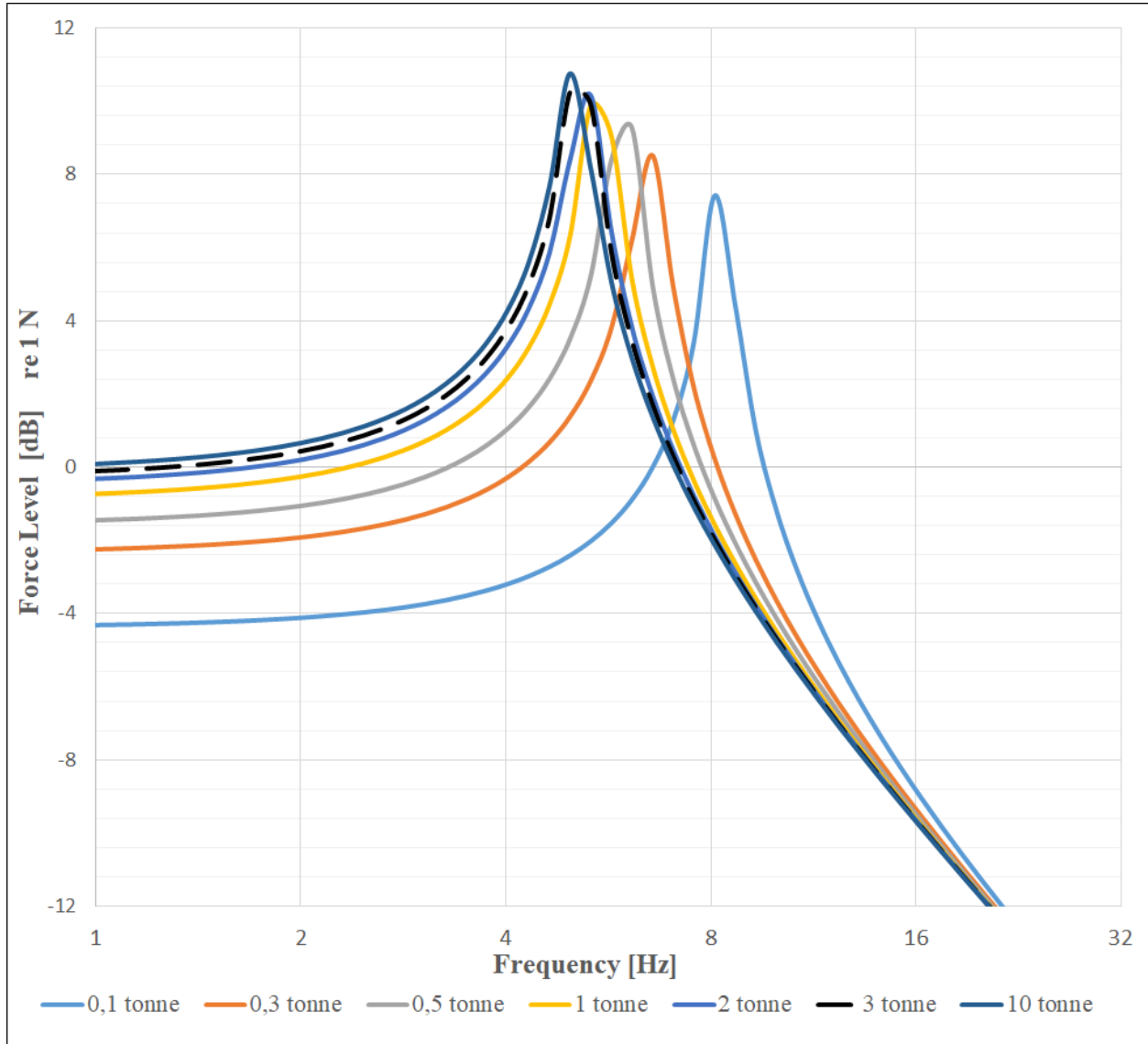
Figure 10: Noise weight analysis.

The figure indicate that resonance (natural) frequency is start to converge with an increase in the engine weight. Lower source weight are results in higher natural frequency. After three-tonnes the force levels are getting stationary.

The selected weight is valid for many ships engine dry weight today. Furthermore, the compensator length analysis in Sec. 6.3 or compensator type analysis in Sec. 6.4 are need to be comparable with each other. The different pipe structures with low engine weight will be result in different force levels on engine foundation for each solutions.

5. Compensator

5.1. What is Compensator?

In resiliently mounted engines, the design and mounting of the piping system must be taken into account. The objective is to ensure that the engine is optimally insulated against the bed plate, but to avoid unnecessary vibrations on the fixed pipe joints.

A compensator is typically designed to accommodate movement and absorb vibrations within piping systems. Compensator must be strong enough to withstand the working pressure, flexible enough to accommodate movements and tough enough to endure cyclic movement. The pressure and flexibility analysis can be examine with modal analysis and finite element analysis.[2]

The compensators can classify due to pressure capacities as :

- High Pressure Compensators *(HPC)*
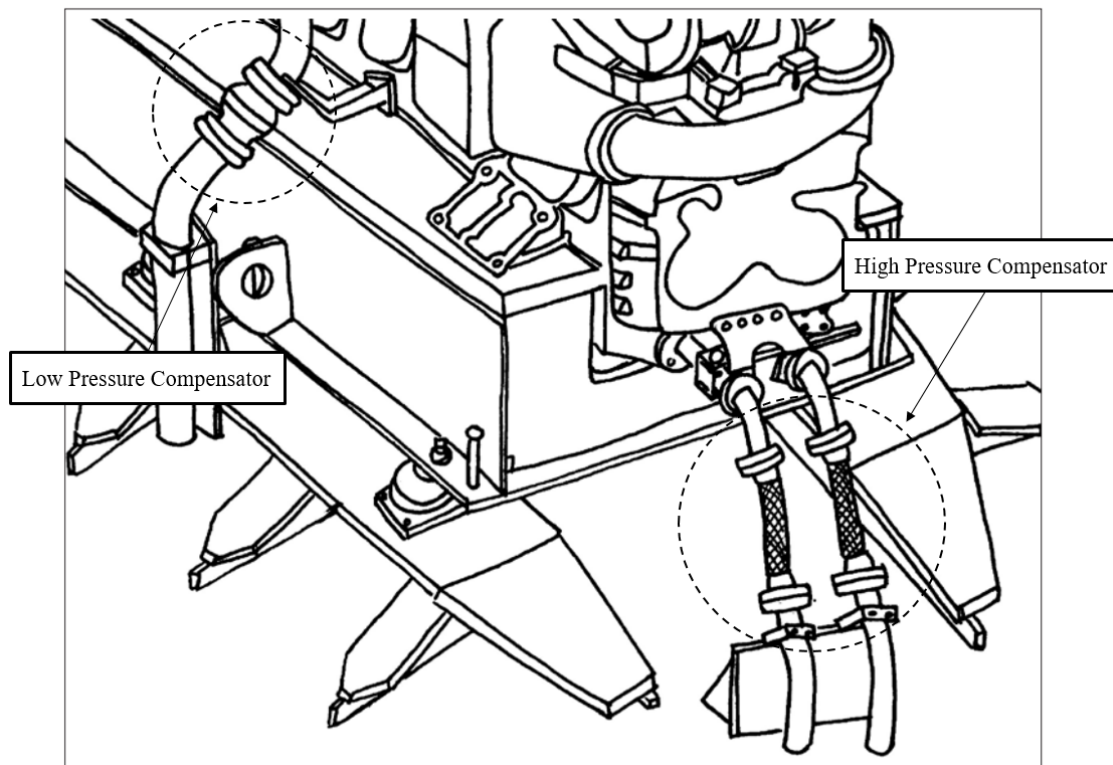- Low Pressure Compensators *(LPC)*

Figure 11: Different compensators on engine.[13]

For all types of fluids, pressures and temperatures there are countless compensator available. They are highly flexible if the tubes are properly mounted. In this thesis main focus of compensator type is selected high pressure compensator. For small diameter, high pressures and high temperatures pipes, *HPC's* are mainly used.

The compensators are typically made of two flanges and an reinforcement of the rubber-coated steel. The compensators are suitable for flexible mounted main engines as they can be flexed, pressurized, stretched or parallelly displaced in accordance with standards.

Flexibility can add the pipe structures as use of expansion joints or compensators. The Fig. 12 shows the movements of the compensators below:
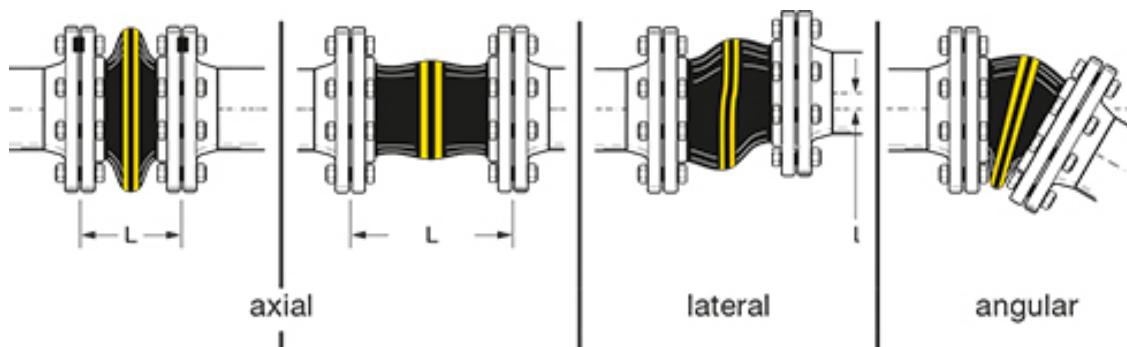
Figure 12: Different compensator movements.[22]

Flexibility analysis is performed in order to investigate the effect from alternating bending moments caused by the harmonic loads are acting from a source or connected pipes. Flexibility assessment is the issue to design the piping systems in such a way that parts of the piping itself act as a spring and release or reduce the internal bending stresses or longitudinal stresses that otherwise would have been destructive for a straight pipe between the noise source and the targets.[16]

5.2. Mechanical Properties

The compensator or flexible pipe can be vary as steel, rubber, fabric or mixed materials. In this study the build material for compensator is determined in order to have advanced features as flexible and both axially and laterally a low spring constant.

DW-ShipConsult company provide the main dimensions of *HPC* from measurement data which are hold before. In order to validate numerical and analytical solutions with test measurements the main dimensions are set similar with compensator test before. The dimensions of circular compensator are given in Tab. 7 below:

Table 7: Main dimensions of compensator.

Length [m]	0,7
Diameter [m]	0,07
Wall Thickness [m]	0,01

Although the main dimensions are provided, the mechanical properties of the compensator is not stated before. Today, the mechanical properties of compensators are highly various due to materials used. One of the challenge of the thesis to set mechanical properties for given main dimensions and dynamic stiffness graph which showed in Sec. 5.3.

Table 8: The mechanical properties of the compensator.

Density [kg/m^{-3}]	2500
Young's Modulus [Pa]	8,2E+08
Poisson Ratio	0,41
Shear Modulus [Pa]	3,2E+08

The main stiffness parameters for this thesis is selected as *Young's Modulus* and *Poisson Ratio*. All the parameters are combined in an engineering perspective and the results are evolved until the numerical solution results are match with the test measurement. The final mechanical properties and results of the compensator are shown in Tab. 8.

5.3. Natural Frequency Analysis of Compensator

In this section, the natural frequency of cantilever compensator is analytically solved. The solution selected by the inputs and analyzed for three different compensator length. Later on, the numerical model solved with Ansys Modal Analysis.

Modal analysis is a method to investigate the dynamic features of a structure under vibrational excitation. Modal analysis can be used to determine a structure's natural frequencies, mode shapes and mode vectors. Modal analysis enables the design to prevent resonant vibrations or vibrate at a defined frequency and provides engineers with an idea of how the design will react to various kinds of dynamic loads. A compensator is one of the structure whose dynamic features can be better researched through modal analysis.

The outcomes are contrasted with each other. Finally, the actual test data is cross-checked with the chosen numerical modal.

5.3.1. Analytical solution of cantilever beam vibration

Give is a cantilever beam of length L with a circular cross-section of inner and outer radius.
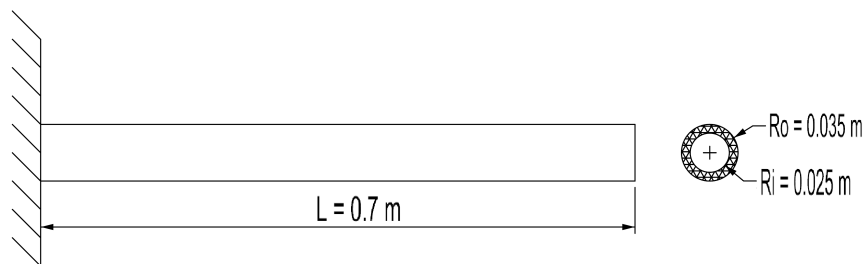
Figure 13: The main dimensions of compensator.

The material properties are given in Sec. 5.2. The analytical solution is appears as:

$$\omega = \frac{\pi}{2l^2}\sqrt{\frac{EI}{\mu}}.C \tag{10}$$

where "f" natural frequencies, "E" the material Young's modulus, "I" the moment of inertia, "μ" unit mass, "l" the beam length, "C" the factor that depends on the vibration mode which is given below :

Modes	1	2	3	4	5
Vibration Mode Factor	0,356	2,232	6,259	12,24	20,244

The factors of vibration can vary depending upon the beam support type and position. *Hütte Des Ingenieurs Handbook* is the basis for the formulations and factors table shown above. [10]

5.3.2. Comparison of Solutions for Different Slenderness Ratio

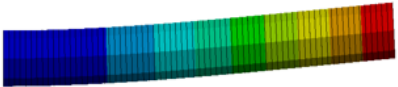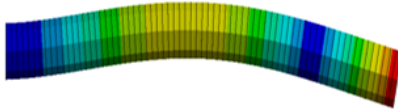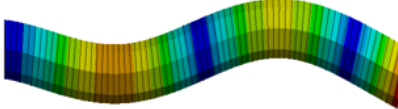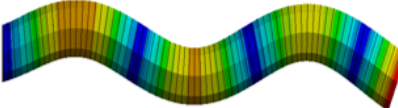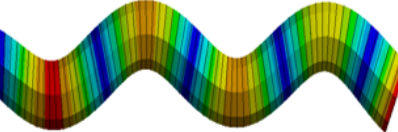The analytical solution of the cantilever compensator is compared respect to the numerical solution. During comparison three different length of compensator is considered. The main objective for comparison between length sizes is the element problems occurring during comparison of two solution. Frequencies of numerical analysis and analytical analysis are shown Tab. 9.

Table 9: The Results "Frequency".

Modes	Numerical Solution Frequency Hz			Analytical Solution Frequency Hz		
	L= 10 m	L= 5 m	L= 0,7 m	L= 10 m	L= 5 m	L= 0,7 m
	0,07	0,28	13,88	0,07	0,28	14,06
	0,43	1,72	81,03	0,43	1,73	88,13
	1,21	4,81	206,78	1,21	4,84	247,13
	2,36	9,40	363,79	2,37	9,47	483,28
	3,90	15,47	539,37	3,92	15,67	799,31

The first view from the table shows that there is a great difference between the short compensator solutions. That's due to the analytical solution is based on *Euler-Bernoulli Beam* theory despite numerical model consist *BEAM*188 as a beam element. *BEAM*188 is based on the theory of *Timoshenko Beam*, which is the theory of shear deformations in a first order: the cross-sectional strain of cross-sections remains flat, and unchanged after deformation.

This difference can observe with relative errors given in following Tab. 10. The cross section areas and mechanical properties same with original compensator.

Table 10: Relative error between solutions.

Modes	L= 0,7 m	L= 5 m	L= 10 m
1	1%	0,2%	0,0%
2	8%	0,2%	0,1%
3	16%	0,6%	0,3%
4	25%	0,8%	0,2%
5	33%	1,3%	0,3%

The analytical solution and numerical solution have relatively small differences in the higher compensator length according to the table given. The 5 meter and 10 meter compensators have a relative error of less than 1 %. The shorter compensator has an error of up to 33 %.

To assess the applicability of the component, the slenderness ratio of the beam structure should be compared as [6] :

$$Slenderness\ Ratio = \frac{GAl^2}{EI} \tag{11}$$

where "G" shear modulus, "E" the material Young's modulus, "I" the moment of inertia, "A" area of cross section , "l" the beam length. The values are defined in mechanical properties Sec. 5.2.

Table 11: Slenderness ratio and element type relation.

Length [m]	Slenderness Ratio	$\delta\ Timoshenko/\delta\ Euler-Bernoulli$
0,7	582,12	0,675
5,0	4158,00	0,987
10,0	8316,01	0,997

The relative difference is decrease with respect to the slenderness ratio increment. Reason why is that the *Timoshenko Beam Elements* are no longer under effect of the shear deformations at high slenderness ratios. It can be stated that the either analytical and numerical solutions are correct. However the geometry is constrained in the given test conditions. Test modal stated by company as Tab. 5.2.

The verification of numerical solution by analytical solution will no longer be valid since the two solutions consider different beam theories. The solutions are extremely irrelevant at small slenderness ratios. Besides that the outcomes of the physical testing can serve as validating the compensator's natural frequencies.

5.3.3. The Validation of Selected Compensator

The *DW-ShipConsult* company provides former test chart about the natural frequencies of desired compensator dimensions. The main dimensions are constrained but the mechanical properties of the compensator is selected through best possible numerical results matched with the physical test results. The material of the compensator will be selected as a rubber steel mixed which leads us to play inputs as density or Young's modulus to get similar results.

The final mechanical properties of the compensator is stated in Tab. 8. The comparison of the numerical results and physical test results are shown Fig. 14 below:
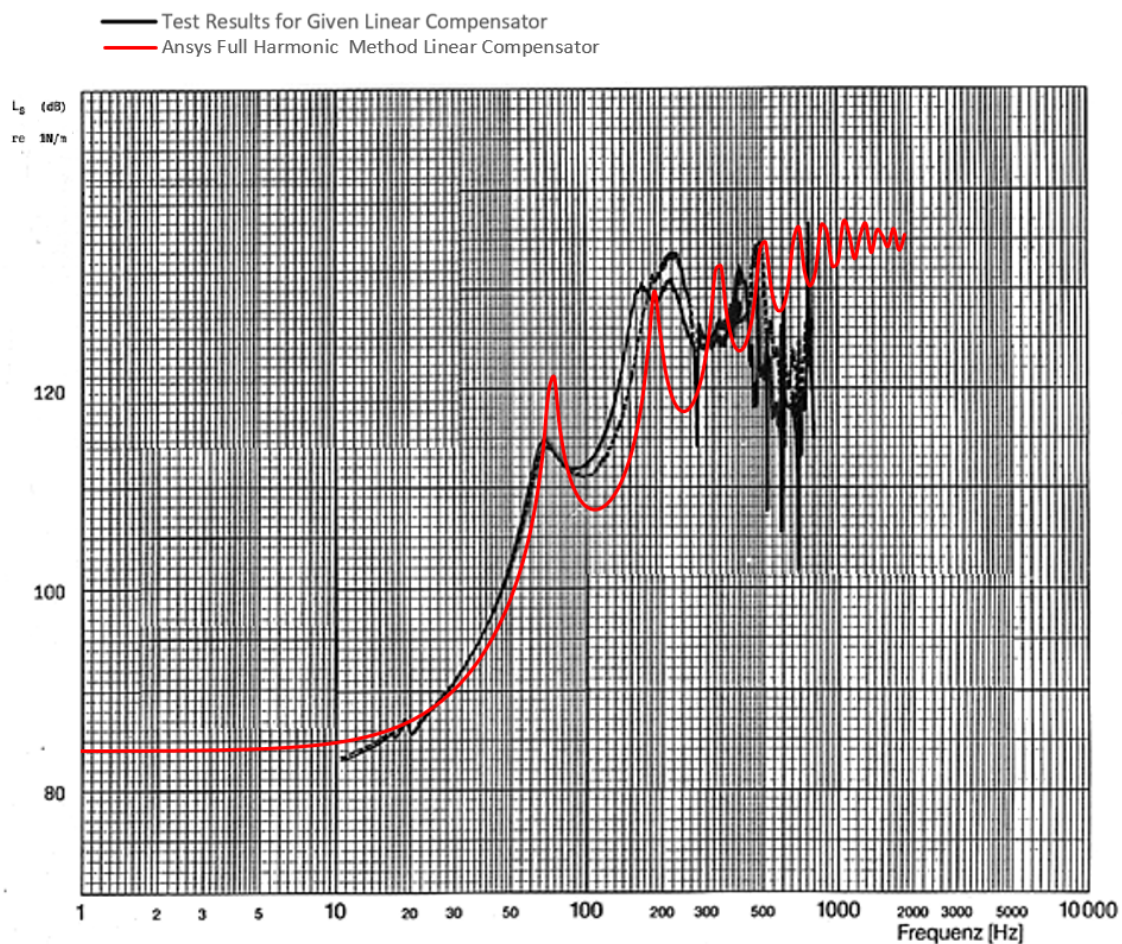

Figure 14: The given data versus Ansys modal analysis.

The figure states that numerical solutions are generally match with the test results. First and second modes are match with same natural frequencies. However the noise levels might look different at resonance points since the uncertainties on damping parameters are effecting on test results. Structural damping is set for *0,03* for all numerical solutions hold on *Ansys Full Harmonic Method.* This verification has significant importance about mechanical properties of the compensator (flexible pipe) used from company database which has no information about mechanical characteristics.

Up to this point, the noise source and compensator is modeled and solved either analytical and numerically. Moreover, the results are satisfied with given data and the models will be connect with each other in following chapters.

6. Harmonic Response Analysis of Piping Systems

Harmonic analysis is used to determine the continuous dynamic state reaction of a structure which is subject to sinusoidal loads. Ansys enables for two different kinds of harmonic loads, which are applied loads or defined excitation. One of can be added to the solution for this research.

Applied Loads   It is the method that applied on this thesis. The load type includes all externally applied loads, elements, gravity and thermal loads. Any number of load cases can be used to identify and include the loading situation in the solution. The same factor and phase angle are applied to load parts for each and every load situation. Although there may be distinct load cases and phase angles, all loads have the same frequency.
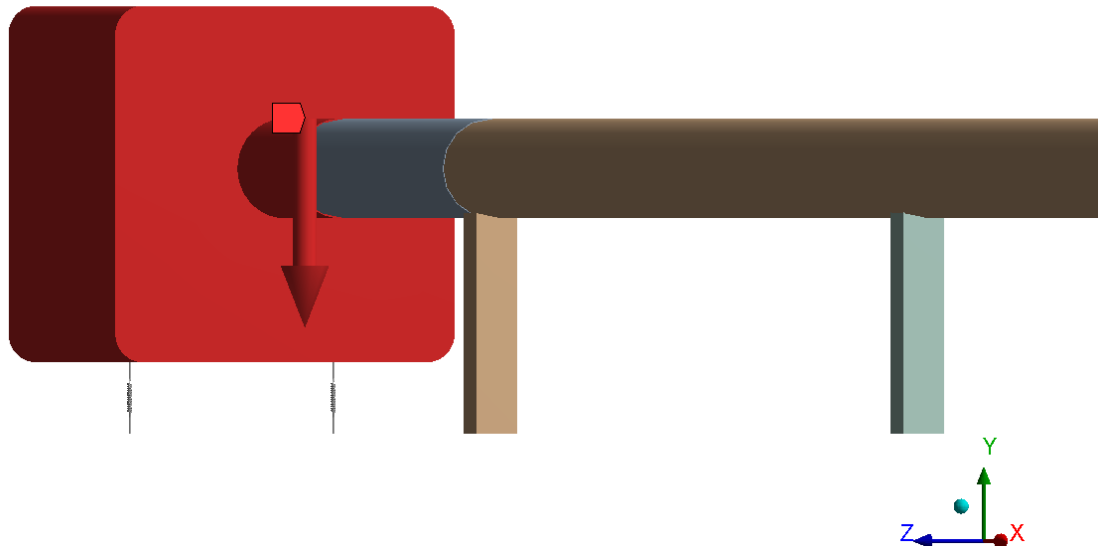

Figure 15: 1 N force applied on y-axes.

Base excitement   The structure is harmoniously excited at the specified degrees of freedom. Excitation is described by a displacement, velocity or acceleration directional vector. This sort of loading is especially helpful for modeling shaker table experiments, as the base nodes are often the places where nodal degrees of freedom are fixed.

Ansys mechanical offers the following solution methods for harmonic analyses:

Mode Superposition   The harmonic response to a specified loading situation is achieved for the *Mode Superposition (MSUP)* method by performing the required linear combinations of the specific solutions acquired from a Modal analysis.

For *MSUP*, it is an advantage to select an existing modal analysis directly since the calculation of the eigenvectors is usually the most costly part of the method. In this manner, the eigenvectors could be efficiently reused by various harmonic analyse with distinct loading conditions.[5]

Full Method   Using the *Full Method*, the appropriate solution of the simultaneous equations of motion provides a harmonic response.

Therefore, the general technique of *Mode Superposition* is generally faster than the *Full Method*. As a vibration analysis takes place, simulation knows what the structure's natural frequencies are. The peak reaction will refer to the structure's natural frequencies in a harmonic analysis. The analytical configurations used to respond harmonically are given in Tab. 12 as follows:

Table 12: Ansys settings for harmonic response.

Frequency Spacing	Logarithmic
Range Minimum	0 Hz
Range Maximum	1000 Hz
Solution Intervals	100
Solution Method	Mode Superposition
Constant Damping Ratio	0,03
Modal Frequency Range	Program Controlled

In this section, firstly, the set-up of the *Finite Element Model* is presented, afterwards the comparison of node number and element type is tackled. Later on, the simulations are run in *Ansys Harmonic Response* with the *Modal Analysis* and lastly, the results are discussed for given topics as below :

- Clamp Location Analysis
- Compensator Length Analysis
- Compensator Type Analysis

6.1. FE model set-up

6.1.1. Modeling

The implementation of the *Finite Element Model (FEM)* is explained in this section. The model is set-up with software *Ansys SpaceClaim*. It is *3D* solid modeling *Computer Aided Design (CAD)* software that works coherently with *Ansys Workbench*. Initially the model created with the volume elements and the compensator used as mentioned in Sec. 5.
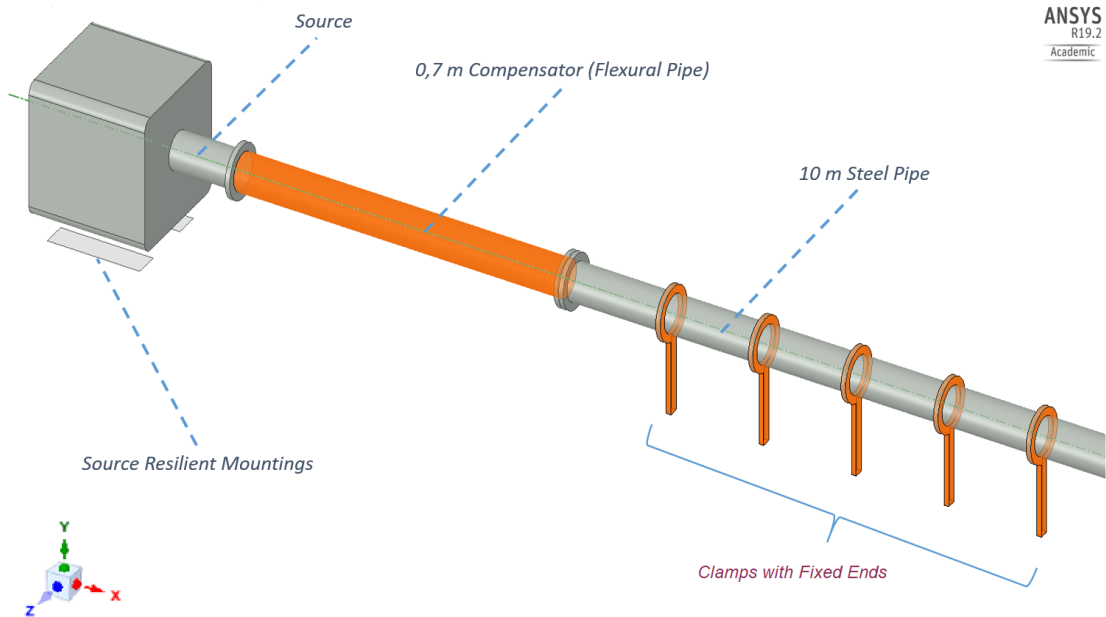
Figure 16: FE model in *Ansys SpaceClaim*.

6.1.2. Meshing

A precise consideration of the mesh quality can be build by sub-domains. In the analysis the model is split into smaller portion to increase the mesh quality. Compare to the whole sttructure the compensator has smaller element size. In this way, the mesh quality on compensator is increased as well.

According to the project task, two details for the mesh are considered. The difference for two models are shown Fig. 17.

Figure 17: Mesh optimization.

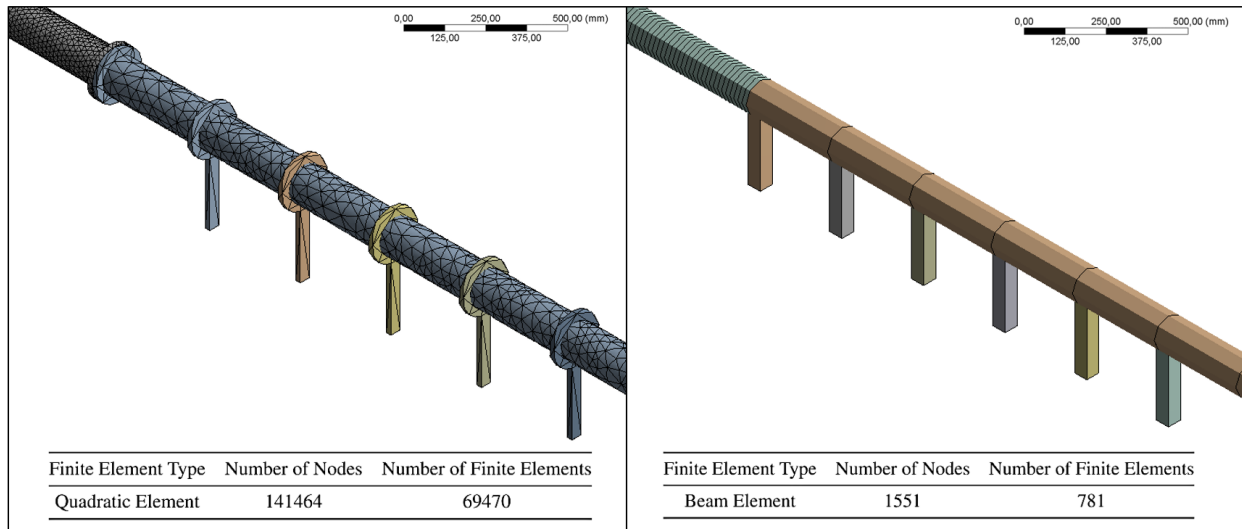The volume components are developed as a solid system, resulting in program creating a large amount of node and element number during meshing. Computation times are rise dramatically. Singularity issues occur extremely in links such as flange surfaces or pipe surfaces.

In order to reduce the computation time of the simulation; the pipes, clamps and flanges are simplified as beam elements instead of volume elements. This lead to number of nodes decrease dramatically. Moreover, the additional surfaces has been removed and the *Computational Time (CPU)* for modal solution decrease from $180 - 240$ second to $20 - 30$ second for each simulation.

6.1.3. Insert of Boundary Conditions

In order to represent the omitted sections of the pipe structure, some application of *Boundary Conditions (BC)* and the loads have been made. First *BC* plotted on the clamp foundations as fixed. Similarly the source resilient mountings which are springs in this case ; are fixed to the surfaces located below source.

During *Harmonic Analysis*, 1 N force applied on noise source in $y - axes$. The clamps and pipes are not rotation restricted. The mechanical and material properties are defined in Sec. 5 .

6.2. Clamp Location Analysis

6.2.1. Clamp Optimization

Pipe clamps are often seen as simple elements used for the connection and fixation of pipes. In case of existing piping, friction based clamps could offer an alternative approach if their design is proven and the occurring loads can be transferred without sliding.

In Ansys, pipe is connected to the supports only by *Manual Contact Region* which basically bonding clamp to pipe consisting of top and bottom parts. A number beam elements provide the necessary force transmission and friction on pipe structure . Main dimensions, mesh properties and boundary conditions of clamps are given Fig. 18 below :

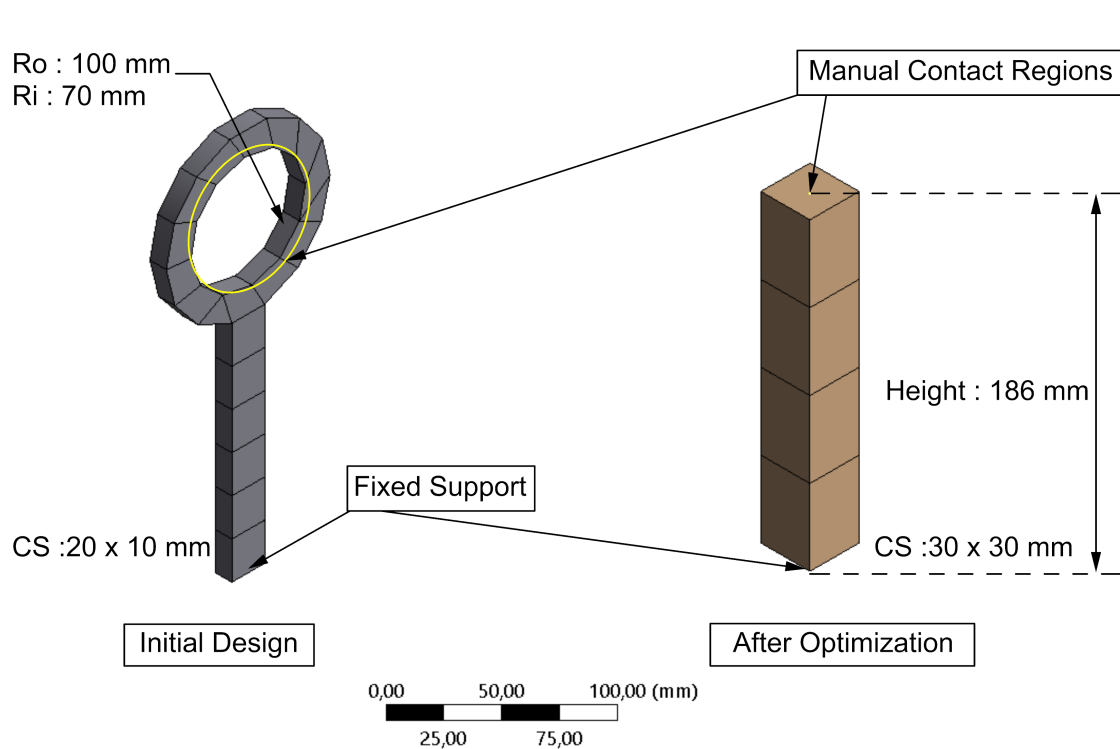

Figure 18: Modeled clamps.

For choosing optimal clamp dimensions (thicknesses, widths, number, diameters, etc.) are set of design rules has been developed. Therefore the optimization on clamps with increase of cross section area and fewer element numbers. The computational time for each simulation is relatively reduced due to number of used elements decreased dramatically for each clamp.

6.2.2. First Clamp Location Analysis

Today, the average clamp distance is around 2 or 3 meter long. However, due to analyse force effects on small displacements, the pipe structure contains 10 stationary clamps which are located at each one meter after compensator in this thesis. However, the location of the first clamp still undefined and the effect of the first clamp location on force transmission from source is still remained unanswered.

To answer this question, the pipe structure has modeled with first clamp which is located in five different location. These locations are *0 mm, 200 mm, 400 mm, 600 mm, 800 mm* away from the 350 mm long compensator. The reaction force at the clamp support is converted to *Force Level* by expressing in decibels below.[26]

$$F = 20.\log \frac{F}{F_0} \;\; [dB] \quad where \;\; F_0 = 1\,N \tag{12}$$

In Ansys, *Frequency Response* is added with force reactions at fixed points. The reaction values are converted into levels and plotted for each scenario. The black curve represent the force at the foundation of the source. The colored curves represent the force level at fixed clamp end in 5 different location. The first clamp location and the force level analysis of each case are show from Fig. 19 to Fig. 23 below:

Figure 19: First clamp location-level analysis with 0 mm distance from compensator.

Figure 20: First clamp location-level analysis with 200 mm distance from compensator.
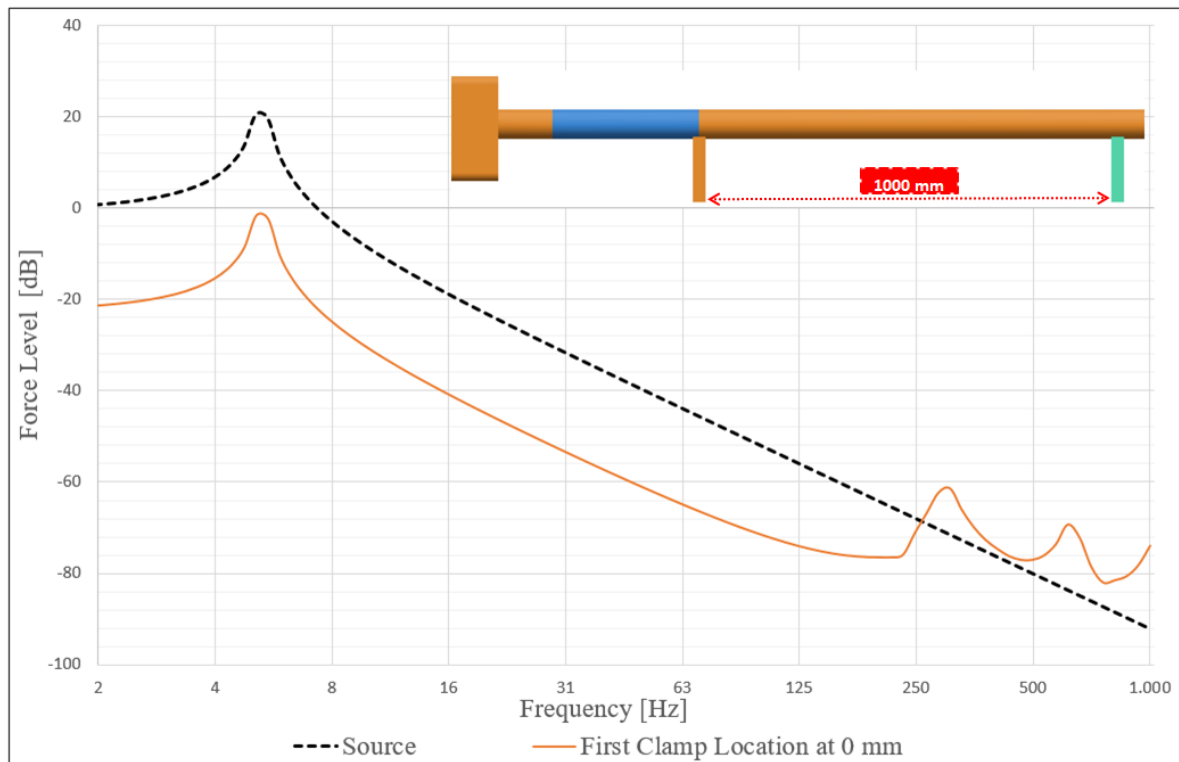

Figure 21: First clamp location-level analysis with 400 mm distance from compensator.
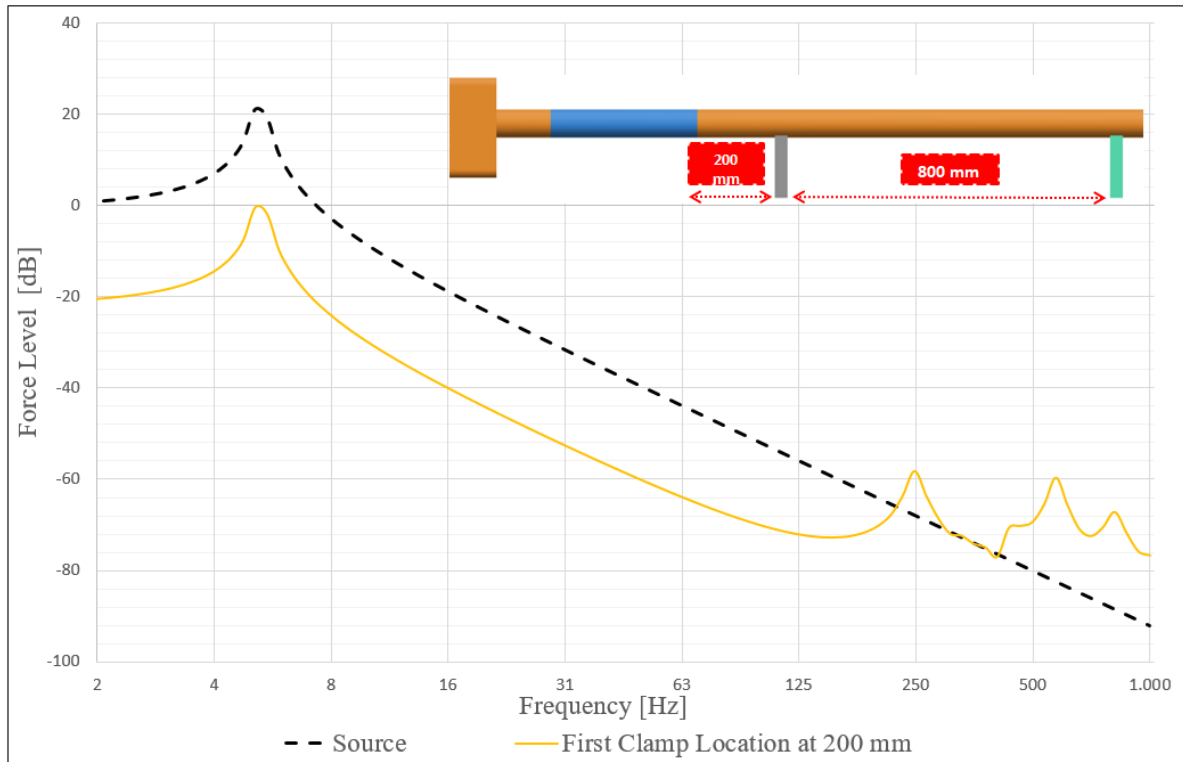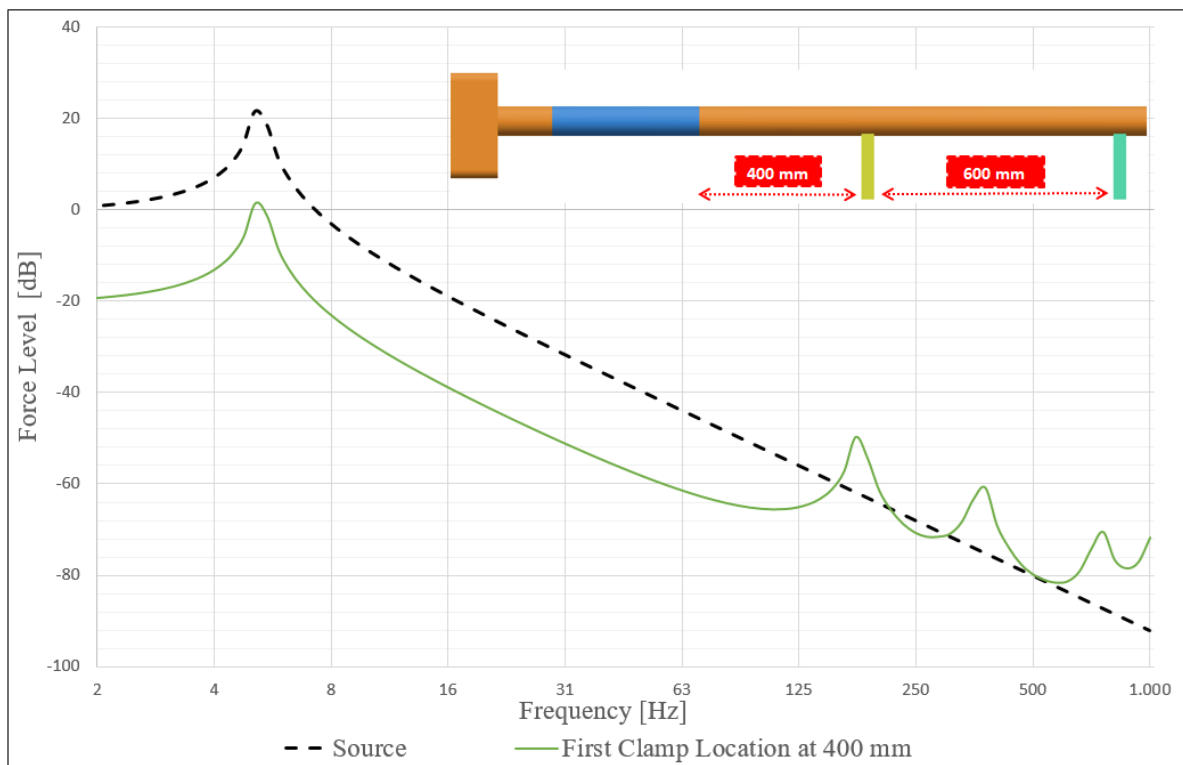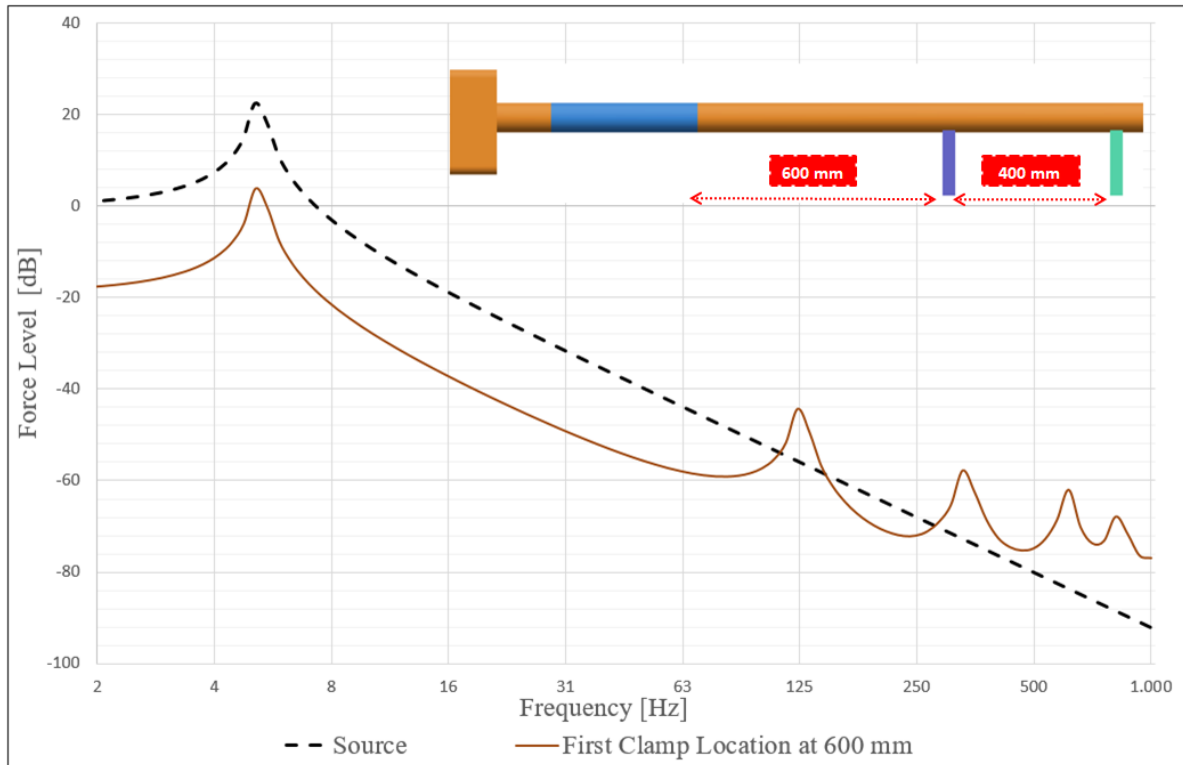
Figure 22: First clamp location-level analysis with 600 mm distance from compensator.
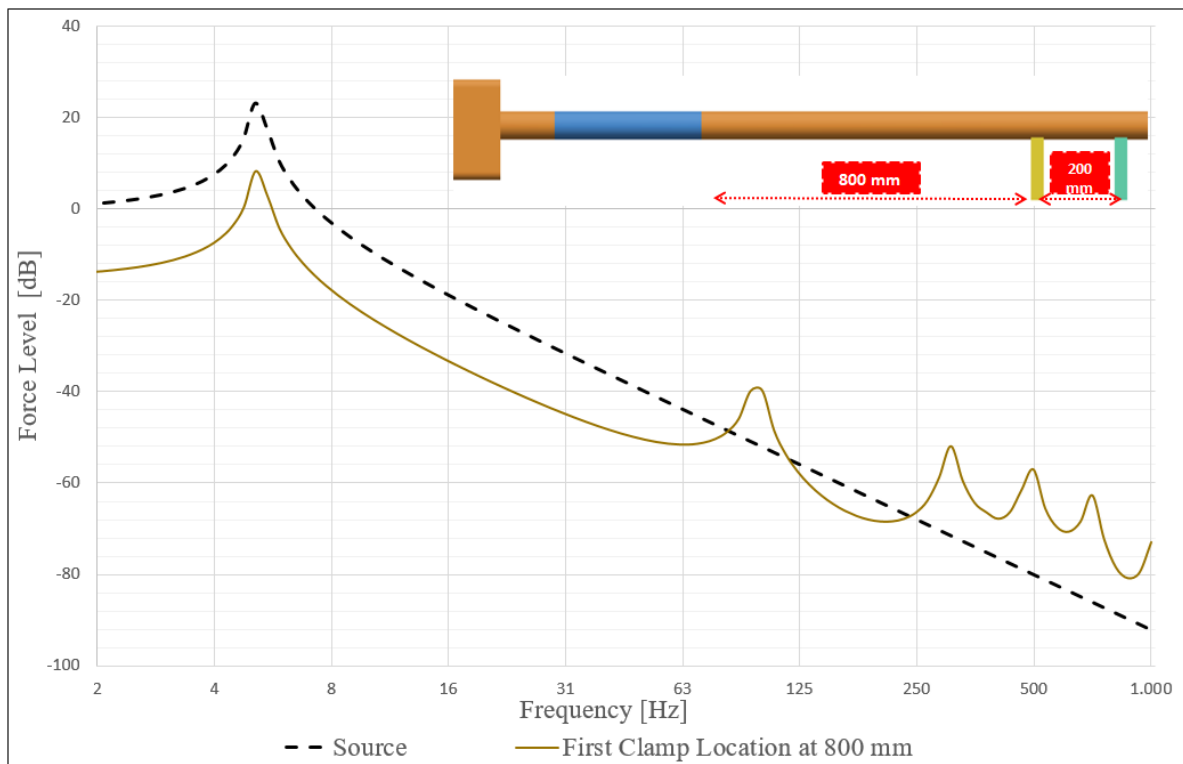

Figure 23: First clamp location-level analysis with 800 mm distance from compensator.

The force levels are showed above with respect to frequency. The peak force levels are loaded at the natural frequency of the source. For five different structure, the source support force levels are relatively similar. The reason for this similarity is the overall stiffness at the source mounts is not influenced by the different pipe connections, because of the small stiffness of the compensator. In the Sec. 4 the reason for chosen noise mass was pointed on this consideration. Source weight above two-tonnes, the natural frequency and force responses on source mounts is not effected largely.
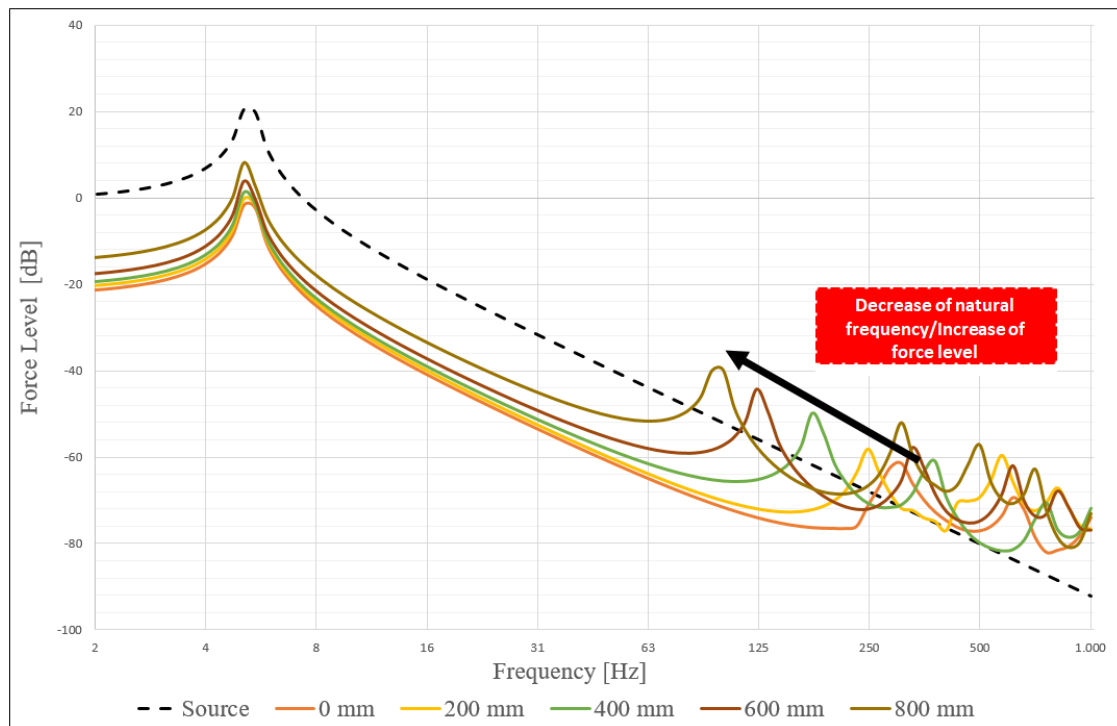
Figure 24: First clamp location-level analysis.

Due to source support force reactions are being relatively similar for each simulation, in the final chart only one source support force level is stated. The location of the first clamp can effect the overall force level seriously. Greater distance of first clamp from compensator results in greater force levels. However, the natural frequency of system is decreases with distance from compensator.

After the first natural frequency of pipe structures the force levels are similar independent of clamp distance. The clamp position can be selected according to the character of the *Structure-Borne Noise* level on the source.

The optimum location for first clamp shown in numerical solution which has highest resonance frequency and lowest force level on the given clamp support. The final figure shows that 0 mm verify the desired conditions.

6.2.3. Clamp Distance Analysis

In the previous section the first clamp location has been varied within different locations. After first clamp location is set to *0 mm* from the *350 mm* long compensator which mean right top of the joint of steel pipe and compensator, first three clamp reaction forces compared with the each other. The next figures shows the force levels at the first three clamps compared with the source force level.
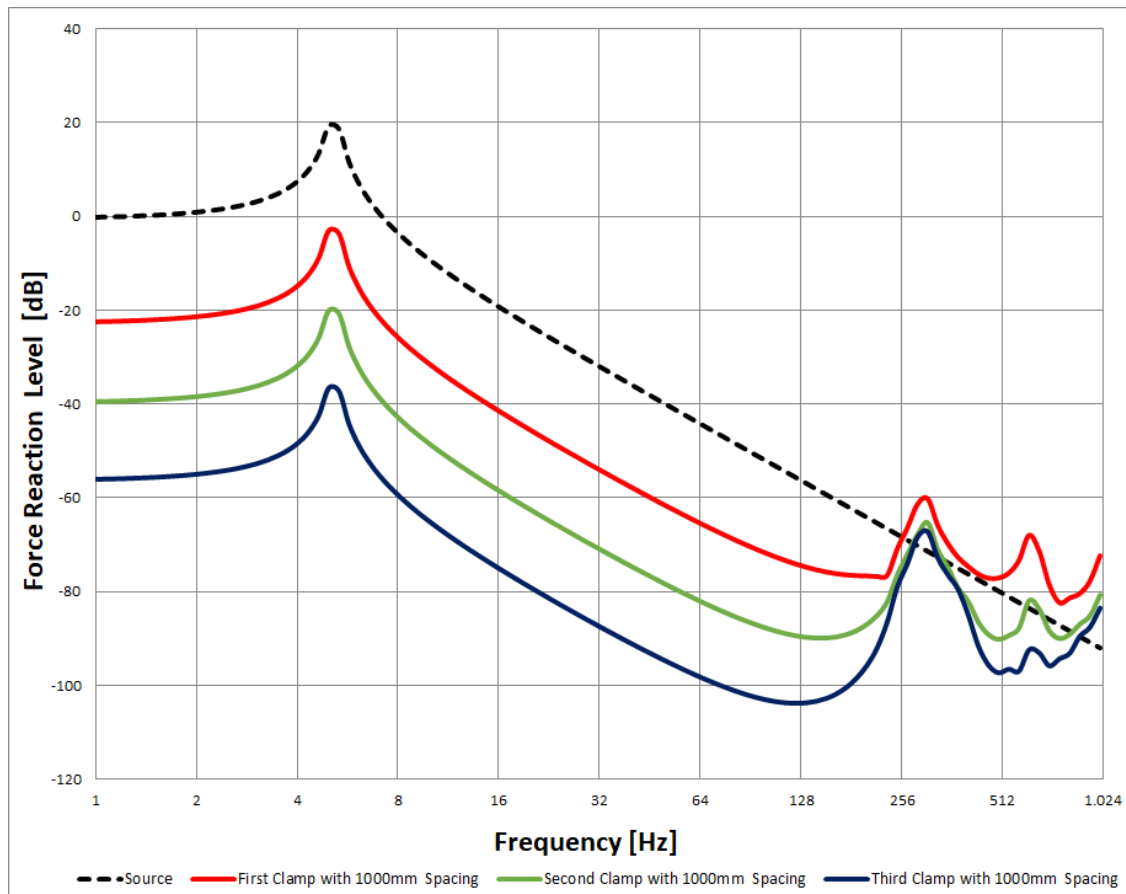
Figure 25: Force levels on clamp while the distance is 1000 mm between each clamp.

The overall pipe structure is considered with one meter clamp spacing with other calculations. The Fig. 25 show the clamps reaction force levels for one-meter spacing between each clamp. If the the reaction force distribution could shown with percentage; it would be stated that the source has over *90%* of overall force reaction and *8 %, 1%, 0,1%* are clamps percentage respectively.

At second and third clamp the force levels are relatively small and not significant to take into considerations up to *250 Hz*. While the spacing is increased to *2000 mm* and *3000 mm* the force reaction levels on each clamp stated in Fig. 26 and Fig. 27.

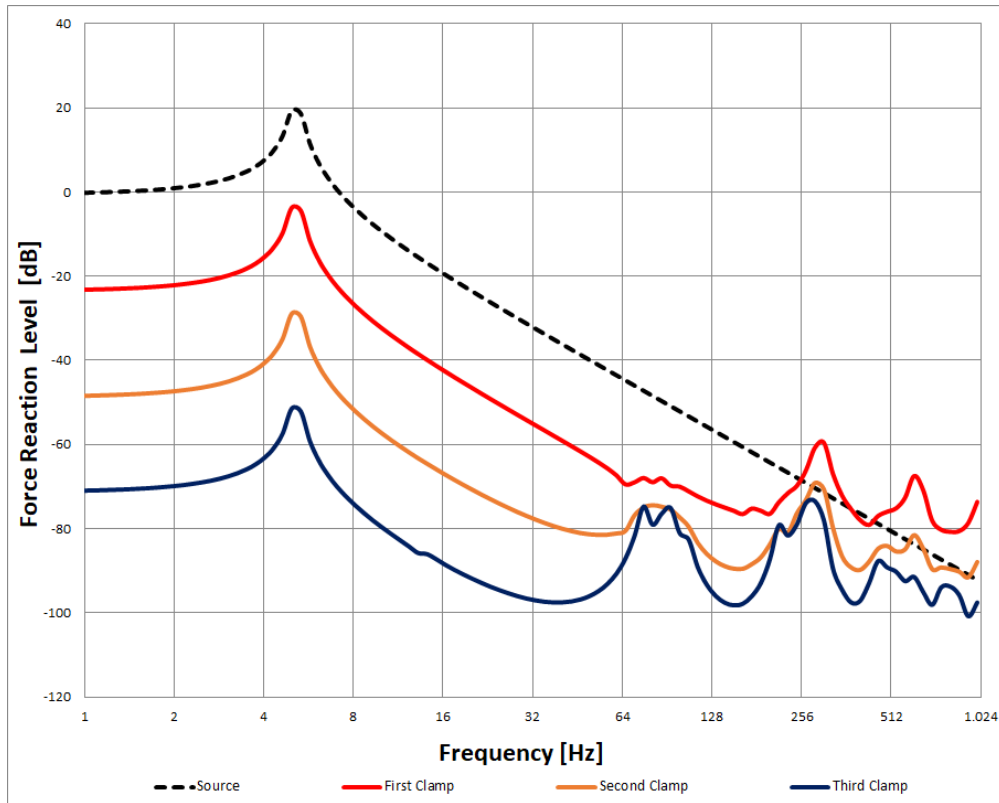**Figure 26:** Force levels on clamp while the distance is 2000 mm between each clamp.
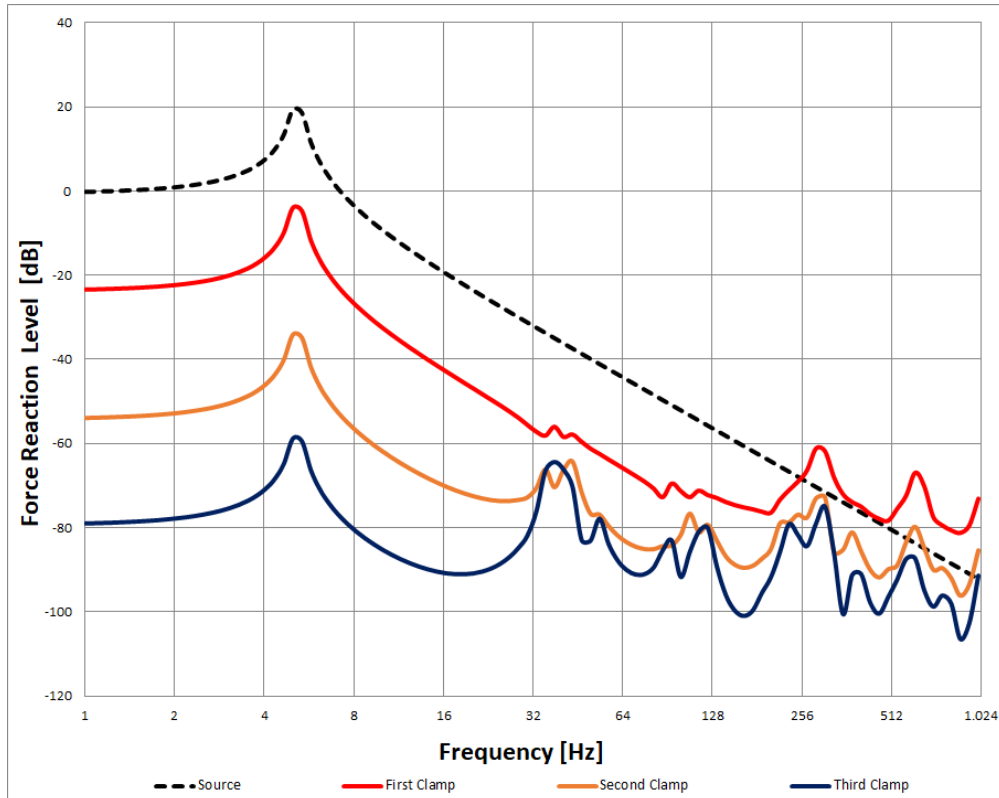
Figure 27: Force levels on clamp while the distance is 3000 mm between each clamp.

The larger spacing result in lower force levels on second and third clamps. However the first clamp reaction forces are relatively higher. It is interesting to state that the clamps after first clamp has no longer high resonance frequencies as *1000 mm* spacing. Also there are new natural frequencies will occur due to the steel pipe which located between these clamps. The last graph shows the first clamp force reaction levels for different spacing in Fig. 28 below:
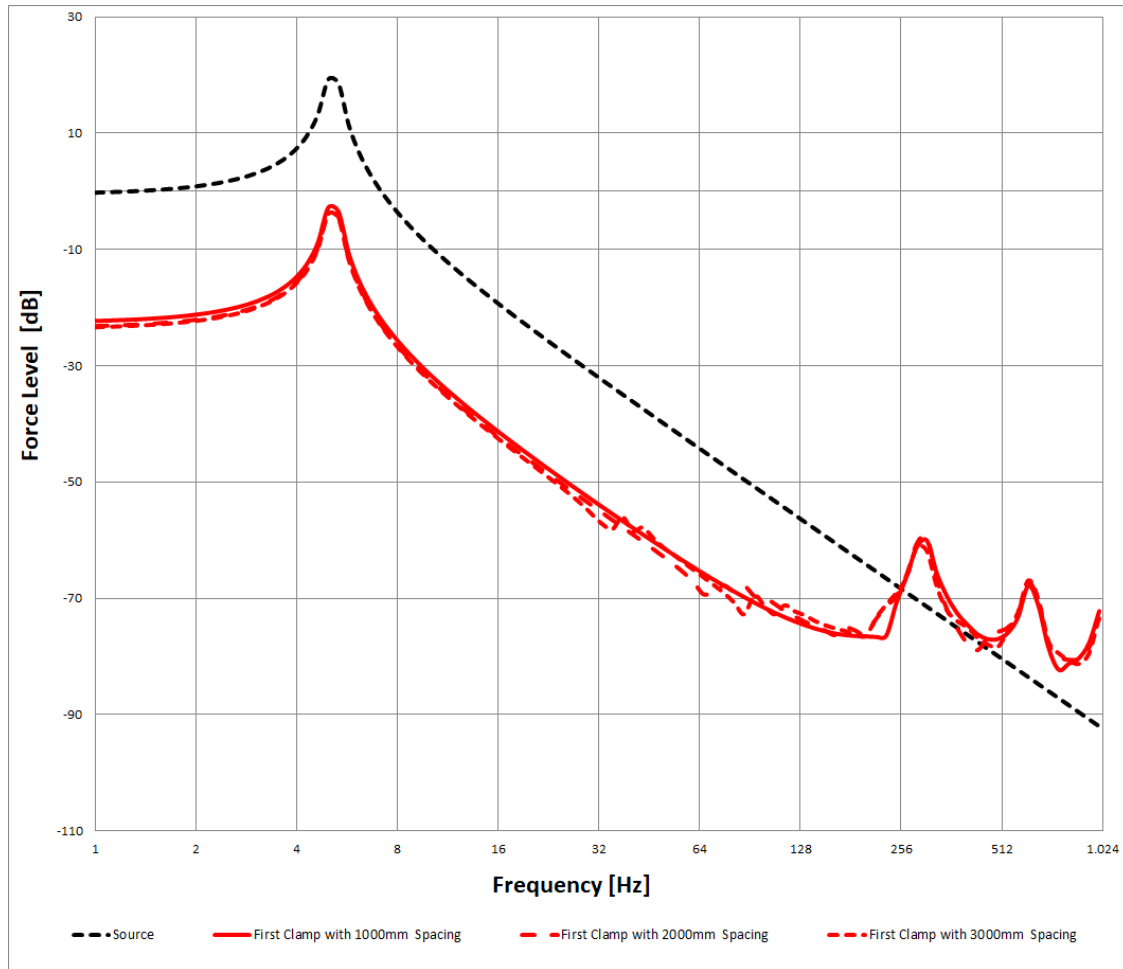
Figure 28: First clamp force levels for different spacing.

The levels for three different spacing is relatively similar. It is shown that first clamp in selected location is no longer under effect of the clamp spacing. There are only minor fluctuations due to the steel pipe natural frequency. That is the fact that analysing the first clamp location will be significant effect on the structure.

Also clamp locations are no longer important at natural frequency which is around *250 Hz* due to similar force levels for all cases. The second and third clamp reaction force levels are approximately *20 dB* drop due to different clamp spacing. The graphs for second and third clamp is shown in App. A.

6.3. Compensator Length Analysis

After the location of the first clamp is set, three different sizes of a linear compensator are modelled and compared. All modelled compensators are linear and have same mesh type.

First compensator is taken as *720 mm* long which is designed due validation of mechanical characteristics of compensator in Sec. 5. This compensator already test analytically and numerically.

Moreover, the *720 mm* is not practicable length in some cases. The second compensator is chosen due to length of common compensator length in today's machinery piping environment. It is taken as *350 mm* length which is also used for the evaluation of first clamp location analysis at Sec. 6.2.

Lastly the length is set for *210 mm* long which is considered as 3 times long the diameter of compensator. The factor three is general pipe length ratio in Ansys. The comparison is shown in Tab. 13. The outer radius, inner radius, density, elasticity modulus, unit mass and cross section areas are same as previous compensator properties and rest is compared below:

Table 13: Mechanical properties of three different length of linear compensator.

	720 mm Compensator	350 mm Compensator	210 mm Compensator
Volume [m^3]	1,36E-03	6,60E-04	3,96E-04
Moment of Inertial I [m^4]	8,72E-07	8,72E-07	8,72E-07
Beam Radial Stiffness [N/m]	2,30E+04	2,00E+05	9,26E+05
Beam Axial Stiffness [N/m]	2,15E+06	4,42E+06	7,36E+06

The table shows that the cross section areas remain same for three compensator and the differences for radial and axial stiffness of the each compensators stated above. Used formulas for Radial and Axial Stiffness is :

$$k_r = \frac{12EI}{l^3 \times F} \tag{13}$$

$$k_a = \frac{EA}{l} \tag{14}$$

Radial stiffness of three compensators are lower than the axial stiffness of the compensator in general. This is due to cubic force of the length in inversely proportional with radial stiffness. More accurate values for radial stiffness can be calculated using advanced computer programs.

As it seen from table the radial and axial stiffness are inversely proportional to the length of the compensator. Radial stiffness is also important for evaluation of stiffness ratios between three modal and noise source. Ratios are shown in Tab. 14 below :

Table 14: Stiffness ratios between source and different compensator lengths.

	Source /720 mm Comp.	Source /350 mm Comp.	Source /210 mm Comp.
Stiffness Ratios	5,37	0,62	0,13

The greater length has lower stiffness which results in greater stiffness ratio. According to this comparison, force levels are expected to be higher at shorter compensators and their supports. This expectation will be verify during comparison of force level tables showed in next charts. The importance of the first clamp location is mentioned in Sec. 6.2 previously.

The force level and frequency responses for selected clamp locations are compared from Fig. 29 to Fig. 31 below:
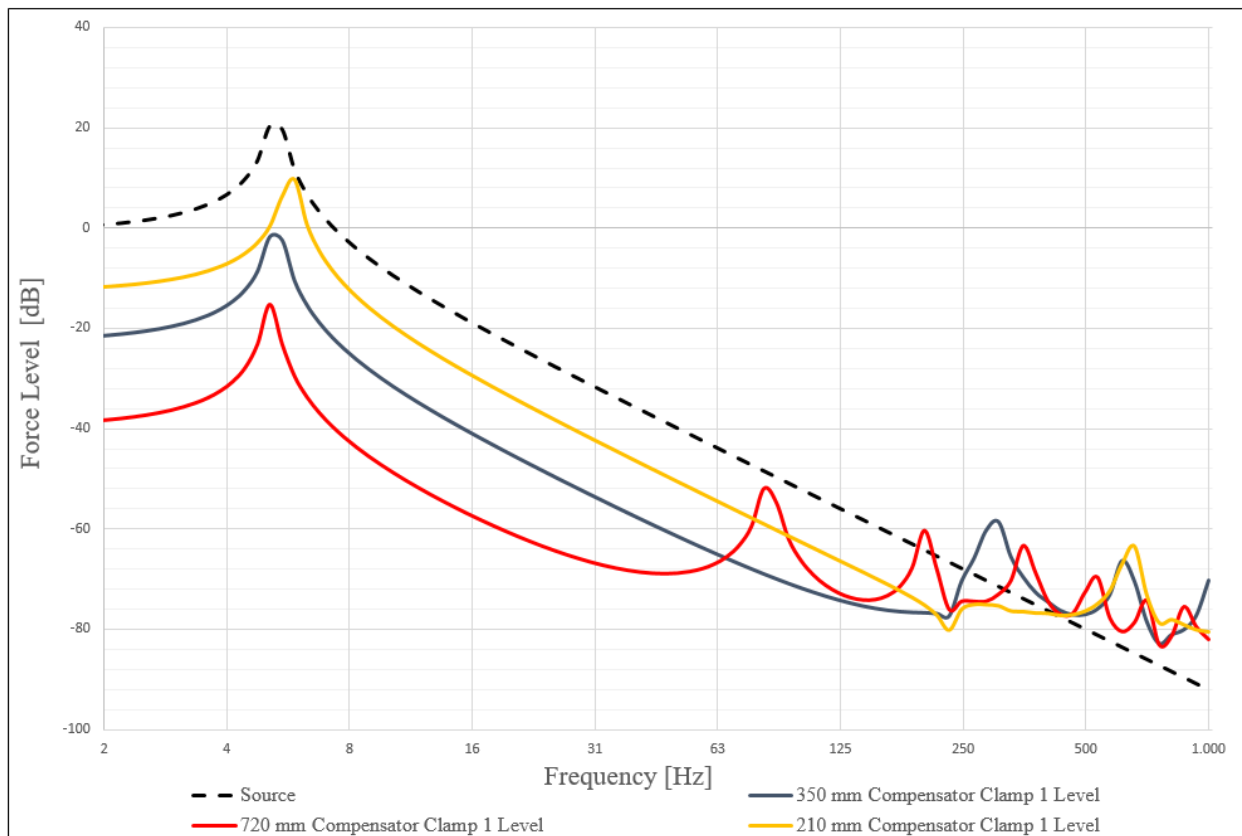

Figure 29: First clamp force levels for three different compensator length.
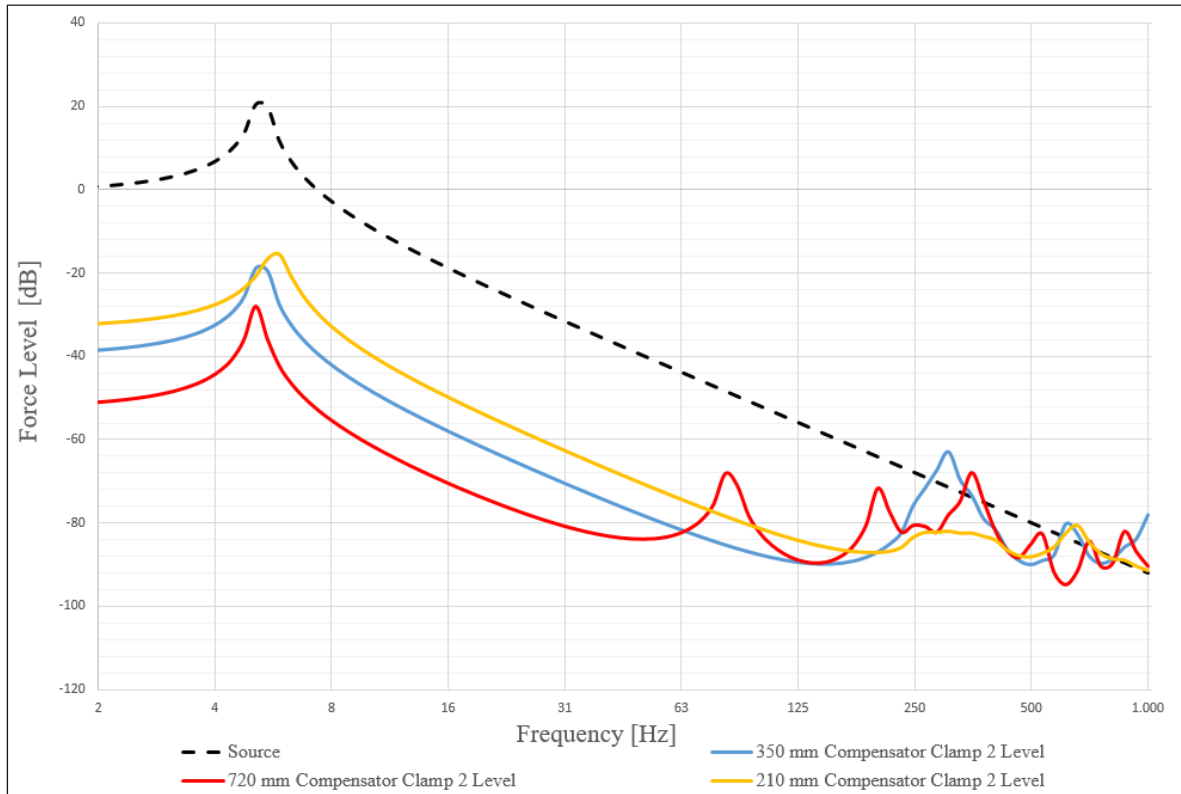
Figure 30: Second clamp force levels for three different compensator length.
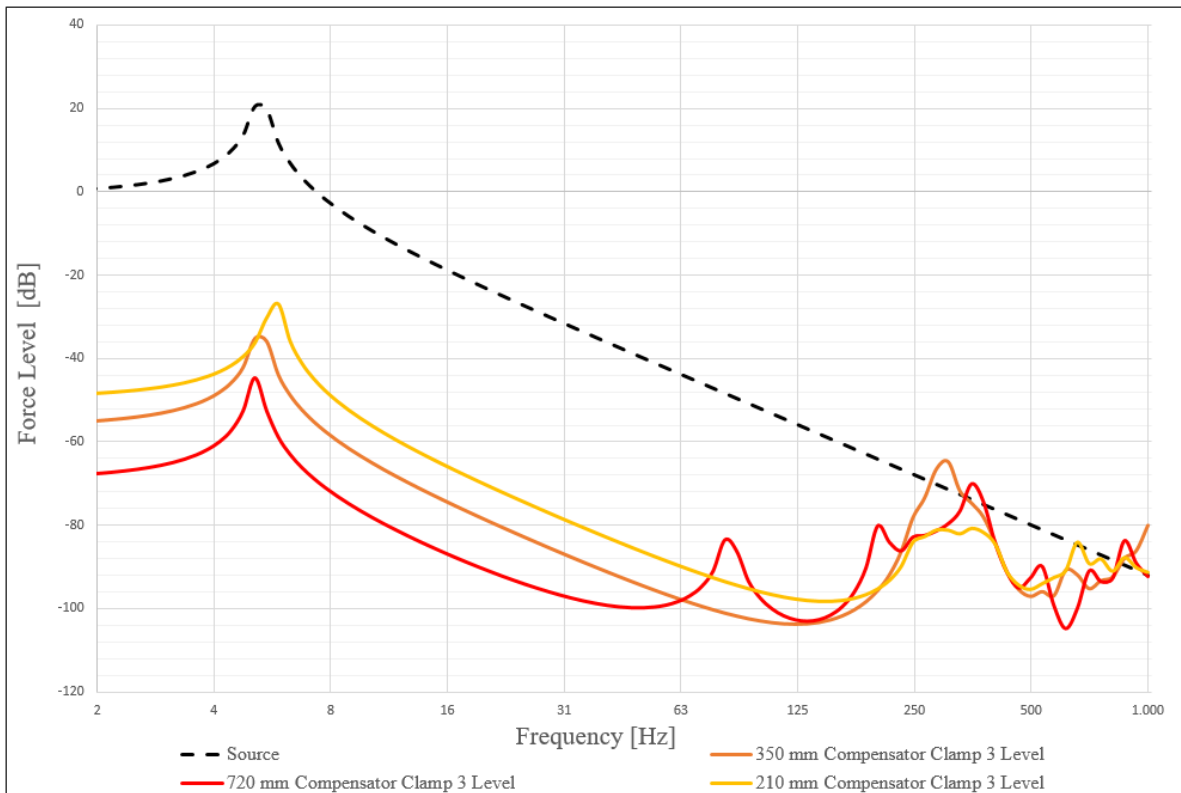
Figure 31: Third clamp force levels for three different compensator length.

The force levels are same for source since the main characteristics are remain the same. However the compensator length has an effect on the resonance free frequency range directly.

The shorter compensators transmit higher reaction forces to the clamps. Due to the higher stiffness of the compensator the natural frequencies occurs in higher frequencies.

With the longer compensator the force levels are lower at low frequencies but the frequency range where transmission via the piping systems dominates shifts to lower frequencies.

The force levels are dramatically reduced at second and clamps which are located 2 and 3 meters from linear compensator. However, above *250 Hz* , force level are no longer under effect of clamp locations. The levels are similar due to the high number of resonances.

6.4. Compensator & Clamp Type Analysis

The importance of the first clamp locations and compensator length are showed in previous sections. The analysis showed above are considered as linear pipe structures where the noise source, compensator and the steel pipes are connected along with $x-axes$.

However, since the machinery rooms are constrained by limited space, the pipe structures can not be designed as linear consistently. In this section, most common pipe structures are modeled through Ansys *SpaceClaim* and analysed with *Mode Superposition*. The considered pipe structures are typical in practice and given as :

- Linear Compensator *350,750,210 mm* length
- Bended Compensator *350,750 mm*
- Dog-Leg Compensators with *210 mm*
- Linear Compensator *350 mm* with Resiliently Mounted Clamps

In the Sec. 6.3 the Linear compensator with different length already evaluated and compared with the each other. The new pipe structures are analysed individually and the results are compared with each other in following section. Each structure analysed with same noise source properties and same harmonic load on given source.

6.4.1. Bended Compensator

The Bended compensators are use in special ships. It is such a useful pipe connections where the pipe lines had to be bended due to design rules or limiting spacing. For instance *REIFLEXA* is one of the company is producing bended compensators today and the typical outfitting of the compensator is shown in Fig. 32 below :

Figure 32: Bended compensators.[22]

The aim to designed such a compensator as stated above is to observe structural behaviour of compensator with respect to its pipe structure during harmonic analysis. The mechanical properties for selected bended compensators are given below :

Table 15: Two bended compensator comparison.

	Bended Compensator 1	Bended Compensator 2
Rotation Degree [°]	90°	90°
Arc Length [m]	0,72	0,35
Outer Radius [m]	0,035	0,035
Inner Radius [m]	0,025	0,025
Density [kg.m^-3]	2500	2500
Elasticity Modulus [Pa]	8,20E+08	8,20E+08
Cross Section Area [m^2]	1,88E-03	1,88E-03
Volume [m^3]	1,35E-03	6,57E-04

The two arc length is set for the bended compensators due to compare linear compensator analysis that hold before. First bended compensator is set for 720 mm long which is designed based on mechanical characteristics of compensator in Sec. 5. The second compensator is taken as 350 mm length which is also used for the evaluation of first clamp location analysis in Sec. 6.2.

It is important to chose these two arc length values in order to standardized for both linear and bended compensator.Bended compensator with 350 mm arc length is show Fig. 33 below.
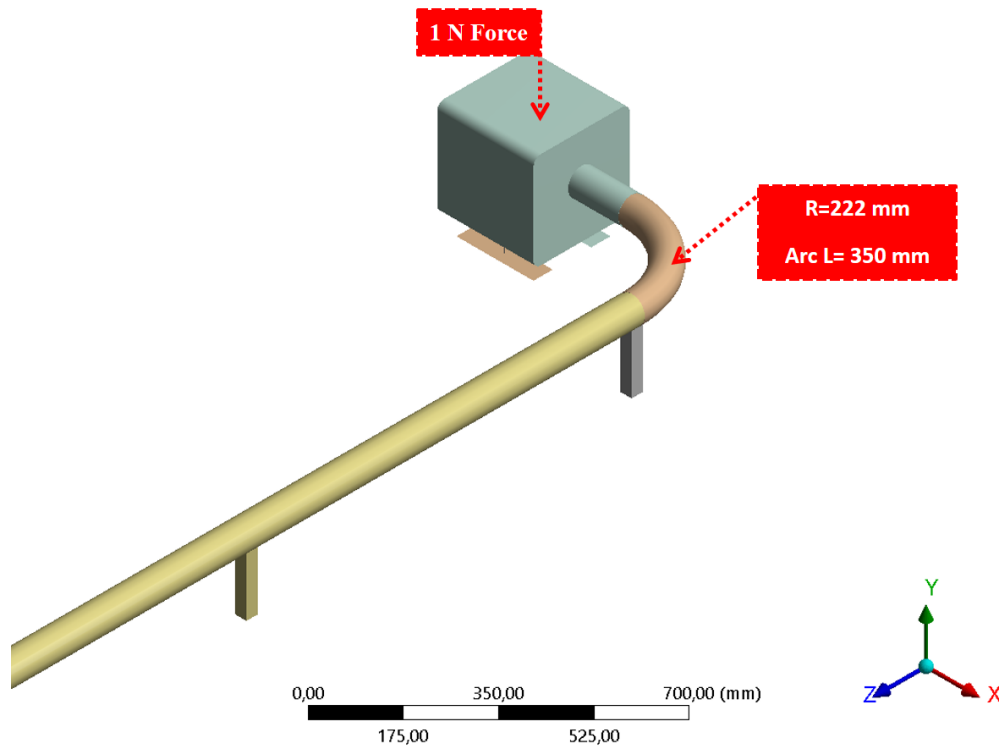
Figure 33: Bended compensator section.

The noise source and clamps remain same positions with respect to linear pipe structure analysis. The number of clamps and length of the steel pipe remained same. The mesh settings are applied identical for each pipe structures where the compensators has 10 *mm* element size and the rest solved with 200 *mm* element size. The Boundary Conditions, reference system and mechanical properties of the structures remain same.

After mesh and boundary conditions are applied on pipe structures, the force levels are evaluated by reaction force action on first three clamps. The force level and frequency chart for two sizes bended compensator showed Fig. 34 below :
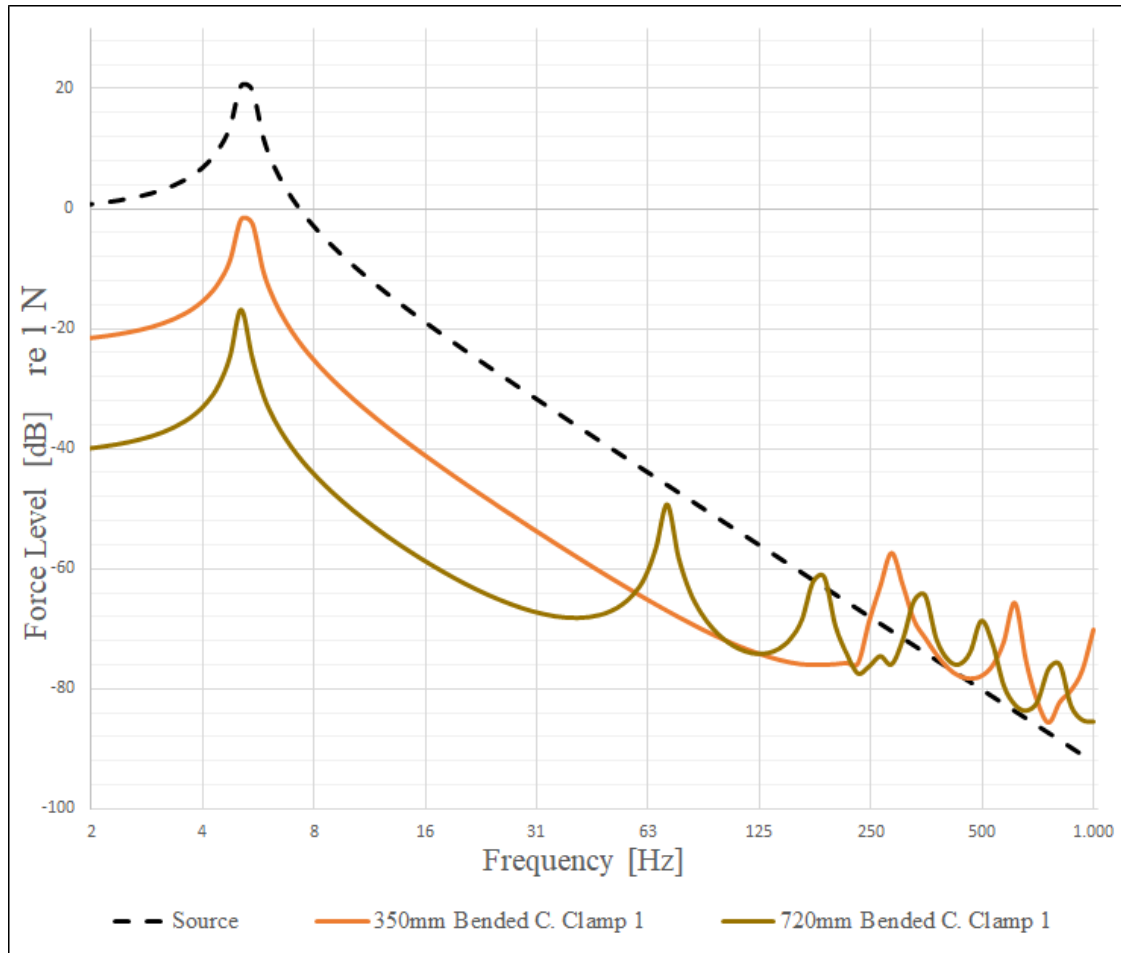
Figure 34: Bended compensator clamps force levels.

The results show that the compensator arc length has a similar effect on bended compensators as linear ones. Longer compensator reduces the systems natural frequencies dramatically. Resonance frequencies occur early stages of solution as 65 *Hz* in case use of 720 *mm* long bended compensators. However the resonance frequencies occur above 200 *Hz* when 350 *mm* long compensators used.

Above frequency of 250 *Hz* the compensator lengths are not important anymore as already observed in linear pipe structure cases. Also the force levels are reduced dramatically after first clamp. The force level- frequency graphs of the first three clamps are showed in App. B for both 350 *mm* and 720 *mm* long compensator.

6.4.2. Dog-Leg Compensator

The focus of the Dog-Leg Flexible Compensator is a simple design as the bended compensators and used in many applications with increased motion capabilities of pipe structure. The compensator is designed to withstand large and irregular movements such as might be caused by tough sea conditions. The desired structure sample and common uses in industry is show Fig. 35 below:
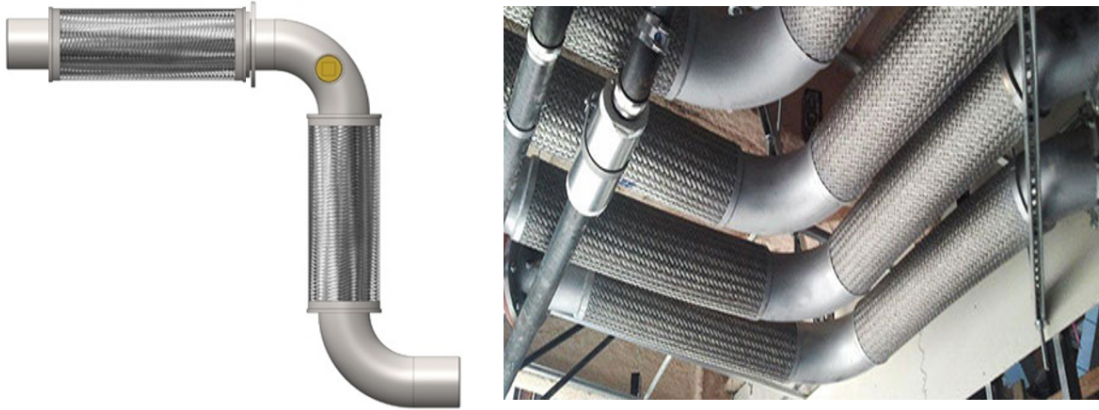
Figure 35: Dog-Leg compensator samples.

The model was conducted numerically using finite element modeling and harmonic simulation. The model used for harmonic analysis is defined Fig. 36 below:
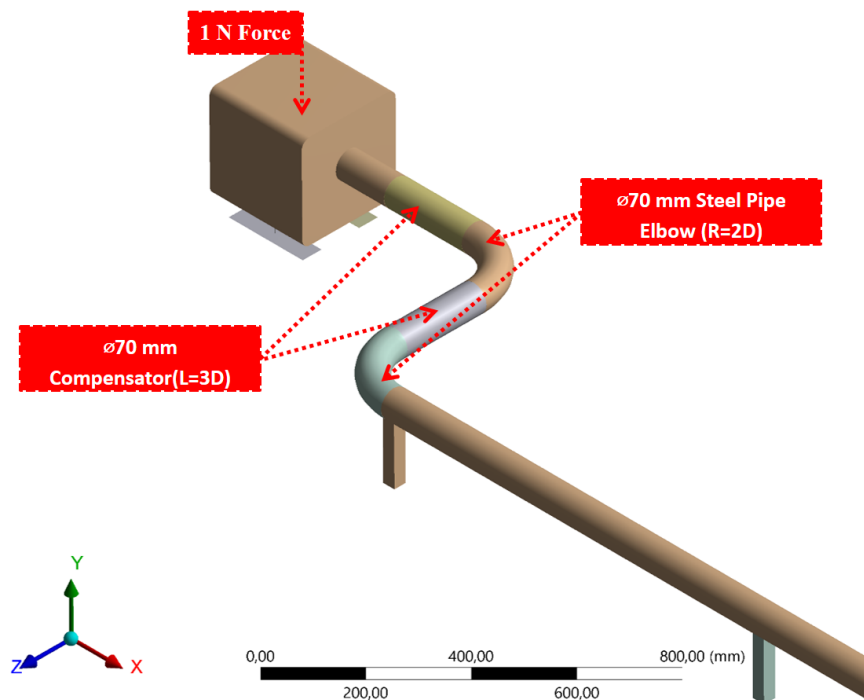
Figure 36: Dog-Leg compensator section.

The compensators are designed with same cross section area. The mechanical properties of the steel pipe and noise source remained same with the clamp spacing.Since there are no desired clamp or support located on the bended steel pipe connections,initial stiffness expectation of the system was lower than the linear and bended compensator pipe structures. Due to the fact that the systems need to be comparable with each other , the compensator length selected as 210 *mm* which is relatively shorter than the other systems.

The force level and frequency chart for two sizes Dog-Leg compensator showed Fig. 37 below :
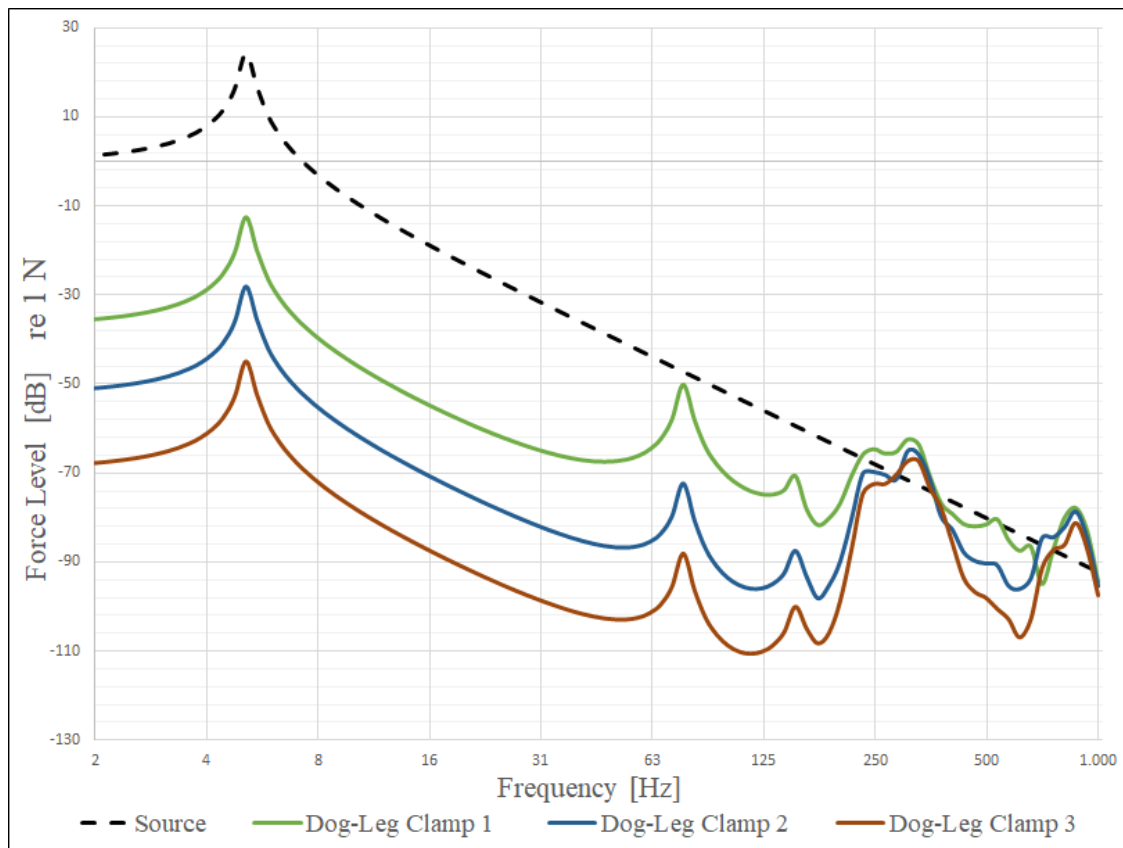
Figure 37: Dog-Leg clamps force levels.

The force levels at the first three clamps are lower than in previous solutions. Due to the fact that two compensators are used, the new levels are reduced but the resonance frequencies remained similar.

It is also important that the resonance frequencies are not effected much since there are no clamp or support located on the steel pipe elbows on the structure. Reduction of the compensator length should result in increase of structural stiffness but longer overall pipe structure with no support located until clamp 1 balanced overall stiffness as indicated linear and bended pipe structures before.

6.4.3. Resiliently Mounted Linear Pipe Structures

In all analysis are hold before, the pipe is supported by pipe clamps to transfer the load to the ship structure. These attachments were assumed rigid. When the system was installed at ambient temperature, all of the floors assumed part of the load distribution.

In the next step the clamps are mounted resiliently. General expected pipe excitation for ship structures is between *0,5- 3 mm* approximately. In this thesis the pipe excitation is constrained as *1 mm*. *10 meter* steel pipe and 0,35 meter linear compensator mass is read by using Ansys *Modal Analysis*. Totally 10 spring are located with *1 meter* spacing which use in analysis before. Finally the resilient support properties are showed Tab. 16 below :

Table 16: The resilient support properties.

Pipe Total Mass [kg]	51,216
Deflection [m]	0,001
g [m/s^2]	9,81
Spring Stiffness Total	502428,96
Number of Springs	10
k_{clamp} [N/m]	50242,896

Since the mass of the pipe structure is smaller compared to the noise source and the number of clamps are 5 times higher, the stiffness of the resilient clamps are relatively lower than the stiffness of springs used for noise source.
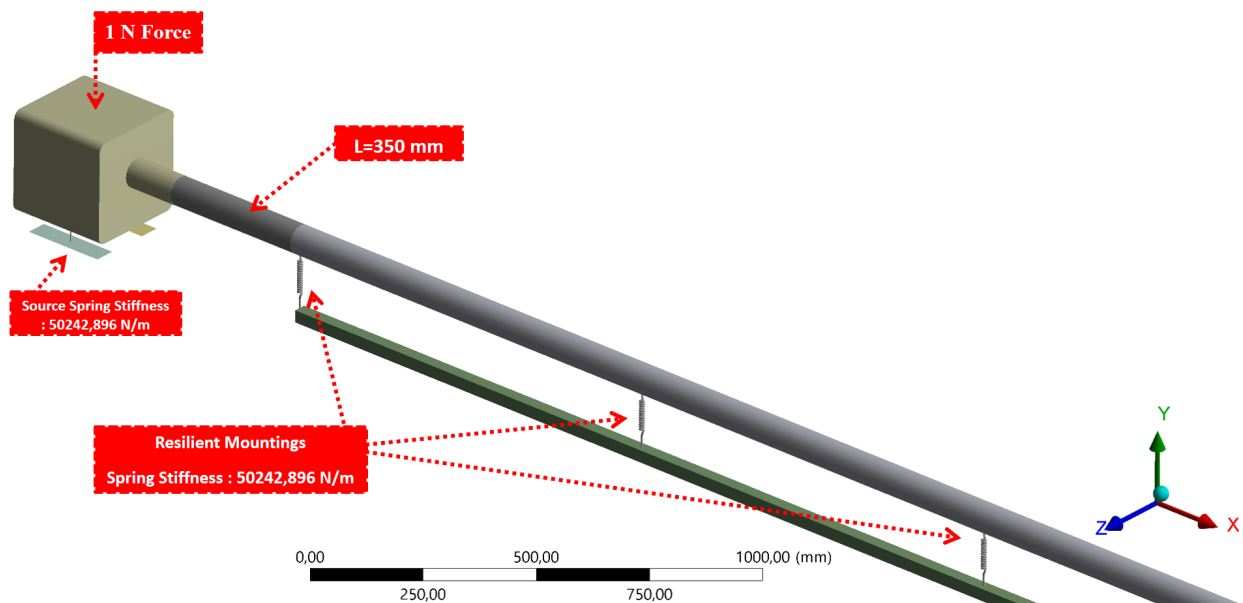

Figure 38: Resiliently mounted spring clamps.

Fig. 38 shows that the pipe structure is designed with the linear 350 *mm* compensator where all the clamps are changed into spring elements. These spring elements represents the new resiliently mounted clamps.

Resilient springs provide variable lifting force during pipe deflection. Force levels for first three clamps shown in Fig. 39 below :
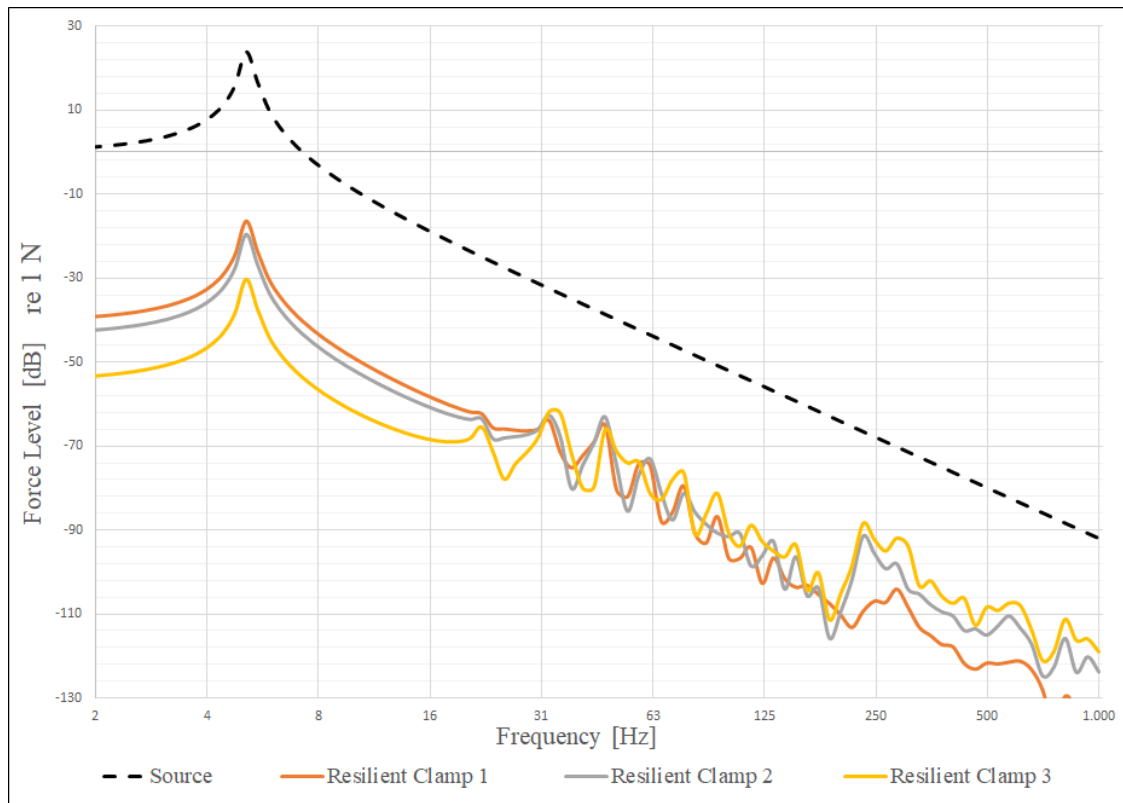
Figure 39: First three Resiliently mounted clamp force level.

The expectation of spring (resilient) mounting on support to provide a reduction in the structure borne noise on supports. Resilient mounted supports isolate the pipe structure from the bed-plate which means that the noise transmission should be reduced effectively.

However, the results show that if there are spring mountings, the load shifts completely as soon as it exceeds the small initial deflection of the first spring connection and this leads to the fluctuation on force levels on clamps.

Neither clamp location nor compensator type effect the force level differences between new type of resilient supports. The structural natural frequencies are completely dominated by noise source.

6.4.4. Results and Comparisons

After all different type of structure is modeled through Ansys *SpaceClaim* and numerically solved with *Modal Analysis* and *Harmonic Response Analysis*, the results of the force levels on first clamps are compared for :

- Linear and Bended Compensators with length of *350 mm* and *720 mm*
- Dog-Leg with *210 mm* Compensators and Linear *210 mm* Compensator
- The Resiliently Mounted pipe and Linear pipe with *350 mm* and *720 mm* Compensators

The first Fig. 40 is important to show the force level and frequency comparison between Linear and Bended compensators. The selected compensator lengths are *720 mm* and *350 mm* for both compensator.
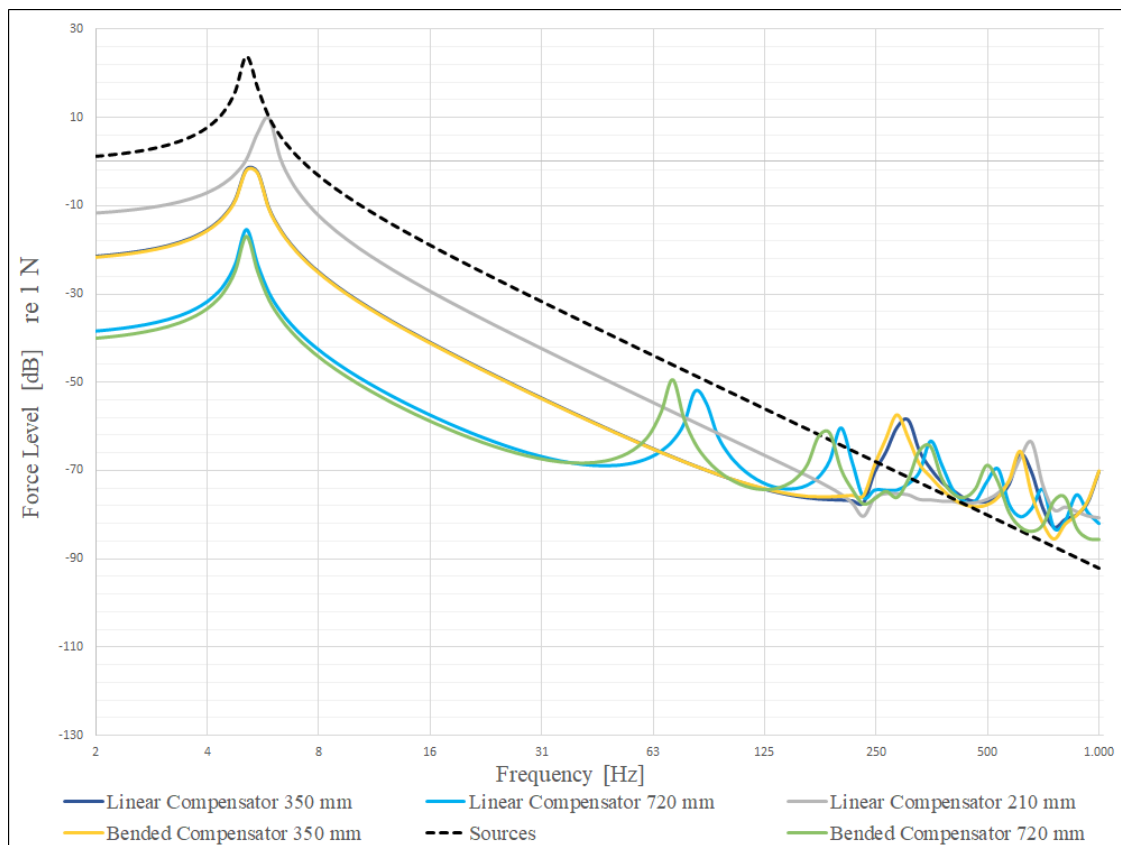

Figure 40: Linear and Bended compensators with *350 mm* and *720 mm* long.

The results are show that the linear compensator and 90°Bended compensators have similar force levels and resonance frequencies. This means that use flexible bends on pipe structures in narrow spaces or the connections where the linear structures will not fit.

For shorter compensators the results are identical and consistent. There is a small differences for longer compensator which is *720 mm* long. The Bended pipe structure has slightly lower resonance frequencies. This result might important in case of high pressure type of compensator design.

Next graph indicates the comparison between Linear and Dog-Leg compensators. The force level and frequency range of selected compensators are shown in Fig. 41 below:
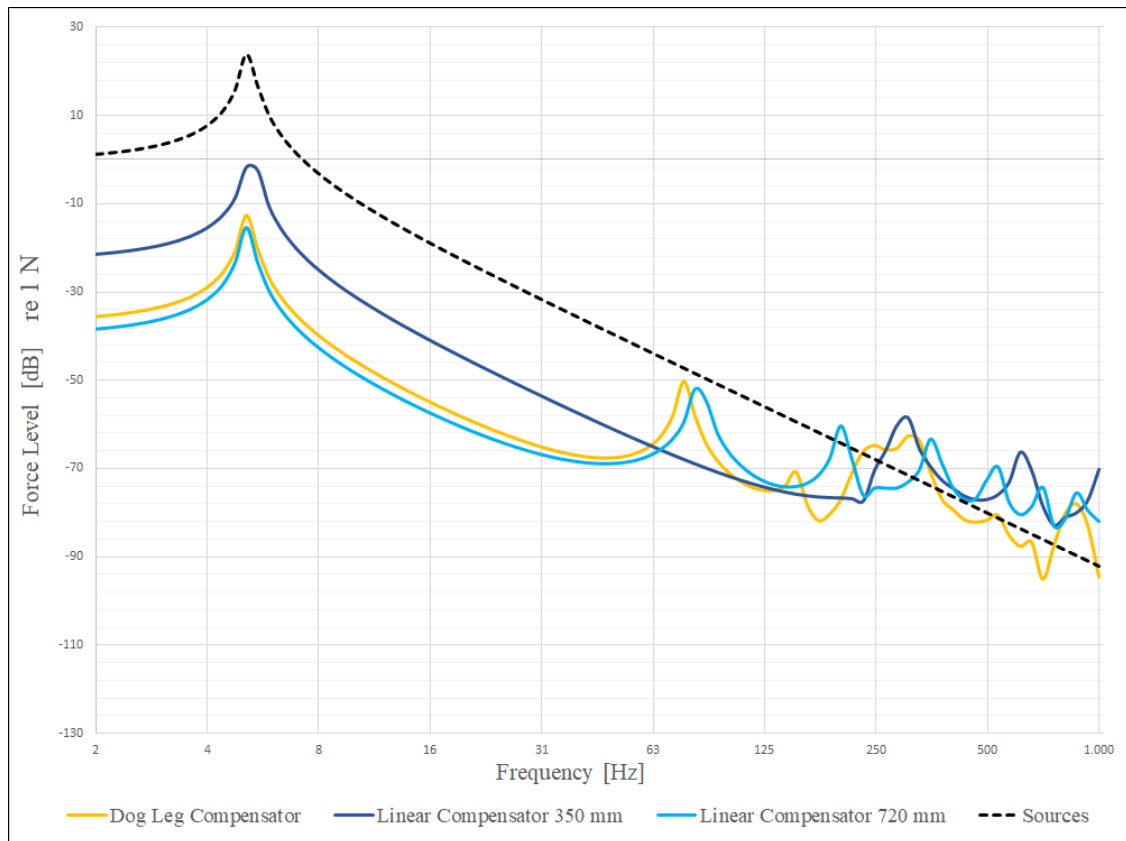
Figure 41: Dog-Leg with *210 mm* Compensators and Linear *210 mm* Compensator

The results show that the Dog-Leg compensators have lower resonance frequencies. Since the total compensator section length is longer than other two linear pipe structure, the force levels matched with the expectation.

Another outcome shows that even if the Dog-Leg pipe section designed with two *210 mm* long compensator, the results are relatively similar with the linear pipe structures with *720 mm* long compensator. This coherence shows that the ships with relatively long *High Pressure Compensator (HPC)* can re-designed with *210 mm* long two compensator and this might increase the feasibility of pipe structure in case of the limited spaces and realistic compensator length use in today ship building industry.

Furthermore, last pipe structure that compensator remained same but the clamps are changed with resilient spring is compared with the same linear structure but rigid clamps below:
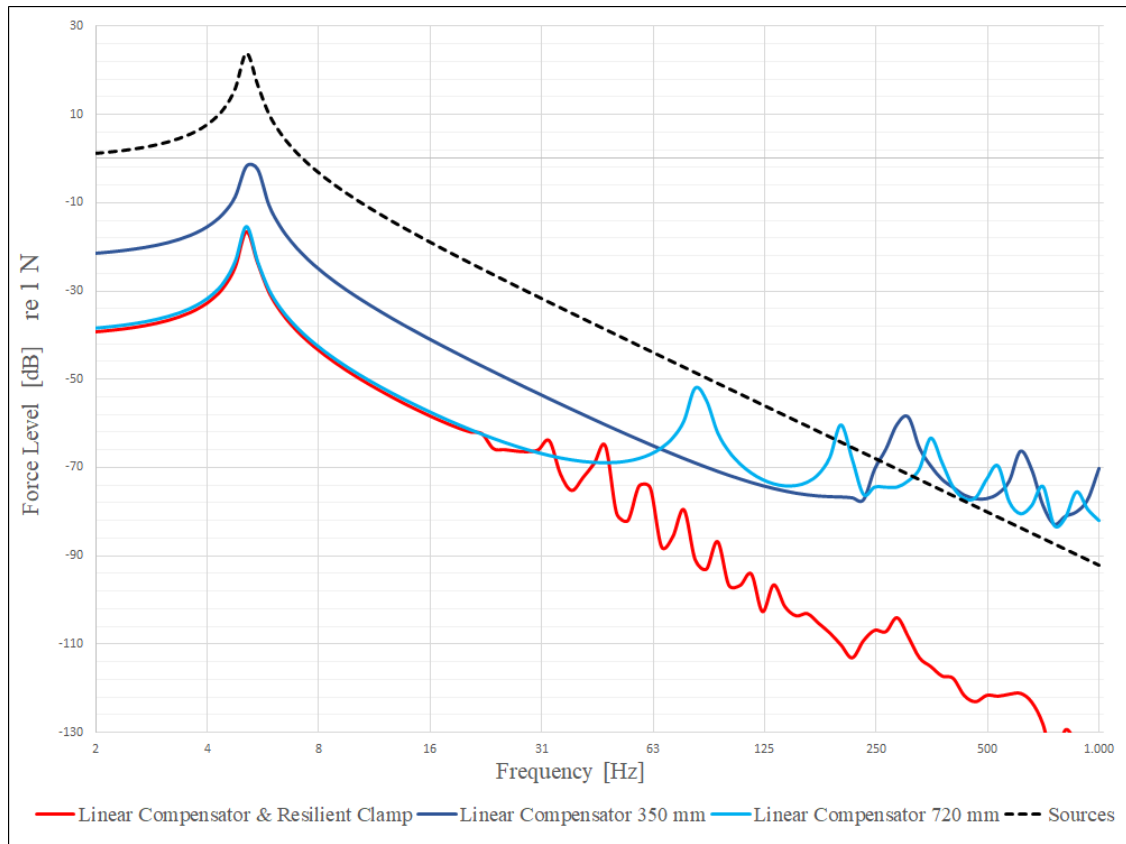
Figure 42: The Resiliently mounted pipe and Linear pipe with *350 mm* and *720 mm* compensators.

At lower frequencies the resilient spring structure has similar path with the linear pipe structure with *720 mm* compensator long. However the path similarity due to the same harmonic response of the identical noise sources acting on both structure.

Clearly the resilient mounted clamps are completely source force level dominant systems. The fluctuations on the curve occurs due to the spring systems located under *10 meter* steel pipe and the natural frequency of the pipe directly leads the noise fluctuations. However the structure is no longer under effect of compensators. Moreover, the *10 meter* long steel pipe will not lead any higher force levels on the whole structure due to its resonance frequencies.

The last Fig. 43 show the general force level and frequency comparison for all different designed pipe structures.

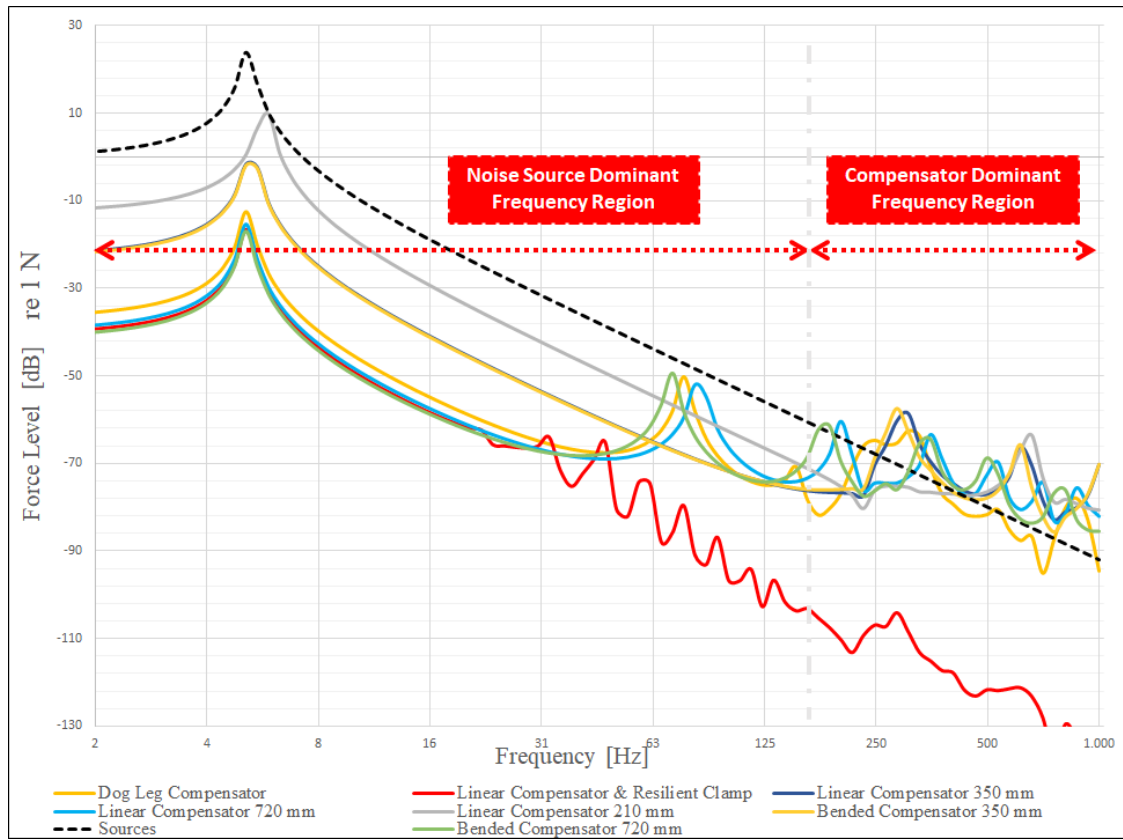**Figure 43:** Comparison of all type of pipe structures.

The relationship between the noise source and the compensators described by the graph above. Bold line separates the zones, which are under either source dominance or compensator dominance. The noise source force level curves are relatively same for each structure since there is no difference for harmonic response on noise source.

According to this graph, Linear and Bended system have similar harmonic responses. Bended systems slightly has lower natural frequency for compensators. Furthermore, Dog-Leg systems follows a similar curve characteristic path as the Linear *720 mm* compensator. Since Dog-Leg structure has two compensators located between the source and the first clamp; the force levels is lower as longer compensators.

Another point state that the structures are no longer under effect of compensators where resilient mounting acting on clamps. It is important to remember that these graphs are valid only for given specific pipe characteristics and designed pipe structures.

7. Case Study : Piping Study of Special Vessel

7.1. Introduction

If ships need to fulfill high requirements on onboard or underwater radiated noise, a noise consultant will usually assist with comprehensive investigations on noise sources and transmission paths. In this case study the noise transmission from a generator engine through a pipe (e.g. cooling water) into the structure was examined.

The following case study was done on a ship which features high demands on confidentiality. Due to that reason, no information can be given on the ship, its purpose, its age or the building yard.

Figure 44: The isometric view of machinery pipe structure.
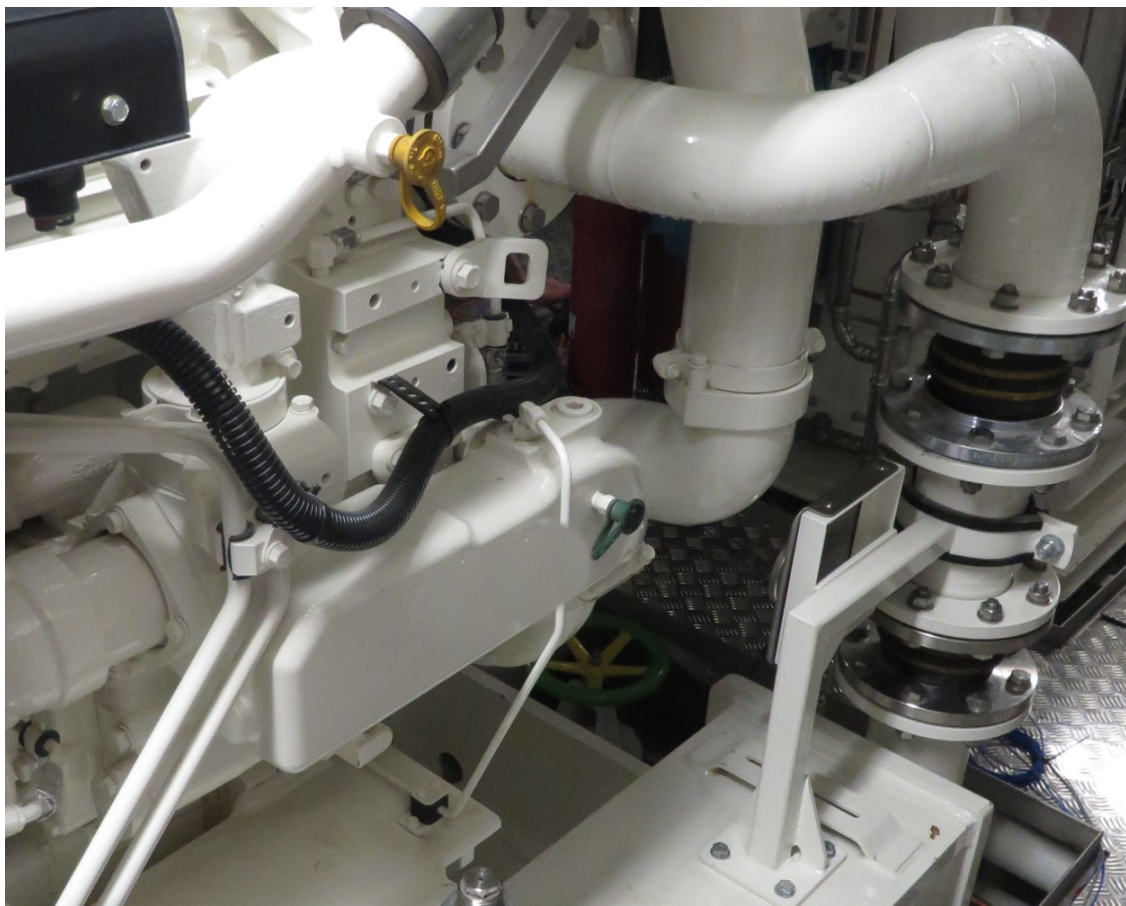
Firstly, test measurement considered to define the Structure Borne Noise transmission. Afterwards, analysis with the *FEM* tool *Ansys Harmonic Response* is carried out. Different set-ups for the *Finite Element Analysis* are tested to afterwards compare the results. Additionally, optimization and recommendations are proposed to improve the noise transmission performance.

7.2. Measurements

Before the measurements the company provide a briefing with the engineers about the strategy and measurement techniques. The hammer test was hold to define the *Structure Borne Noise* transmission. All the measurements were hold on-board of the ship.

This is often also known as Modal Testing. It is a method of testing that allows us to calculate the natural frequencies (modes), modal masses, modal damping ratios and mode shapes of a test structure.[12]

In theory, it would expect that impact the structure under test with a perfect impulse. This would be of infinitely short duration. This would result in a constant amplitude in the frequency domain. However, in real life, such an impulse is not possible. Instead, the frequency range is known.

The duration of this test is directly related to the force frequency. Hammer tests (modal testing) are usually performed with a unique hammer with a loading cell in its tip to assess the impact force. In this measurement, a standard hammer where load cell is not placed is used.
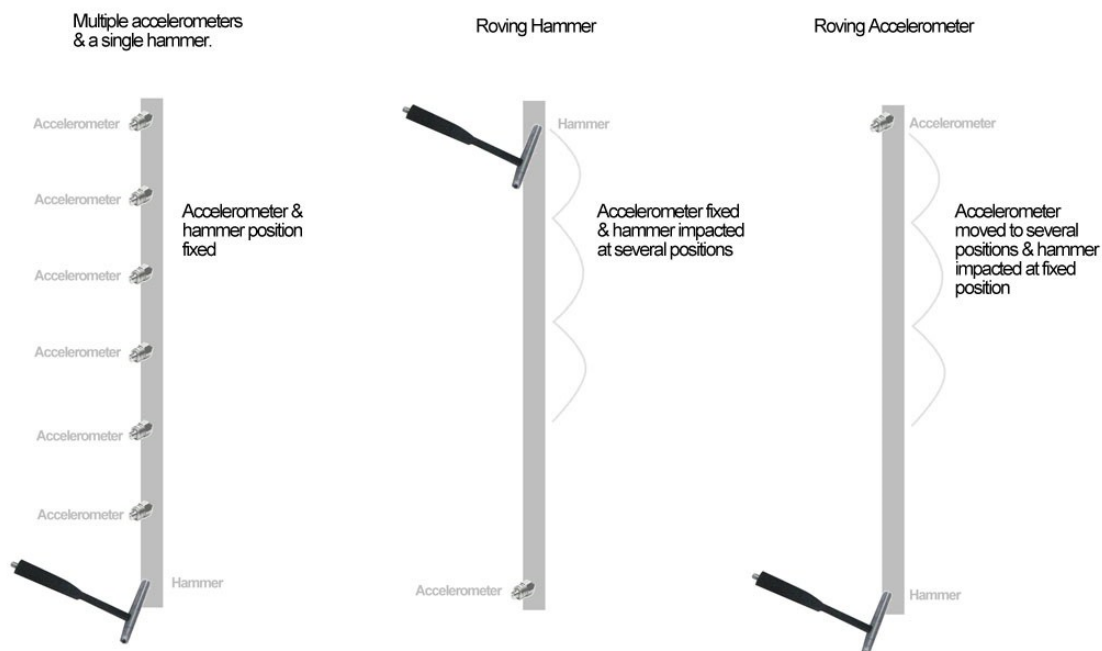

Figure 45: Three different way of hammer test.[12]

The Fig. 45 show the three common way of the hammer test which are:

- Set the accelerometers on the structure and the impact once at many positions. It's time-efficient because a single effect and data capture are required. In fact, to perform average, several impacts are held, but it is still a quick test. Nevertheless, it would take a big investment in transducers and an equally big investment in a measurement scheme with sufficient channels to record all reactions simultaneously.

- A single accelerometer can be fixed to one position and then structure has impact at several locations. This is known as a *'roving hammer'* test. This uses the least resources, but takes longer as we have to make several measurements. This is the most common form of hammer impact testing.

- The structure impacts at a fixed position and moves around several locations with a single accelerometer. This is referred to as a test of *'roving accelerometer'*. Although this remains effective in terms of transducers and measurement systems, it is less effective in time, since it takes time to move an accelerometer. This technique is generally used in circumstances where accelerometers can be fixed by space constraints, but there is not enough space for a hammer to be used.[4]

In this study, the hammer test placed with the first way which is stated above as multiple accelerometers and single hammer. The initial expectation was perform hammer test from the engine to the first clamp with single test location.

Since the pipe system is not linear and not rigidly supported; the system divided into three section and hammer test applied for each section individually.
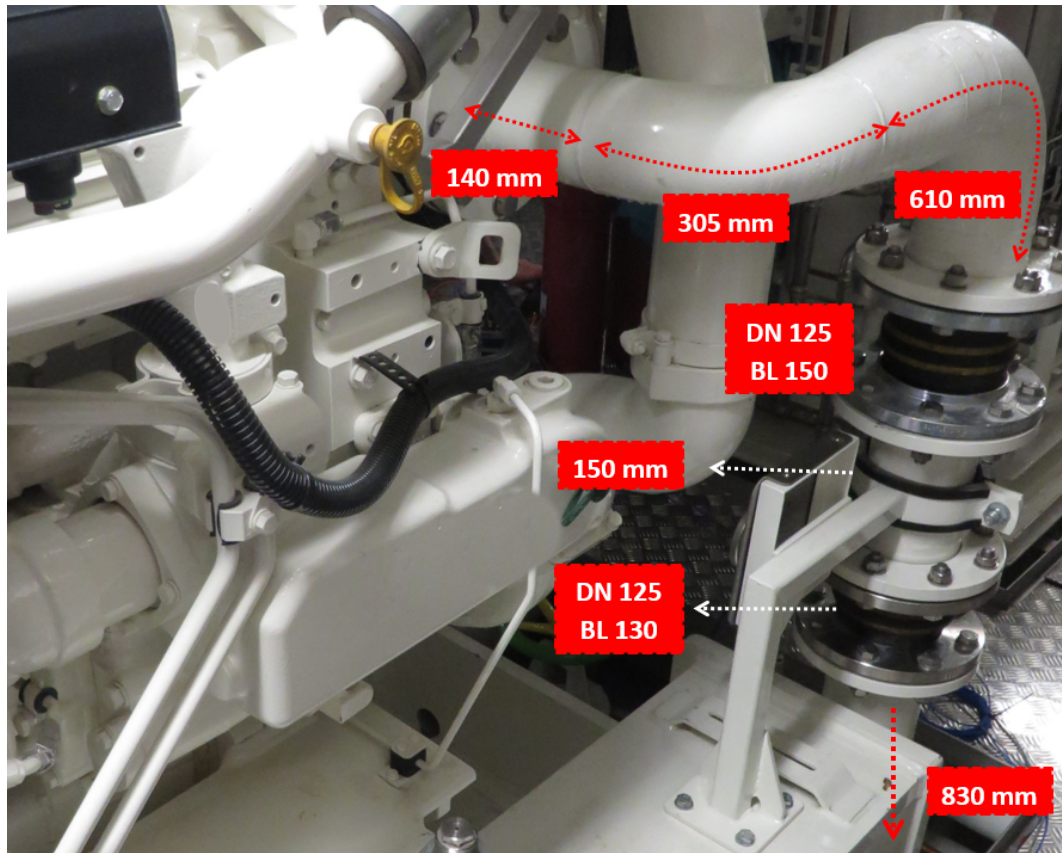
The pipe structure is showed on the Fig. 46.

Figure 46: Measured dimensions of pipe structure.

As it seen from the figure above, the noise source is the engine with its intermediate mass. The engine is double resiliently mounted to the ship hull. Pipe lengths are shown in the figure for better visualisation. The other data taken from measurement is listed in Tab. 17 below:

Table 17: The data sheet for measurement.

Engine mass[kg]	19779
Intermediate mass [kg]	10000
Steel pipe diameter (avg.) [m]	0,15
Steel pipe wall thickness [m]	0,004
Compensator type	DN 125

The collected data is essential for the Ansys *SpaceClaim* modeling. After all the data and lengths are measured, the test started. The first measured section start from the engine to the first flange,second section is start from the first flange to the end of the second compensator and last section start from the second compensator to the first clamp. The hammer test arrangement for *Section I* is shown in Fig. 47.
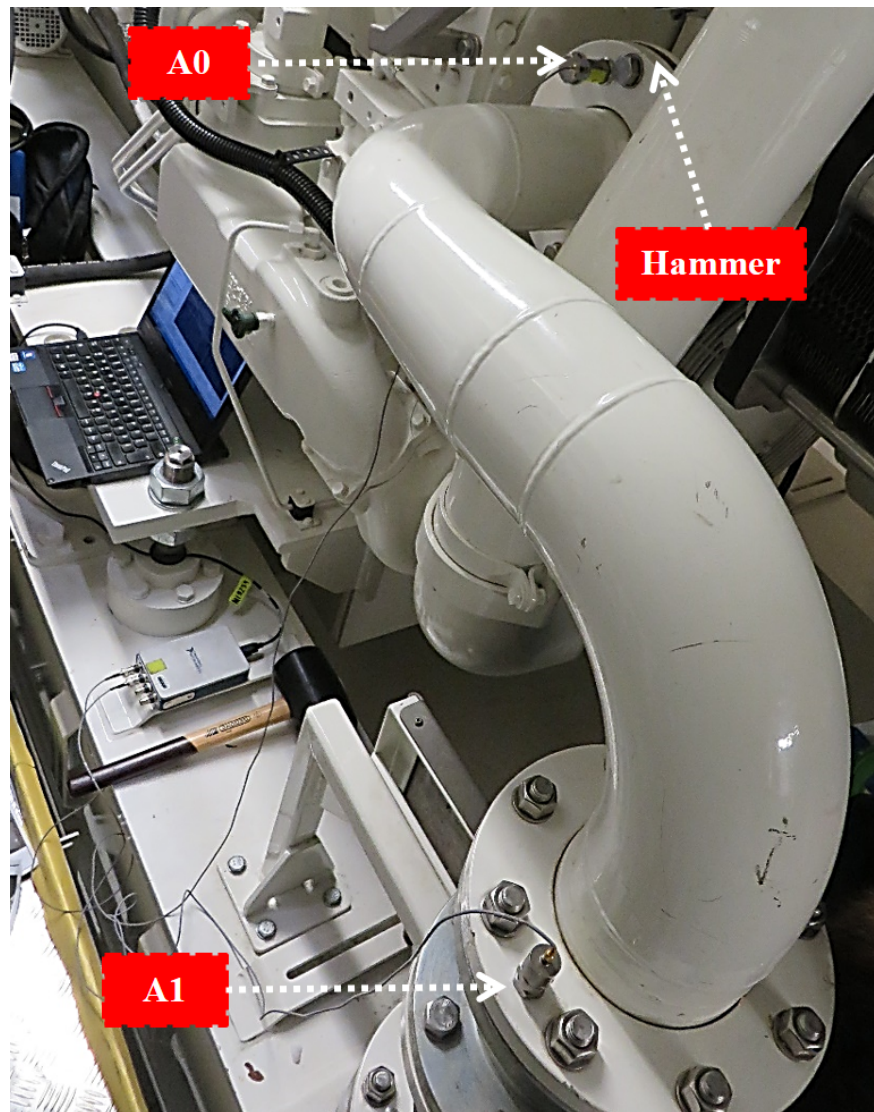
Figure 47: Test 1 for *Section I*.

The Structure Borne Noise transmission for *Section I* is set for the hammer test. Two accelerometers are used for the tests and the hammer is hit by a stationary point in a certain time. First accelerometer is set on top flange which is located at engine and pipe 1 connection. Second accelerometer is set on the bottom flange which is located at the pipe 1 and first compensator connection. The point where the hammer impact is selected as top flange described above. Both accelerometers are connected to *Analogue-Digital converter Amplifier* which reads real time velocity levels on the selected locations.

The location of the top flange is not enough spacious to impact as planned. To validate the final result for pipe section one, the hammer is also impacted from to bottom flange where the second accelerometer is located and finally the result for *Section I* taken as average of both test.
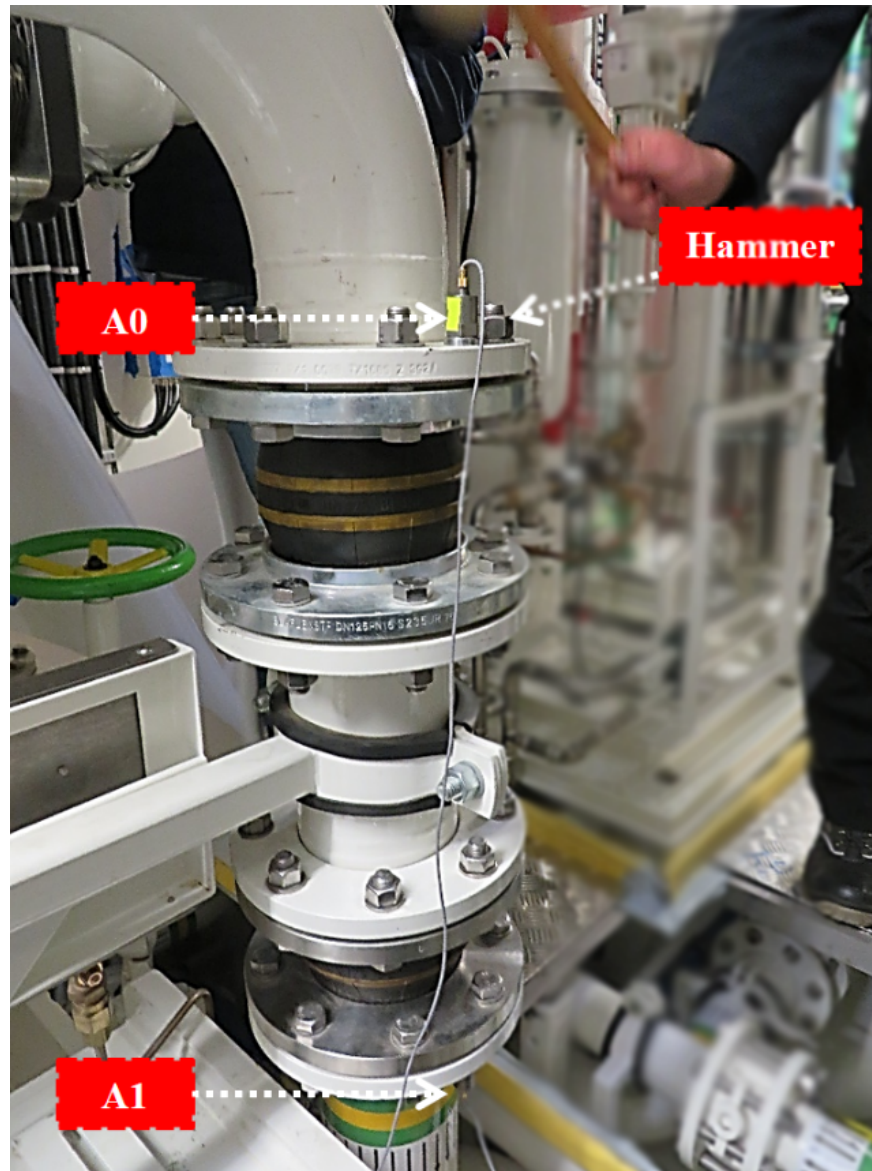
Figure 48: Test 2 for *Section II*.

The test for *Section II* is shown Fig. 48 above. The pipe section consist of two low pressure compensator and a support which connected directly to the intermediate mass. As structural design considerations the intermediate mass is not appropriate location to connect a support. To see the effect of these two compensator and support; first accelerometer is located on flange between first pipe and first compensator. Second accelerometer is located on the flange which located between second compensator and third pipe. The point where the hammer impact is selected as top flange and velocity levels on the selected locations are read by *Analogue-Digital converter Amplifier*.
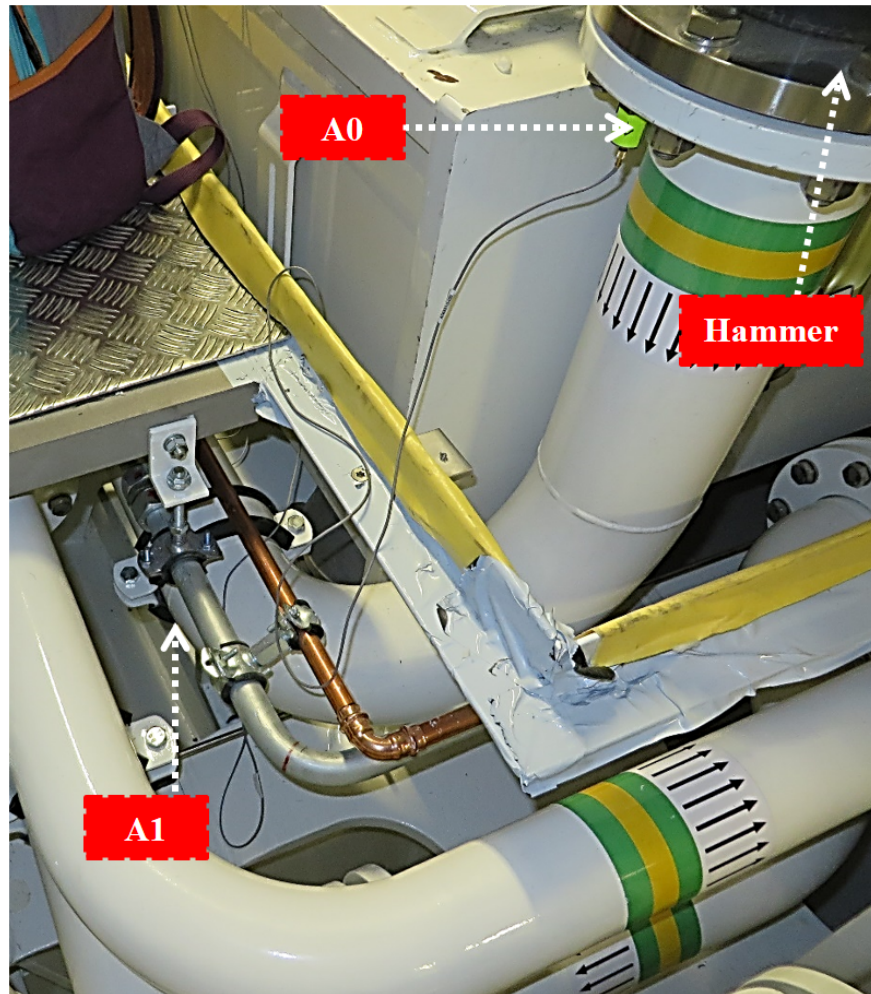
Figure 49: Test 3 for *Section III*.

The last SBN transmission test applied on pipe *Section III* which is located from the bottom flange of second compensator to the fist clamp of the pipe structure which is located under engine. First accelerometer is located on the second compensator bottom flange and second accelerometer is located top of the fist clamp. The first clamp is a bended clamp and connected directly to the hull. The hammer impact location is selected as bottom flange of second compensator and velocity levels on the selected locations are read by *Analogue-Digital converter Amplifier*.

After the measurements are completed the data are transferred to the excel to observe transmission loss along the each pipe. The transfer functions are showed in Fig. 50 for three pipe structure.
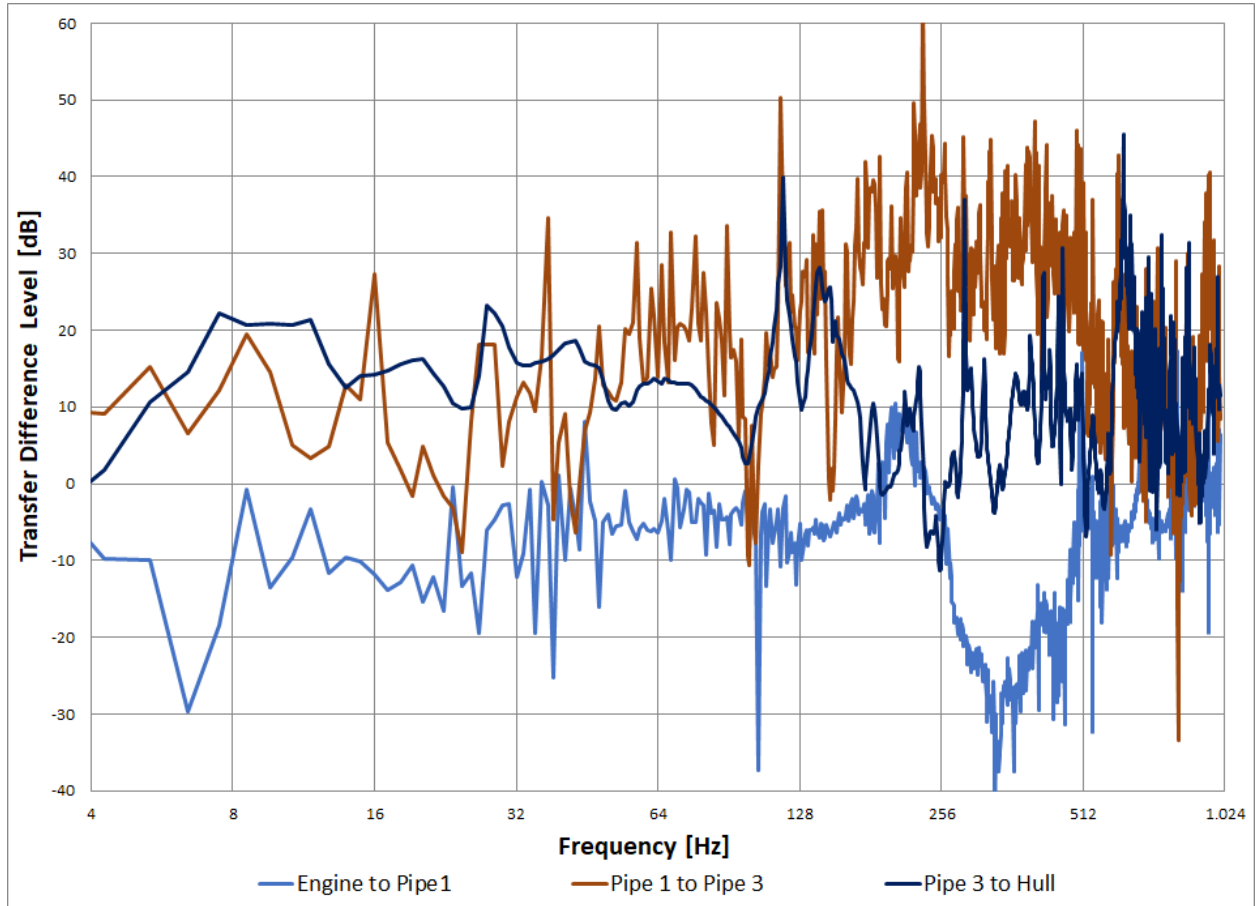
Figure 50: Transfer functions for three pipe section.

The three test is performed with different time spans and different hammer locations. The velocity levels on the accelerometers are not comparable with each other since he values are not read on the same measurement. Although the accelerometers are not comparable with each other; the noise transmission differences which mean transfer functions are key parameter to compare these three measurements.

Although the transfer differences showed above graph, it is also possible to take *Energetic Average* these difference for reduce the fluctuations and unexpected jumps and bumps. The formula for the energetic average of differences is given below equation:

$$L = 10\log \sum_{i=1}^{n} \frac{10^{\frac{L_i}{10}}}{n} \tag{15}$$

Here the *n* values are set for 7. The number of averaged levels can be selected as different values as well. The final transfer difference levels are shown in Fig. 51.
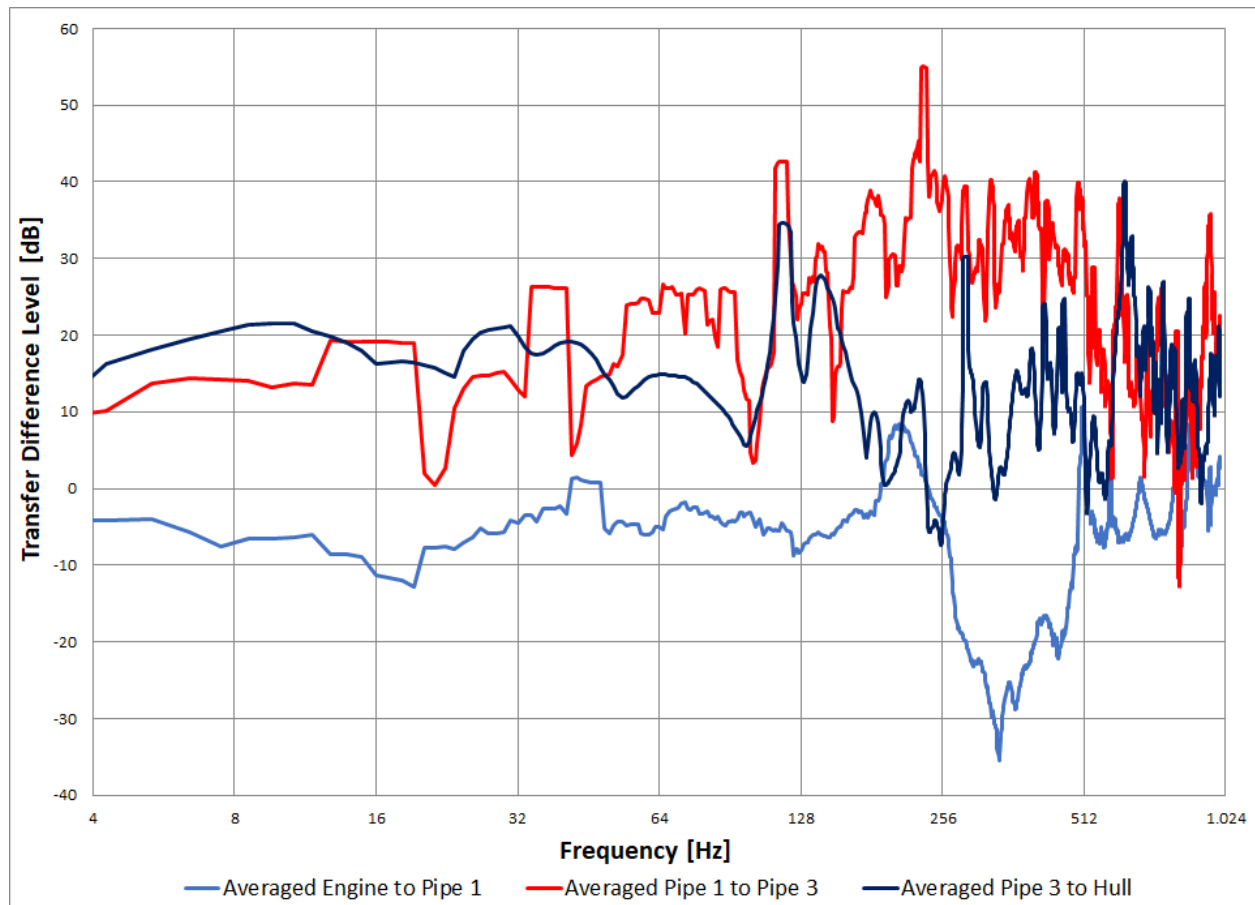
Figure 51: Averaged transfer functions for three pipe section.

The energetic averaged of transfer functions are showed above. The transfer function from engine to pipe 1 will be negative since the engine stiffness is much higher than the pipe so that there will be noise increment instead of noise reduction. Also the transmission difference will be around *10 dB*.

The second transfer function from pipe 1 to pipe 2 is showed with the red curve on Fig. 51. This pipe structure consist two compensator and one support.Since these elements on the pipe leads to the noise reduction; the transmission loss is positive and around *10 dB*.

The last transfer function from pipe 2 to hull has larger noise reduction since the clamp is located on the hull. The transmission loss is positive and around *20 dB*.

7.3. Harmonic Response Analysis with Ansys

This case study covers the Structure Borne Noise (SBN) transmission analysis from the double resiliently mounted source to the ship via the pipe and two compensator. The criterion for the comparison is the velocity levels acting on the noise source mountings to the first clamp. After measurements the pipe structure is modelled with Ansys *SpaceClaim* and harmonically analyzed with *Ansys Harmonic Response*.

The pipe structure is modeled with beam elements with given pipe dimensions and mechanical properties in Sec. 7.2. The mesh settings are applied different for beam elements and solid elements. Selected element length for solid elements is *500 mm* and for beam elements is *50 mm*. Final meshed model is showed in Fig. 52 below :
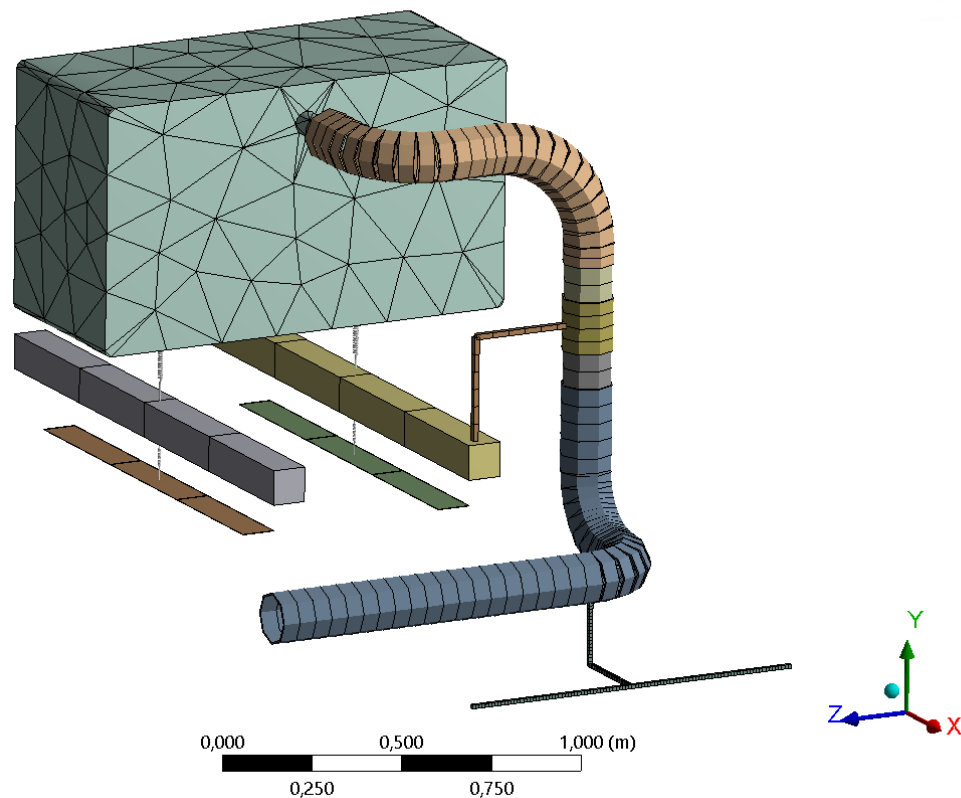
Figure 52: Full model of the pipe structure with selected mesh properties.

Bottom spring stiffness for double resiliently mounted structure should calculate with total mass of the engine and intermediate mass. The medium springs can only be function of the engine mass. The deflection of the engine and intermediate mass is set for *10 mm* as previous single *DOF* systems. The overall spring stiffness is calculated according to the formulation in Sec. 4 and shown in Tab. 18.

Table 18: The spring stiffness of the double resilient mountings.

	Engine	Intermediate Mass + Engine
mass [kg]	19779	29779
Deflection [m]	0,01	0,01
Spring Stiffness Total	1,94E+07	2,92E+07

After applied all design parameters on the model; the final model for harmonic response analysis is shown in Fig. 53 below :
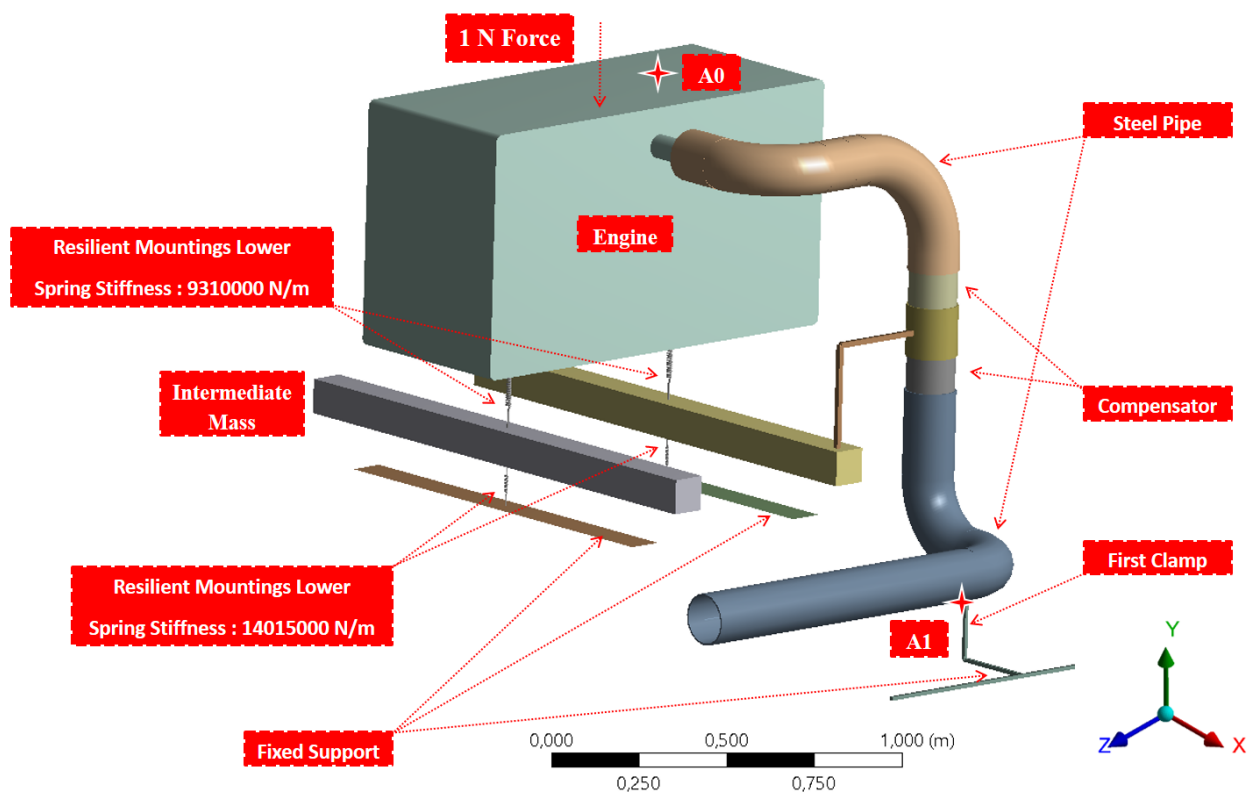
Figure 53: Boundary conditions and structural properties of modal.

All the boundary conditions are applied as showed above. During harmonic response analysis *1 N* force applied on *y-axes* to the engine like previous harmonic analysis of the linear pipe structures. During the design of the model some of the design parameters like wall thickness of steel pipe or support cross section areas remained unanswered due to limited time of the measurement. However the final assumptions are considered with the past experiences about pipe structures.

Table 19: Ansys settings for harmonic response

Frequency Spacing	Linear
Range Minimum	1,0667 Hz
Range Maximum	1000,55 Hz
Solution Intervals	938
Solution Method	Mode Superposition
Constant Damping Ratio	0,01
Modal Frequency Range	Program Controlled

The final harmonic response analyse inputs are showed in Tab. 19. The frequency range is set as equivalent to the test measurements frequency range with an linear increment Later on the logarithmic scale will apply on both solutions. The damping ratio is taken as *0,01* due to corresponding measurement values and *Mode Superposition* method is applied.

Due to use of beam elements instead of solid elements for computational time optimization, it is clearly to see that the number of intervals are above 900. That is lead to high required time for solutions and computational time is approximately *600 second* for each solution.

The first velocity respond with respect to given frequency range is read from the engine surface in *y-axes* as showed *A0* in above figure. The second velocity respond read from the first clamp of structure which connected directly to the hull. It is shown in Fig. 53 as *A1* on *z-axes*.

Since Ansys allow to have direct harmonic response from engine to the first clamp in single analyse, the structure can analyse as whole and the difference level between two points estimate directly. The results of *Ansys Harmonic Response Analysis* is showed in the following section.

Lastly, the hammer test applied for each pipe section in three dimensions. However, the results were not comparable with Ansys model since each test are hold in different time interval and all the accelerometer are relocated for each measurements. The results were compiled with *Visual Studio Code* in regards of *CPU* time of each natural velocity level frequency response graph. The energetic average of the natural frequencies for each pipe section shown in App. D. The *VS* code for analysis also given in App. E.

7.4. Results and Comparison

The *Structure Borne Noise (SBN)* transfer functions are compared according to velocity level differences for both numerically and test measurements. The result are compared in Fig. 54 below :
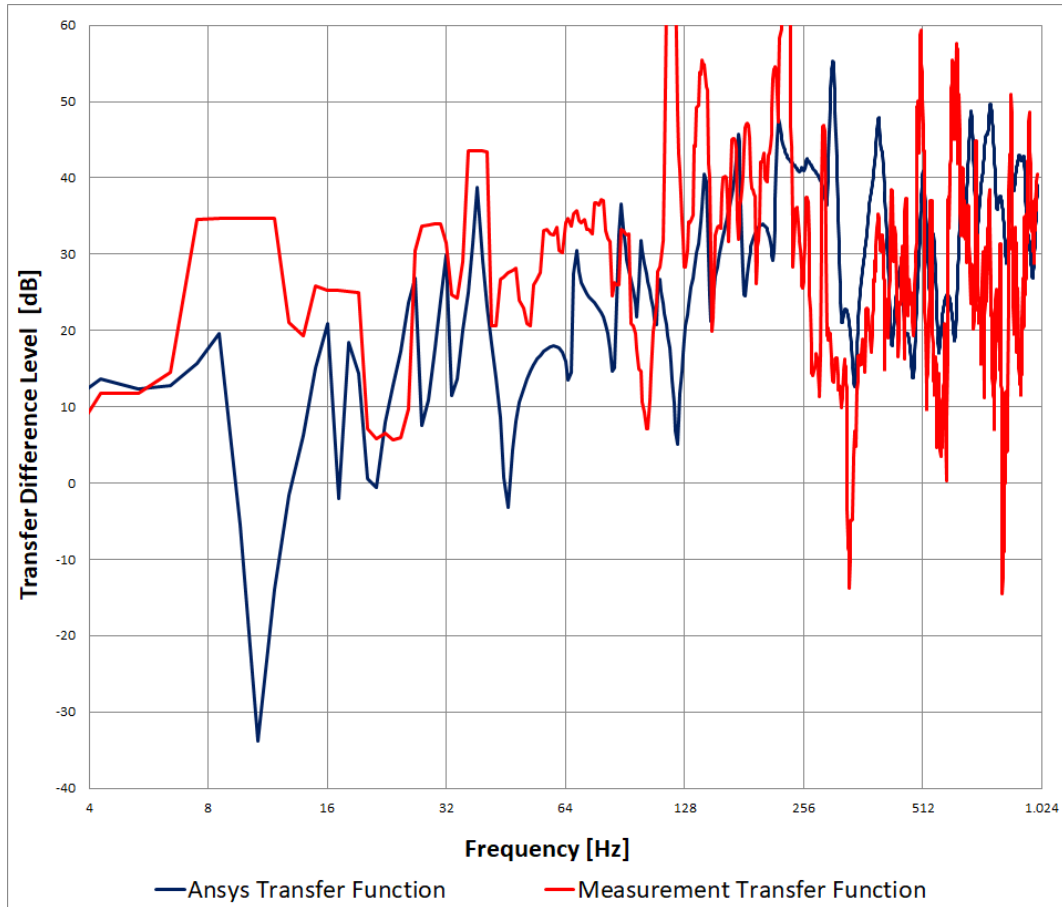

Figure 54: Transfer functions from the source to the first clamp of structure

The measurement transfer function is shown with its energetic averaged values. In general the values match with minor error. In measurements, the extreme low and high frequencies are usually neglected due to heavily inconsistent natural frequency of the individuals.

Beside that, the transfer differences are coincide after *16 Hz* for both function. The main instruments that lead these results are the first and second compensators. The average noise transfer from the engine to the first clamp of the pipe structure is around *20 dB*. Both numerical and test results are satisfied the average expectation of noise transfer difference level.

The final reaction force levels for source and first clamp are shown in Fig. 55.
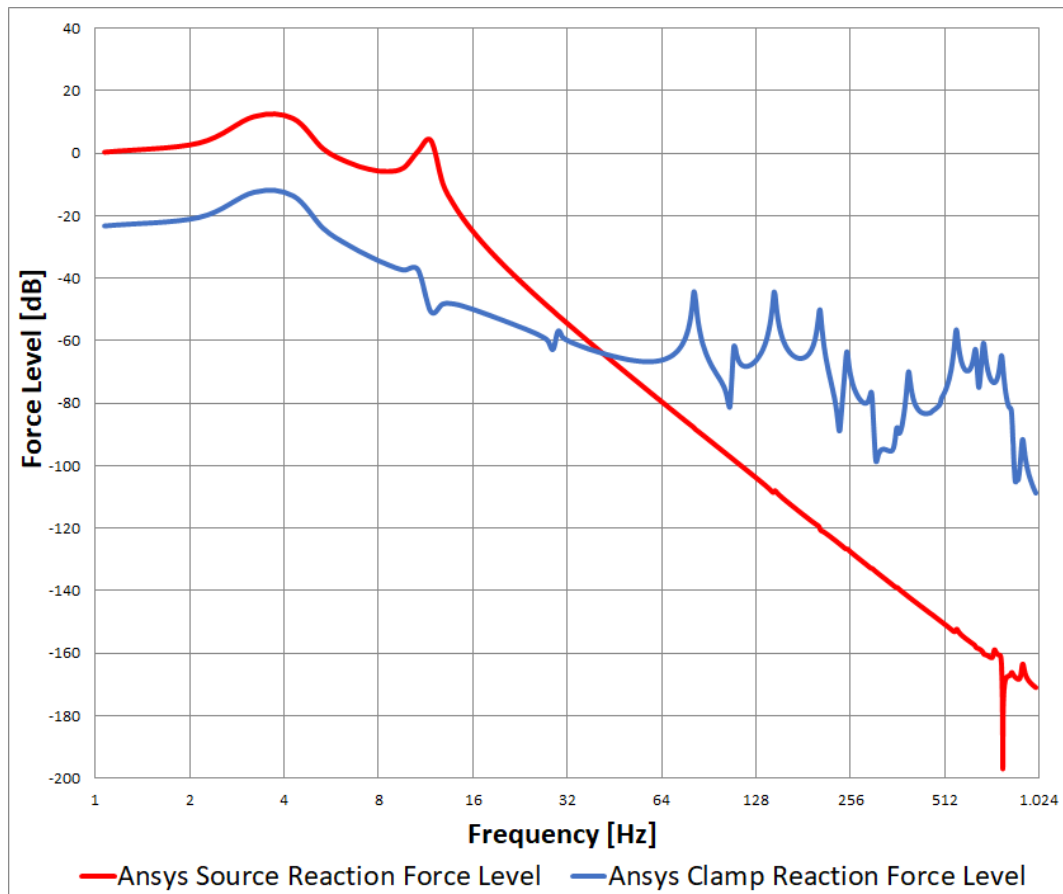
Figure 55: Source and clamp reaction force levels in given pipe structure.

The results are shows that the structure become easily pipe dominant in early frequencies. For such a massive machinery systems this is serious issue to be solve. After *40 Hz* the structure become under effect of pipes and this could lead resonance in early stages of operation.

Since the all dynamic forces on source and intermediate mass is not showed in this harmonic response analysis, the source reaction force level might become imperfect in real problem. Nevertheless, in real life the results would not be irrelevant from Ansys results as shown above.

One of the main reason for this problem is the pipe support between intermediate mass and steel pipe. The support has no effect since it is not stiffened enough for this pipe connection. However the support might reduce noise if its connected to the hull more stiffer surfaces.

If the pipe support is stiffened by making the Young's modulus 10^4 times higher than defined in the real structure [6], the reaction force levels would be in Fig. 55.
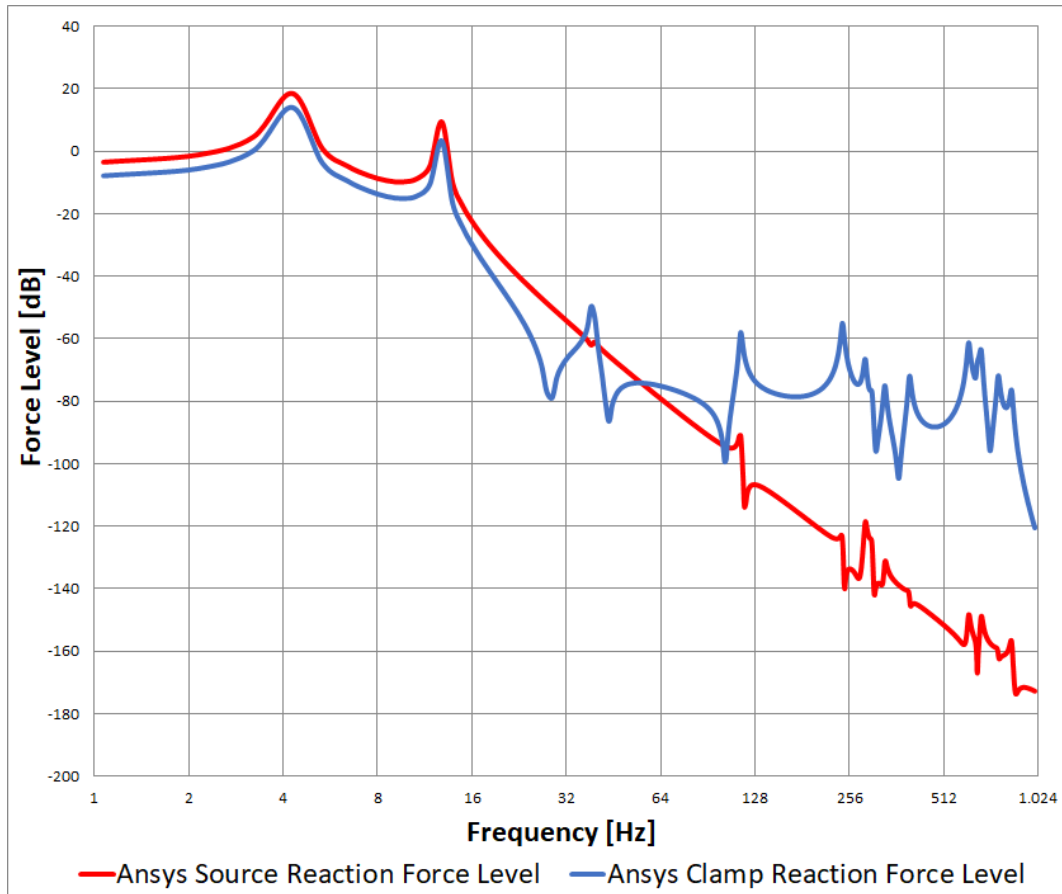
Figure 56: Source and clamp reaction force levels in case of stiffened intermediate mass support.

The results show that the pipe structure with stiffened pipe support have similar response levels. When the pipe support become highly stiff, the system by-passing the engine and its intermediate connection. It is becomes single degree of freedom system with only intermediate mass springs to the hull. The reason for similar levels can explain with the axial stiffness of the compensator highly similar with stiffness of the resilient mountings.

Defined compensators have relatively high stiffness than the real case in order to meet the transfer difference levels for numerical and test results. Furthermore, the compensators with reduced axial stiffness and stiffened pipe support relationships is shown in App. C as well.

To sum up, the pipe supports which are connected directly to the intermediate masses must be stiffened enough. The effect of the compensator stiffness should be considered for each solution step. These are the important outcome for the future *SBN* studies. Also the results are heavily depends on environmental changes and specific conditions. The accuracy is proportional with the quality of data taken from measurements that applied on model.

8. Conclusions

The objective of the thesis *"Structure Borne Sound Transmission Along Piping on Ships"* is to combine knowledge and experience in the area of noise (sound) transmission of piping at most common machinery pipe structures. The noise transmission of the this study concern the source, compensator, pipe structure, source and pipe support. By setting up numerical and analytical solutions for pipe components the noise transmission on structure harmonically resolved in the most efficient way for each component and the selection of convenient countermeasure also be verified according to ultimate results.

As a start point, one of the most common pipe structure is divided into main components as source, compensator, steel pipe and clamps. An analytical approach is compared to calculations by the *FE* method for noise source. Therefore, the resilient mounts are introduced and the numerical model is set up. The analytical and *FEM* calculations are performed afterwards. The results are compared for various source mass. The most appropriate mass is selected for noise source ultimately.

Later on, a compensator is created with cantilever beam modal solutions with a performed test. Two different beam element are compared in respect of their slenderness ratios. This is intended to observe the validity of the numerical model and set up the standardized mechanical properties of the compensator. As a result of simulation, the dynamic stiffness of the compensator correspond to the expected phenomena.

As a first approach to the *Harmonic Response Analysis*, whole pipe structure is modeled and assembled. The solid pipe and clamps are optimized to beam element in order to reduce mesh error and computational time. The rest of the structure is taken into account via boundary conditions and restraints.

The clamp location has varied within different locations. The second and third clamp reaction force levels are compared with respect to the first clamp. The location of the first clamp can effect the overall force levels seriously. As a result, greater distance of first clamp from compensator results in greater force levels. Optimum location of the first clamp and spacing of other clamps are selected due to clamp dominated and source dominated frequency ranges and force levels.

The study of the compensator length and noise transmission analysis is hold afterwards. The stiffness relationship is calculated of three length of the compensator. The greater length has lower stiffness which results in greater stiffness ratio. Later on the force level on clamps for selected compensator lengths are compared. With the longer compensator the force levels are lower at low

frequencies but the frequency range where transmission via the piping systems dominates shifts to lower frequencies.

To evaluate effect of the compensator on noise transmission, different type of compensators are modeled and harmonically analyzed. The force transmission levels are compared within each other. It becomes clear that the linear compensator and 90°bended compensator force levels and resonance frequencies are fulfill each other if the conditions are similar. Moreover, the dog leg compensators have increased transmission loss and lower resonance frequency due to its double compensators.

As a last approach to the *Harmonic Response Analysis*, all rigid clamps are changed into resilient mountings. The relationship between the noise source and the compensators are described. The results show that the resiliently mounted clamps are completely source dominant systems. It is interesting to show that how the compensator become negligible in these kind of systems. The further studies can be shape around resiliently mounted clamps instead of compensators.

In this thesis, a special ship has experienced as a noise transmission study with its machinery pipe structure. The hammer test has been used for this study. Experiences were obtained by performing several test with vibration specialists onboard. The study highlights the choice of measurement methods, measurement settings, measurement standard as well as how results from the measurement are analyzed and presented. Results are compared with numeral model of the structures, a few improvements and recommendations were made for future machinery pipe structure design.

It is possible to draw the following results as each vibration problem of the pipe needs an in depth knowledge of active processes, surrounding machines, and vibration supports. The selection of measuring devices is mainly governed by frequency range that captures the vibration motion. The selection of measuring points is chosen primarily based on the measuring location's experience and accessibility. However, a calculation where the pipe resonance frequency and velocity levels can demonstrate hot spots in measuring positions is preferable.

The different tasks for the analysis are all answered and justified in the thesis. Even tough the pipe vibration problems at ships are often complex, the performed studies are enable more detailed understanding of these problems. The results obtained with modal and harmonic response analysis are provide an overview of the capacities, advantages and drawbacks of the pipe structure for futher studies.

References

[1] Beta Machinery Analysis. "Vibration Control Strategies for Reciprocating Compressors". In: (2009). Ed. by BETA MA.

[2] J.M.J.F. van Campen. "FEA case Study: Rubber expansion joint for piping systems". In: (2015). Ed. by TANIQ BV.

[3] J. S. Carlton and D. Vlasic. "Ship vibration and noise: Some topical aspects". In: *Lloyd's Register Technical Papers* (June 2005).

[4] A. Collet and M. Kallman. "Pipe Vibrations Measurements". In: (Feb. 2017). Ed. by ENERGIFORSK-ISBN 978-91-7673-351-6.

[5] Ansys 17.0 Documentation. "Harmonic Response Analysis". In: (2017). URL: `https://www.sharcnet.ca/Software/Ansys/17.0/en-us/help/wb_sim/ds_harmonic_analysis_type.html` (visited on 06/01/2019).

[6] Ansys 18.2 Documentation. "Stiff Beam". In: (2018). URL: `https://www.sharcnet.ca/Software/Ansys/18.2.2/en-us/help/wb_sim/ds_stiff_beam.html` (visited on 07/09/2019).

[7] Siemens Experimenter. "Natural Frequency and Resonance". In: (2018). URL: `https://community.plm.automation.siemens.com/t5/Testing-Knowledge-Base/Natural-Frequency-and-Resonance/ta-p/498422` (visited on 04/09/2019).

[8] P. Guillaume. "Modal Analysis". In: *Department of Mechanical Engineering,Vrije Universiteit Brussel* (2010).

[9] A. Harish. "What Is Modal Analysis and Why Is It Necessary?" In: (2019). URL: `https://www.simscale.com/blog/2016/12/what-is-modal-analysis/` (visited on 06/12/2019).

[10] Akademischen Verein Hütte. "Hütte Des Ingenieurs Tashenbuch". German. In: (1955). Ed. by Verlag von Wilhelm Ernst& Sohn.

[11] T.Carter M. Alf and L. Canals. "Maritime Medicine: Main noise sources on board ships". In: (2014). Ed. by ISBN: 978-82-999303-0-7 Norwegian Centre for Maritime Medicine.

[12] C. Mason. "What Is A Hammer Test Or Hammer Impact Test?" In: (2013). URL: `http://blog.prosig.com/2013/02/11/what-is-hammer-impact-testing/` (visited on 07/02/2019).

[13] The Danish Fishermen's Occupational Health Services. "How to handle noise and vibrations in ships". In: (Apr. 2008).

[14] G. Novac T. Pazara M. Pricop and C. Pricop. "The application of new noise and vibration standards onboard ships". In: (2018). Ed. by IOP Conf. Series: Earth and Environmental Science 172 (2018) 012027.

[15] K. K. Singh V. Kumar and S. Gaurav. "Analysis of Natural Frequencies for Cantilever Beam with I- and T- Section Using Ansys". In: (Sept. 2015). Ed. by International Research Journal of Engineering and Technology (IRJET) e-ISSN: 2395-0056.

[16] Det Norske Veritas. "Structural Analysis of Piping Systems". In: *Recommended Practice DNV-RP-D101* (2008).

[23] D. K. Wittekind. "A simple model for the underwater noise source level of ships". In: *Journal of Ship Production and Design, 30(1):1–8* (Feb. 2014).

[24] D. K. Wittekind. "Ship Acoustics - Chapter 1. Basics". In: *Lecture slides* (2013).

[25] D. K. Wittekind. "Ship Acoustics - Chapter 2. Sources and Primary Measures". In: *Lecture slides* (2013).

[26] D. K. Wittekind. "Ship Acoustics - Chapter 3. Secondary Measures and Sound Propagation in the Ship". In: *Lecture slides* (2013).

Web Figures

[17] *Web image available from.* URL: https://www.earq.com/hearing-loss/decibels (visited on 05/12/2019).

[18] *Web image available from.* URL: https://www.navalhead.it/services/design/ (visited on 05/18/2019).

[19] *Web image available from.* URL: https://upload.wikimedia.org/wikipedia/commons/0/07/Resonance.PNG (visited on 06/19/2019).

[20] *Web image available from.* URL: http://www.nauticexpo.com/prod/volvo-penta/product-21503-266901.html (visited on 04/08/2019).

[21] *Web image available from.* URL: https://www.paulstra-industry.com/elastomer-mounts-g9-en.html (visited on 04/08/2019).

[22] *Web image available from.* URL: https://reiflexa.net/en/products/ (visited on 07/05/2019).

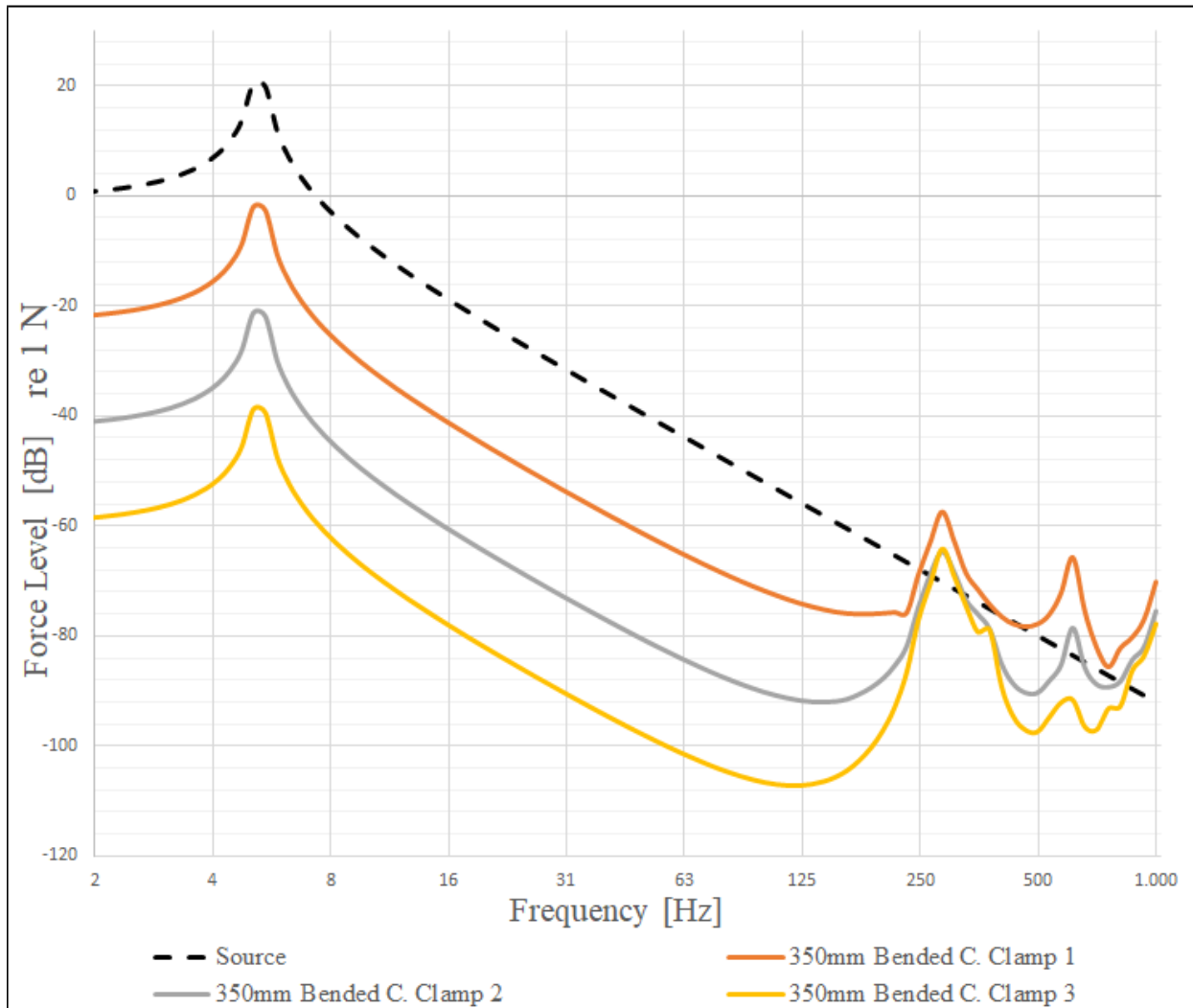# A. Clamp Spacing Force Levels

A.1. Second Clamp Force Levels
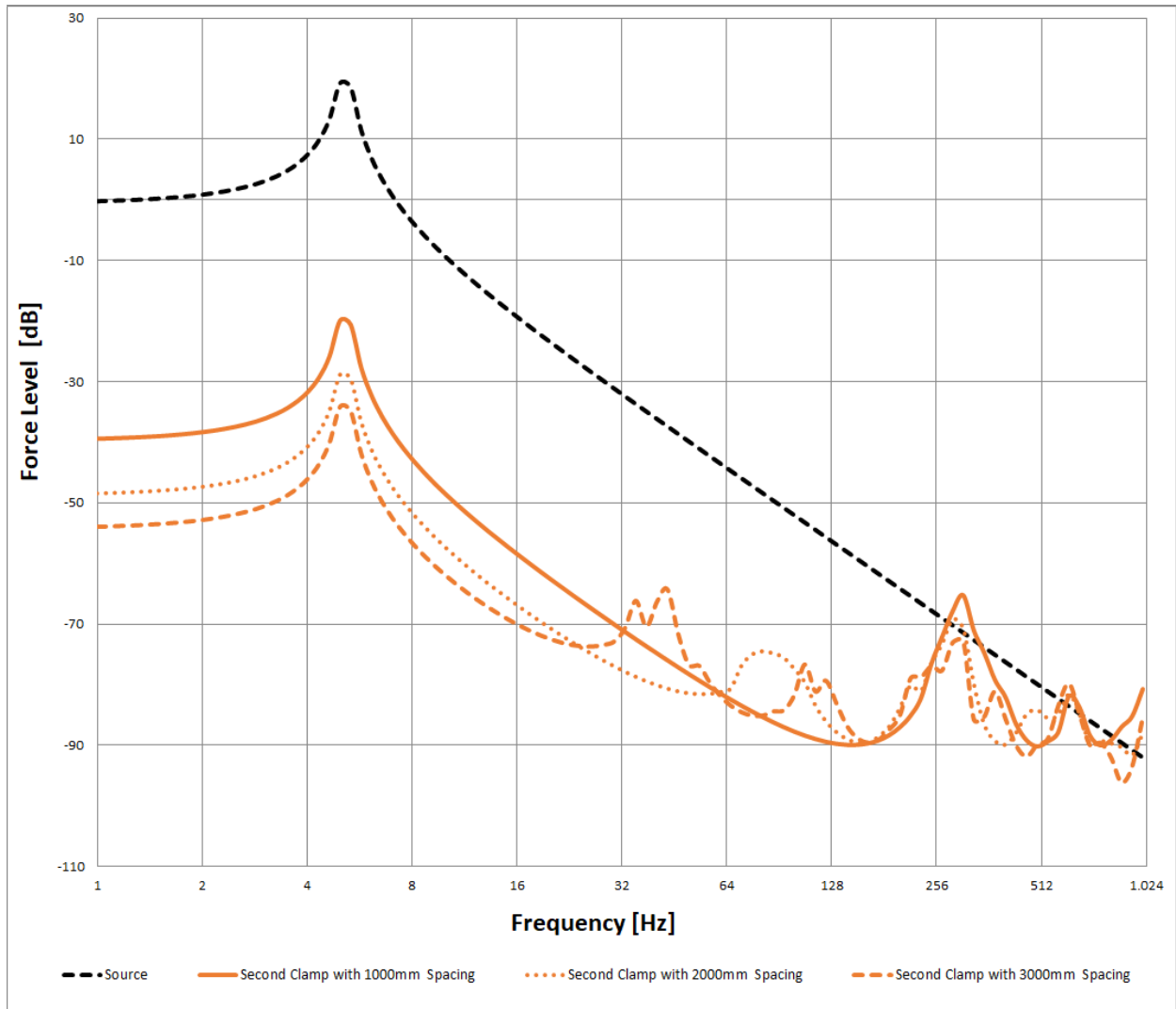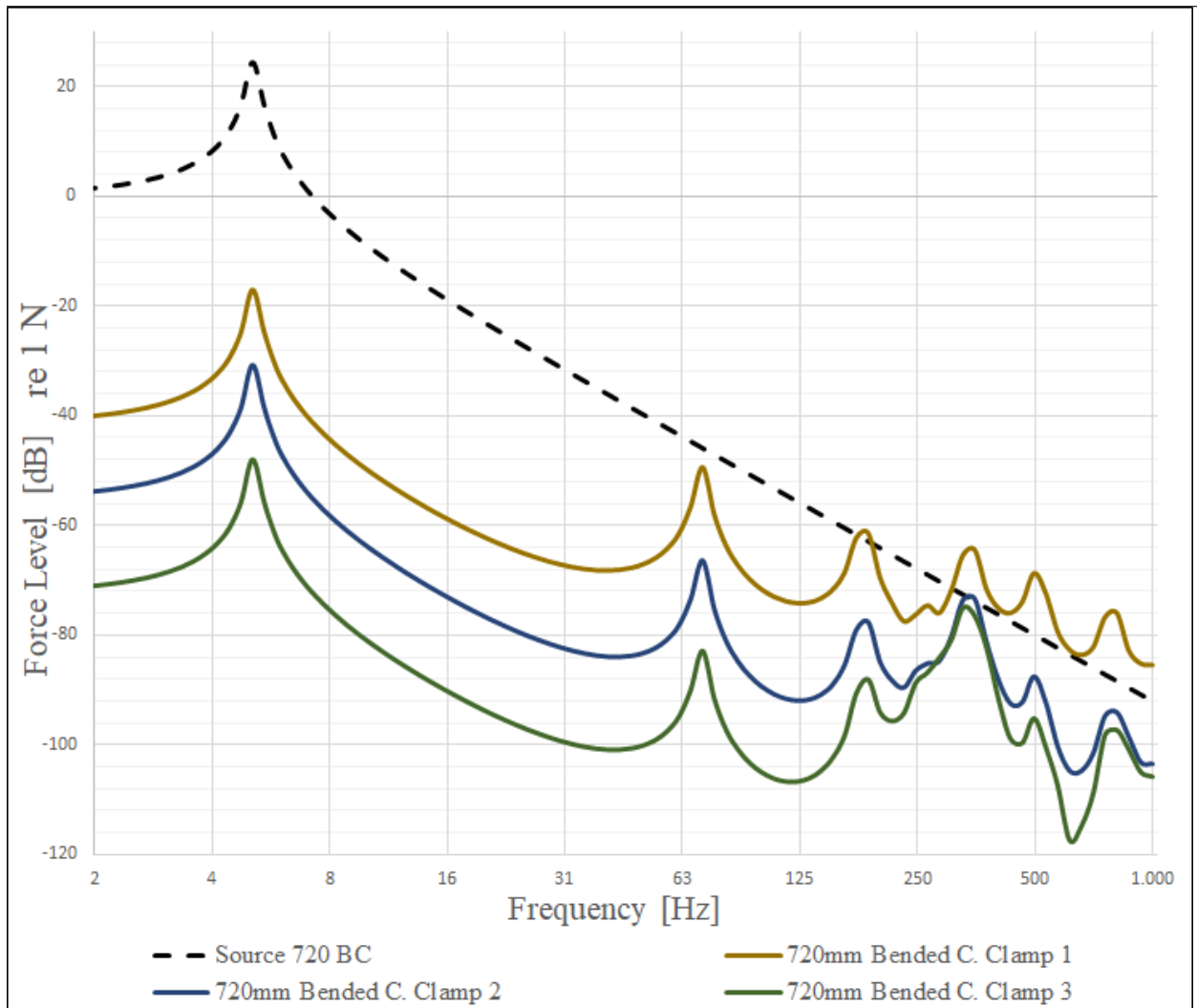
A.2. Third Clamp Force Levels
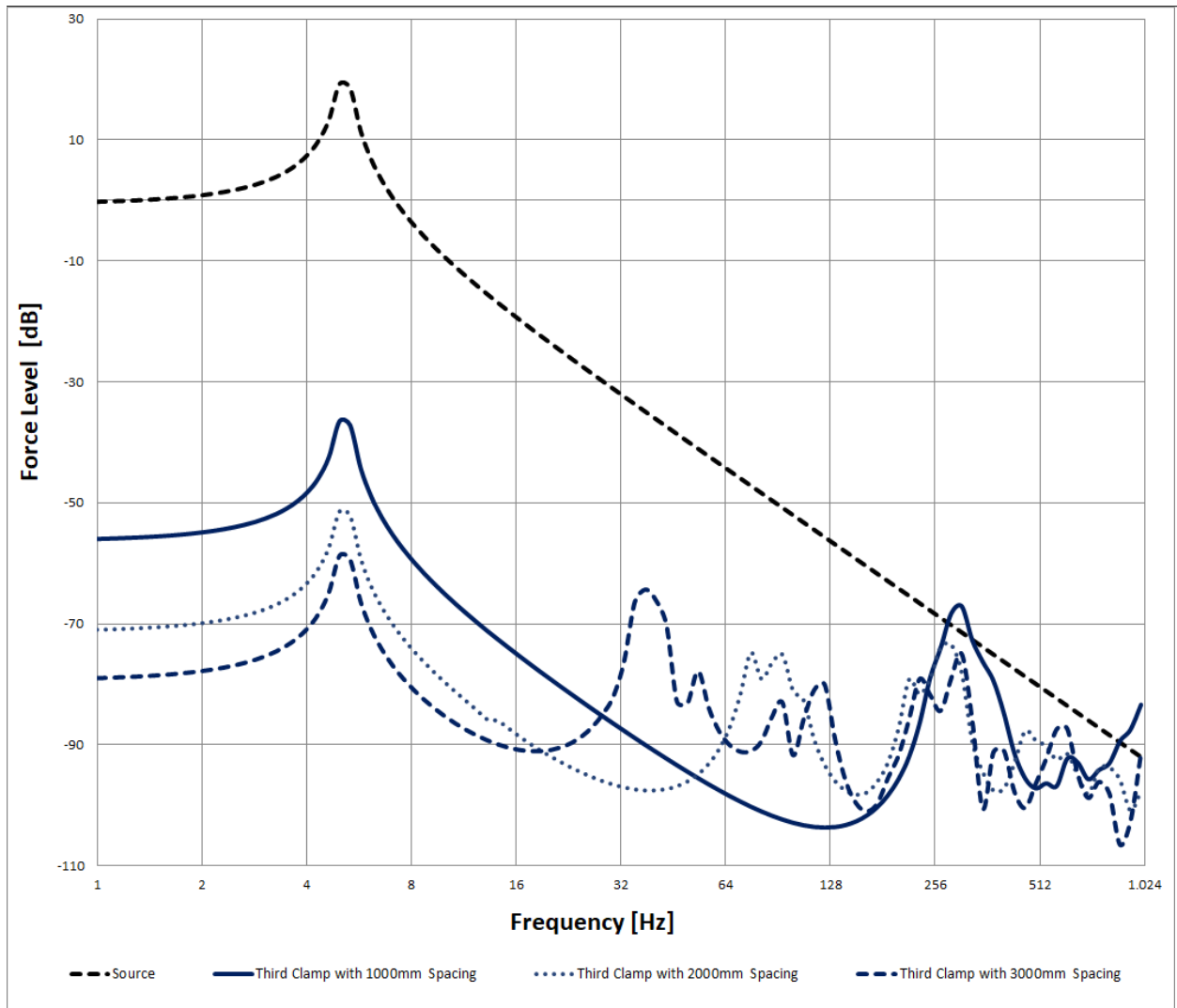
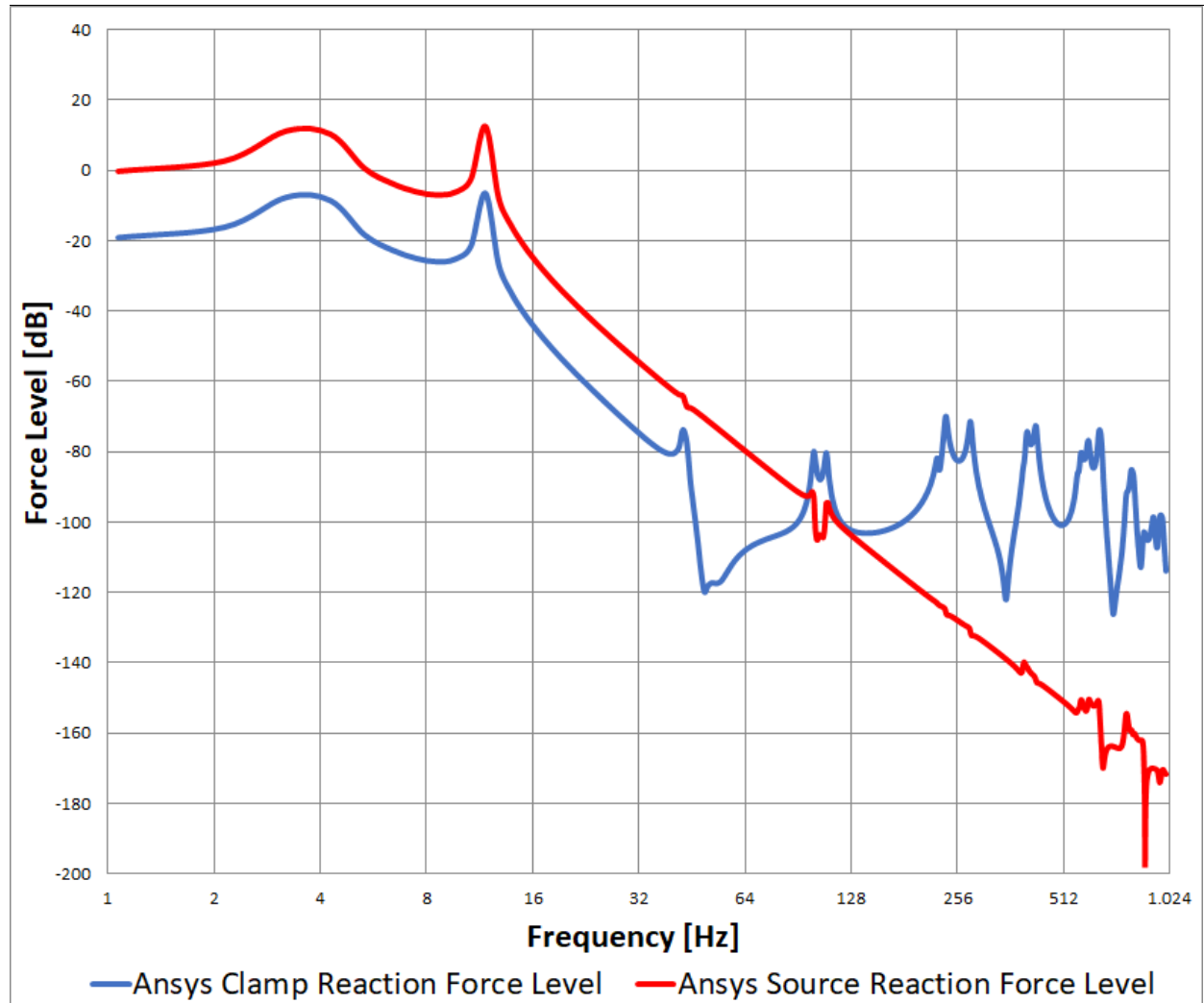# B. Bended Compensator Clamp Force Levels

B.1. 350 mm Compensator

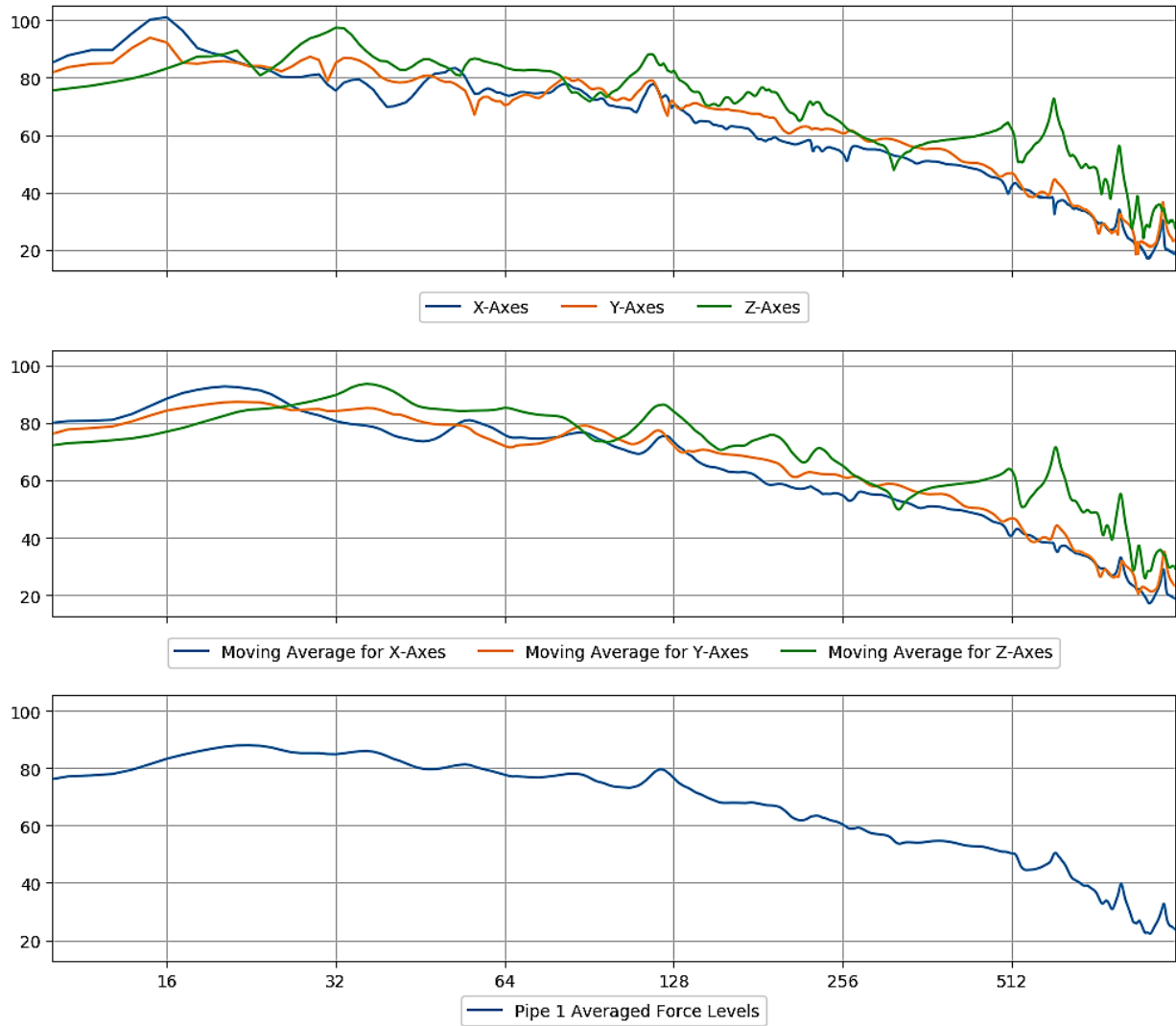## B.2. 720 mm Compensator

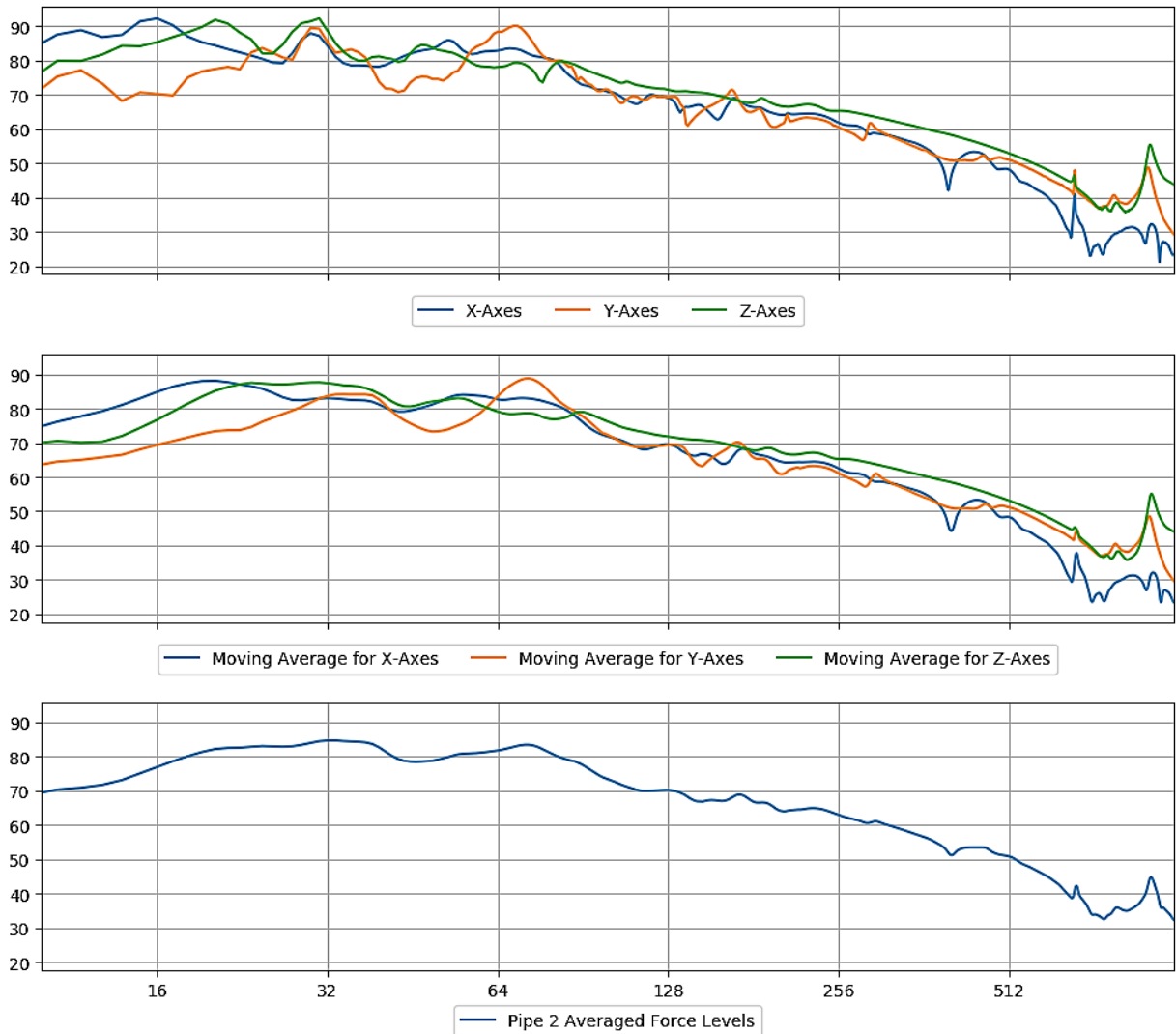## C. The Reaction Force Levels for Compensator with Reduced Stiffness
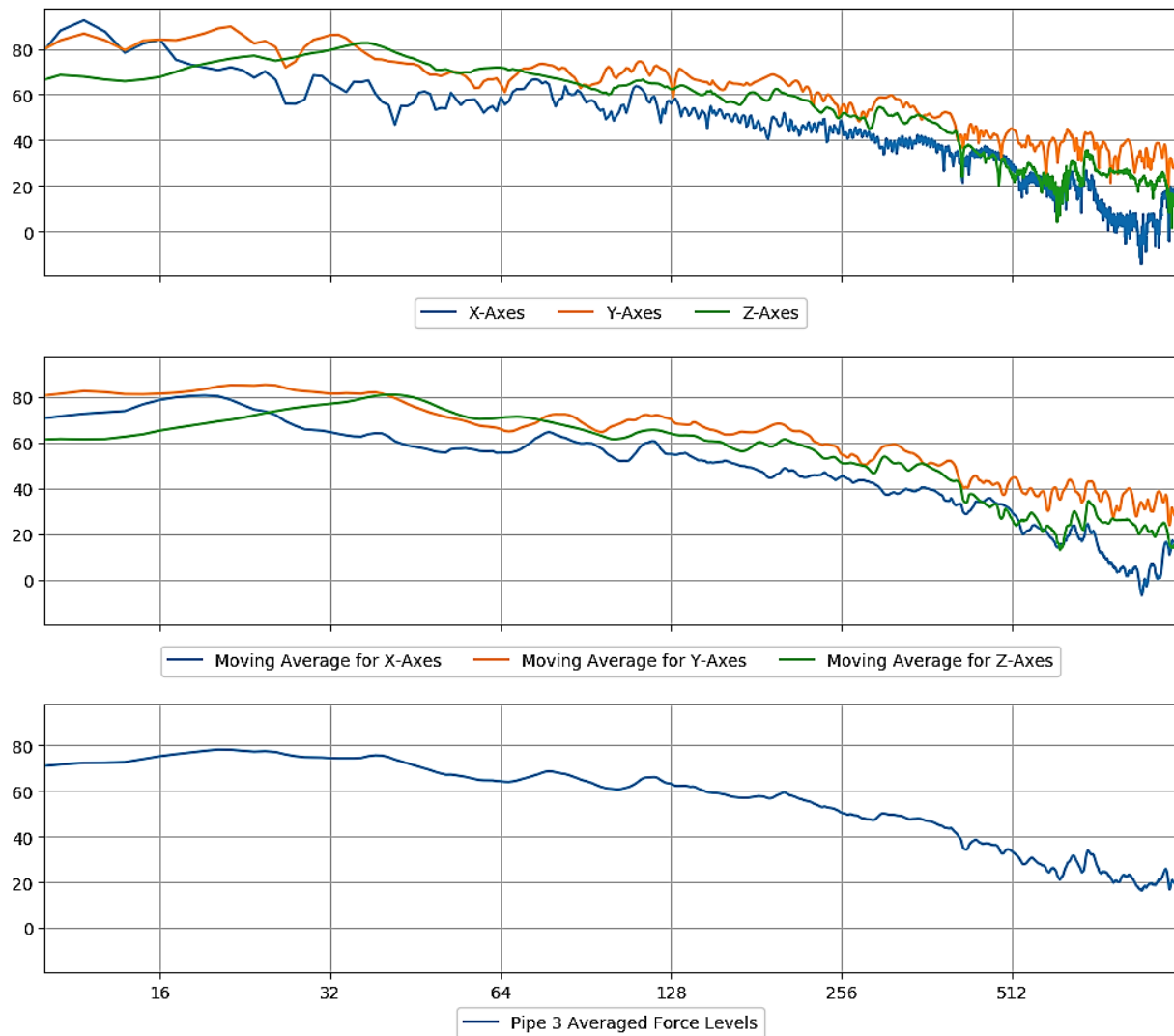
D. Natutal Frequency Test Measurements

D.1. Pipe Section 1

D.2. Pipe Section 2

D.3. Pipe Section 3

E. Visual Studio Code for the Case Study

```python
1 import pandas as pd
2 import matplotlib.pyplot as plt
3 from matplotlib.ticker import ScalarFormatter, FormatStrFormatter
4
5
6
7 # importing the excel file
8 df = pd.read_excel(
9     "C:\TransferFunction\pipes_final_v4.xlsx",
10     sheet_name = 0,
11     index_col =0)
12 print(df.info())
13 columns = ['X-Axes','Y-Axes','Z-Axes']
14
15 window = int(10)
16 df_smooth = df.rolling(window).mean()
17 df_smooth['Pipe 1 Averaged Force Levels'] = df_smooth.mean(axis=1)
18
19 xlim=(10,1000)
20
21 f, (ax1, ax2,ax3) = plt.subplots(3,1, sharex=True,sharey=True)
22 df.plot(y=columns,logx=True, xlim=xlim, ax=ax1)
23 df_smooth.plot(y=columns,label=['Moving Average for X-Axes','Moving
      Average for Y-Axes','Moving Average for Z-Axes'],logx=True, xlim=
      xlim,ax=ax2)
24 df_smooth.plot(y=['Pipe 1 Averaged Force Levels'],logx=True, xlim=xlim,
      ax=ax3)
25 ax1.set_xscale('log', basex=2)
26 ax2.set_xscale('log', basex=2)
27 ax3.set_xscale('log', basex=2)
28 ax1.grid()
29 ax1.legend(loc='upper center', bbox_to_anchor=(0.5, -0.05), ncol=3)
30 ax2.grid()
31 ax2.legend(loc='upper center', bbox_to_anchor=(0.5, -0.05), ncol=3)
32 ax3.grid()
33 ax3.legend(loc='upper center', bbox_to_anchor=(0.5, -0.1), ncol=1)
34 ax1.xaxis.set_major_formatter(FormatStrFormatter('%.0f'))
35 ax2.xaxis.set_major_formatter(FormatStrFormatter('%.0f'))
36 ax3.xaxis.set_major_formatter(FormatStrFormatter('%.0f'))
37 plt.tight_layout()
38 plt.subplots_adjust(left=None, bottom=None, right=None, top=None,
      wspace=None, hspace=0.3)
39 #plt.savefig('00Pipe_1.png')
```

```python
40 plt.show()
41
42 print('--- END ---')
43
44 # importing the excel file
45 df = pd.read_excel(
46     "C:\TransferFunction\pipes_final_v4.xlsx",
47     sheet_name = 1,
48     index_col =0)
49 print(df.info())
50 columns2 = ['X-Axes','Y-Axes','Z-Axes']
51
52 window = int(10)
53 df_smooth = df.rolling(window).mean()
54 df_smooth['Pipe 2 Averaged Force Levels'] = df_smooth.mean(axis=1)
55
56 xlim=(10,1000)
57
58
59
60 f, (ax1, ax2,ax3) = plt.subplots(3,1, sharex=True,sharey=True)
61 df.plot(y=columns,logx=True, xlim=xlim, ax=ax1)
62 df_smooth.plot(y=columns2,label=['Moving Average for X-Axes','Moving
      Average for Y-Axes','Moving Average for Z-Axes'],logx=True, xlim=
      xlim,ax=ax2)
63 df_smooth.plot(y=['Pipe 2 Averaged Force Levels'],logx=True, xlim=xlim,
      ax=ax3)
64 ax1.set_xscale('log', basex=2)
65 ax2.set_xscale('log', basex=2)
66 ax1.grid()
67 ax1.legend(loc='upper center', bbox_to_anchor=(0.5, -0.05), ncol=3)
68 ax2.grid()
69 ax2.legend(loc='upper center', bbox_to_anchor=(0.5, -0.05), ncol=3)
70 ax3.grid()
71 ax3.legend(loc='upper center', bbox_to_anchor=(0.5, -0.1), ncol=1)
72 ax1.xaxis.set_major_formatter(FormatStrFormatter('%.0f'))
73 ax2.xaxis.set_major_formatter(FormatStrFormatter('%.0f'))
74 ax3.xaxis.set_major_formatter(FormatStrFormatter('%.0f'))
75 plt.tight_layout()
76 plt.subplots_adjust(left=None, bottom=None, right=None, top=None,
      wspace=None, hspace=0.3)
77 #plt.savefig('00Pipe_2.png')
78 plt.show()
79
80 print('--- END ---')
81
```

```python
82 # importing the excel file
83 df = pd.read_excel(
84     "C:\TransferFunction\pipes_final_v4.xlsx",
85     sheet_name = 2,
86     index_col =0)
87 print(df.info())
88 columns3 = ['X-Axes','Y-Axes','Z-Axes']
89
90 window = int(10)
91 df_smooth = df.rolling(window).mean()
92 df_smooth['Pipe 3 Averaged Force Levels'] = df_smooth.mean(axis=1)
93
94 xlim=(10,1000)
95
96
97
98 f, (ax1, ax2,ax3) = plt.subplots(3,1, sharex=True,sharey=True)
99 df.plot(y=columns3,logx=True, xlim=xlim, ax=ax1)
100 df_smooth.plot(y=columns,label=['Moving Average for X-Axes','Moving
       Average for Y-Axes','Moving Average for Z-Axes'],logx=True, xlim=
       xlim,ax=ax2)
101 df_smooth.plot(y=['Pipe 3 Averaged Force Levels'],logx=True, xlim=xlim,
       ax=ax3)
102 ax1.set_xscale('log', basex=2)
103 ax2.set_xscale('log', basex=2)
104 ax3.set_xscale('log', basex=2)
105 ax1.grid()
106 ax1.legend(loc='upper center', bbox_to_anchor=(0.5, -0.05), ncol=3)
107 ax2.grid()
108 ax2.legend(loc='upper center', bbox_to_anchor=(0.5, -0.05), ncol=3)
109 ax3.grid()
110 ax3.legend(loc='upper center', bbox_to_anchor=(0.5, -0.1), ncol=1)
111 ax1.xaxis.set_major_formatter(FormatStrFormatter('%.0f'))
112 ax2.xaxis.set_major_formatter(FormatStrFormatter('%.0f'))
113 ax3.xaxis.set_major_formatter(FormatStrFormatter('%.0f'))
114 plt.tight_layout()
115 plt.subplots_adjust(left=None, bottom=None, right=None, top=None,
       wspace=None, hspace=0.3)
116 #plt.savefig('00Pipe_3.png')
117 plt.show()
118 print('--- END ---')
```